20-WATT HIGH IMPACT TRAVELING-
WAVE TUBE AMPLIFIER

By

Edward R. Dornseif

9 February 1968

Contract No. 951287

Final Report

Watkins-Johnson Company
3333 Hillview Avenue
Palo Alto, California

20-WATT HIGH IMPACT TRAVELING-
WAVE TUBE AMPLIFIER

By

Edward R. Dornseif

9 February 1968

Contract No. 951287

Final Report

Watkins-Johnson Company
3333 Hillview Avenue
Palo Alto, California

TABLE OF CONTENTS

TABLE OF CONTENTS

TABLE OF CONTENTS

LIST OF ILLUSTRATIONS

LIST OF ILLUSTRATIONS

LIST OF ILLUSTRATIONS

LIST OF ILLUSTRATIONS

LIST OF ILLUSTRATIONS

TABLE OF TABLES

TABLE OF TABLES

SECTION I

INTRODUCTION

A. DESCRIPTION OF REPORT

This report describes in detail a program to design and develop a traveling-wave tube amplifier (TWTA) consisting of a traveling-wave tube (TWT) and a band reject and harmonic filter (filter). The TWTA is for a space communication application requiring operation during and after high impact shocks to levels of 10,000 G for 1 millisecond duration.

The report is divided into four major sections: 1) End Item Amplifier, 2) Engineering Model TWT Development, 3) TWT Reliability and Life, and 4) Recommendation for Additional Development.

The report is organized in a way that will hopefully result in a clearer and more logical exposition, not to present a chronological development. The report progresses from the general to the specific and from the total amplifier to its component parts.

The report has been written to benefit developers of future high shock resistant hardware, not necessarily just traveling-wave tubes. It is assumed that the reader has some familiarity with the subject matter.

An attempt is made to clarify the initial evaluation of the development task, the preliminary approach to the problem and the logical steps taken to complete the task.

B. HISTORICAL REVIEW

This review describes the development and research efforts performed to obtain the 20 watt, S-band amplifier.

1. Program Objective. The program had as its objective a TWT amplifier which had:

- high impact shock capabilities
- long life with high reliability
- the required power output
- high RF/DC efficiency, and
- high non-operating temperature capability

The high impact capability remained as the one completely new and unexplored environment for these two devices (TWT and filter).

2. Period of Effort. The development program was begun on 13 January 1966 and completed with the delivery of the end item amplifier on 31 October 1967 - a period of 20 months excluding a 6-week period during which the program was in a hold category.

3. Results. The program concluded with the delivery of a prototype amplifier which, while not to full specification, did satisfy the principle objective of the program. An engineering model TWT was tested to near specification limits of shock loading with a large degree of success. Specifications, such as power output, gain, noise figure, size, weight, temperature, and non-operating temperature, were met. Efficiency and input VSWR were not met on the deliverable device but can be met with relatively little additional effort. A number of additional specification items remain to be tested by the contracting agency, the Jet Propulsion Laboratory.

This report describes in detail the problems encountered in developing the TWTA with particular attention being devoted to the high impact requirement. Since the filter was furnished on a fixed-price basis by Rantec Corporation*, only the TWT development is described in detail in this report.

4. History. A brief historical review is presented here to describe the approach used to develop such a high impact device.

Initially it is difficult for the developer of a sophisticated device to comprehend the implication of a 10,000 G impact. It is not difficult to perform a few elementary calculations to determine the numbers. As an example, for the case of a uniform deceleration, the impact level is proportional to the velocity squared and inversely proportional to the deceleration distance. The engineering model TWT was impacted at 110 mph with a deceleration distance of 0.575 in. for an average level of 8500 G. To anyone who has not seen and heard such an impact, it is difficult to get a "feel" for the problem - to become calibrated at these impact levels. However, take the familiar example of an automobile traveling at 110 mph impacted against a concrete wall. The deceleration distance (displacement of the front end) is 4 to 6 feet, or less than 1/100th of the TWT impact level. It is not difficult to get calibrated in these terms.

* Rantec Corporation, Division of Emerson Electric, Calabasas, California

A thorough mathemetical analysis of the dynamics of a 10,000 G, 1.0 ms shock pulse is impractical for such a device as a TWT which may use over 200 separate parts in some 45 assemblies. Such an analysis would have to consider the frequency domain response of the pulse and the corresponding response of the assembly under test. However, it is reasonable to assume since the peak loading is at $\omega = 0$ (D.C. or static acceleration), a static analysis is quite appropriate with firm consideration given to the lower resonant frequencies.

Using this approach for the initial design, parts, materials, and interfaces were designed to withstand the forces experienced during a constant deceleration of 10,000 G with allowance for adequate safety margin.

With the initial design, key units were tested under statically loaded conditions to check the calculations. However, at this point further design changes were principally determined by the empirical approach based on high impact tests.

The development effort progressed from key parts, to minor subassemblies to major subassemblies, to the completed tube. Using this approach, the design of progressively larger elements of the TWT could be certified as acceptable. In this manner, the specific damage could be analyzed in order to isolate the cause of the failure, whether materials, interface, design or geometry. If complete assemblies were tested at high levels at the start of the program, the problems/failures could not be adequately separated, identified, and corrected.

SECTION II

END ITEM AMPLIFIER

A. DESCRIPTION OF THE END ITEM (PROTOTYPE) AMPLIFIER

The prototype amplifier consists of two RF components: 1) traveling-wave tube amplifier, and 2) a combined band reject and harmonic filter. An integrated TWTA which includes the power supply, housing, and related hardware has not been defined at this time. Without a definition of the interfaces between the two RF components, the impact development portion of the program has been restricted to determining the shock capability of the separate devices.

The TWT, Watkins-Johnson Company Model WJ-398, is a medium-power, periodic-permanent-magnet focused tube which utilizes metal-ceramic construction throughout. The tube weighs 3.12 pounds, with a total containment volume of 60 cubic inches and a long axis dimension of 11 inches. A photograph of the prototype model TWT is shown in Fig. 1.

The RF filter, Rantec Corporation Model FS-607, combines both a band reject and low pass filter in a common package. The filter weighs 0.53 ounces, with a total containment volume of 12.7 cubic inches and a long axis dimension of 6.75 inches. A photograph of the prototype model filter is shown in Fig. 2.

B. PERFORMANCE OF THE AMPLIFIER

The principal acceptance test results for the TWT and filter are shown in Table I. The complete Watkins-Johnson Company acceptance test results, as well as the test sequence are shown in Appendix I. Additional acceptance testing will be conducted by the contracting agency at the Jet Propulsion Laboratory; therefore, complete test results are not available at this time.

Table II shows the performance of the prototype amplifier with respect to the specification requirements.

C. DESCRIPTION OF THE TRAVELING WAVE TUBE

1. Performance of the TWT. The broadband performance characteristics of RF power output, saturation gain, and beam and overall efficiency for the TWT are shown in Fig. 3. As shown, the saturation power output is greater than
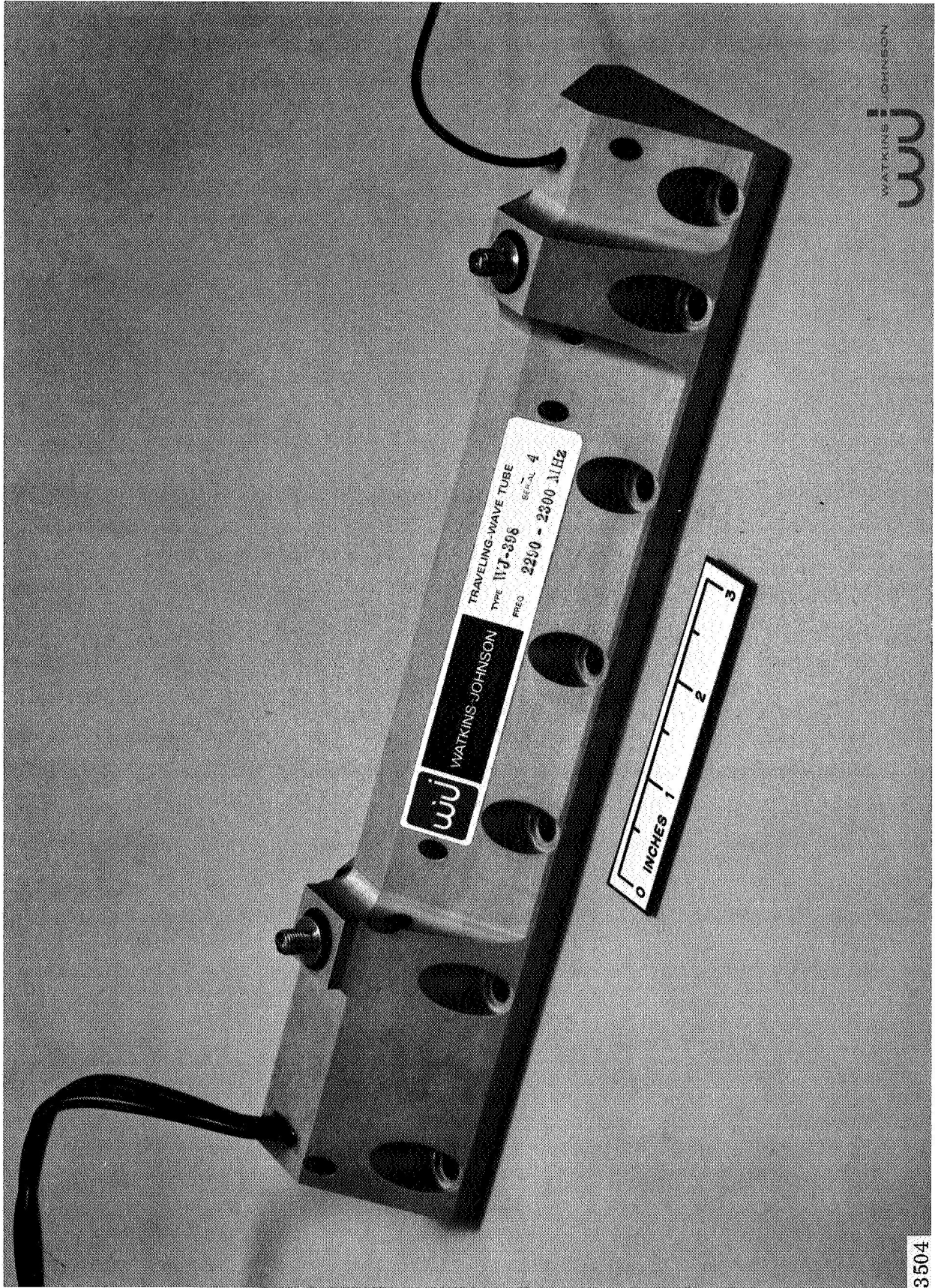
Fig. 1 – Photograph of the prototype model WJ-398 TWT.
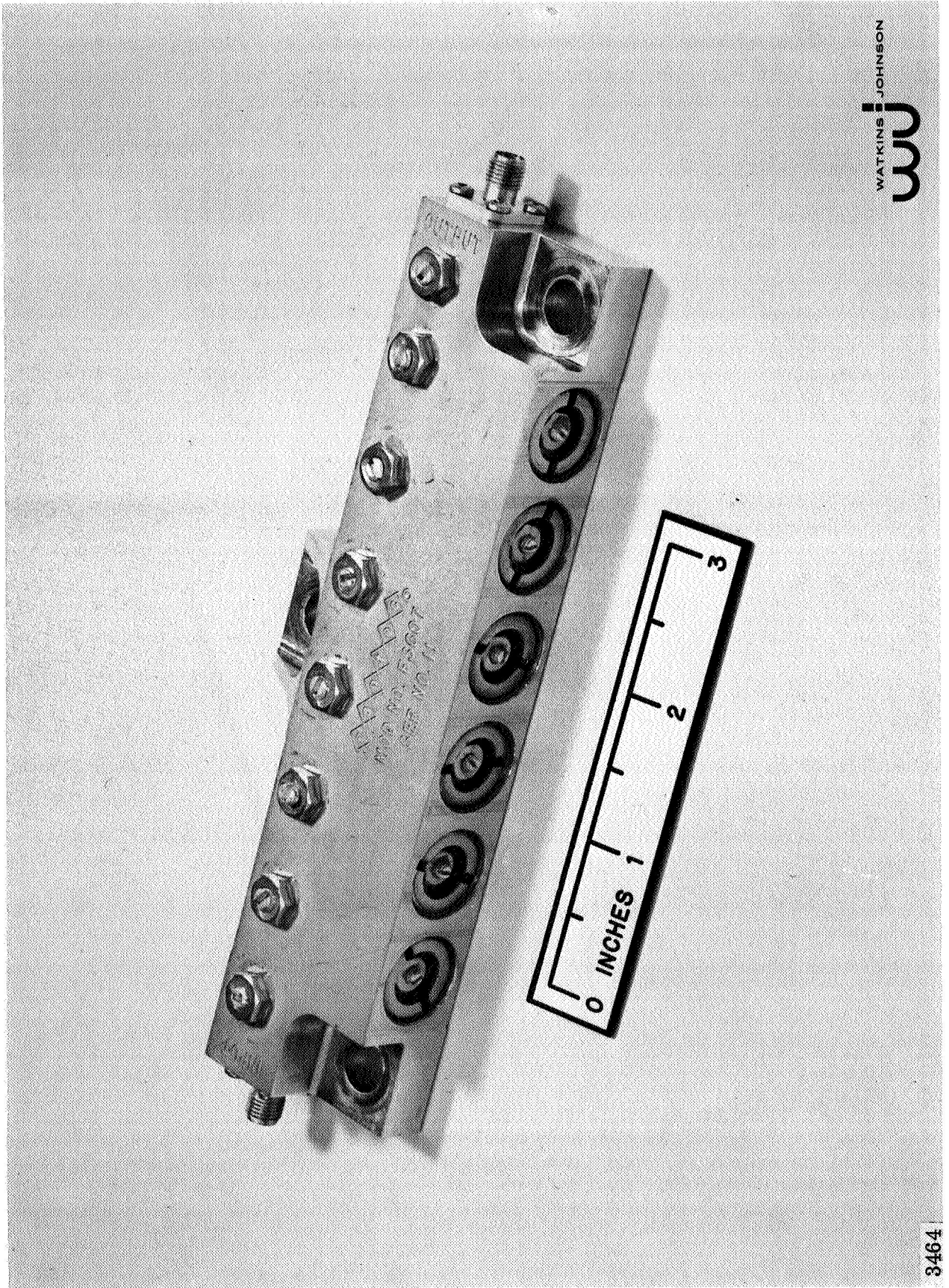
Fig. 2 – Photograph of the Rantec Corporation model FS-607 band reject and harmonic filter.

TABLE I

END ITEM TWT AND FILTER * FINAL PERFORMANCE RESULTS

Frequency	2300 MHz
Power Output	21.85 watts
RF Drive	2.25 dBm (41.24 dB gain)
Primary Power	75.19 watts (29.1% efficiency)
Operating Input VSWR	1.30:1 (1.45 max.)
Minimum Power Output with 5:1 Load	42.9 dBm
Small Signal Noise Figure	23.6 dB

Weight:

TWT	3.12 lbs.
Filter	0.53 lbs.
Total	3.65 lbs.

* WJ-398 S/N 4 traveling-wave tube and Rantec FS-607 S/N 11 band reject and harmonic filter.

TABLE II

SPECIFICATION AND ACHIEVED PERFORMANCE

Parameter	Specification Value*	Measured Value
Frequency range	2290 - 2300 MHz	Specification met
Power Output at Sat., CW	20 watts min.	Specification met
RF Input at Sat.	18 dBm max.	Specification met, 2.25 dBm
Input power (primary)	60 watts max.	75.19 watts
Short term stability	0.4 dB max. peak-peak variation in sat. gain within bandwidth DC-50 KHz	To be evaluated at JPL
Long term stability	0.5 dB max. decrease in sat. gain over 20,000 hrs.	To be evaluated at JPL
Operating input VSWR	1.2:1 max.	1.45:1 max.
Load VSWR	5:1 without instability or degradation of life of tube. Incident RF output power shall be plus 42 dBm min.	Specification met 42.9 dBm min. power output
Modulation bandwidth	0.3 dB max. variation of the phase modulation sidebands as the frequency of the modulating signal is varied from 10 Hz to 5 MHz with constant mod. index	To be evaluated at JPL
Phase jitter	12° peak to peak max. during vibration: 30° max. peak to peak during shock	To be evaluated at JPL
Noise figure	35 dB max.	Specification met, 23.6 dB
Harmonic outputs	30 dB below carrier	To be evaluated at JPL
Spurious output	- 155 dBm in any 20 Hz band between 2.108 GHz and 2.128 GHz	To be evaluated at JPL
Magnetic leakage	5 gamma max. measured at a distance of 3 feet	To be evaluated at JPL
Design Operating Life	20,000 hours	To be evaluated at JPL

TABLE II (Continued)

Parameter	Specification Value*	Measured Value
Changing magnetic field	1/2 gamma max. variation at rate less than 60 cps measured at distance of 3 feet	To be evaluated at JPL
Weight	4.5 pounds max.	Specification met, 3.65 lbs.
Packaging:		
RF connector	OSM jack	Specification met
DC power connection	12 inch flying leads	Specification met
Volume	Contained within rectangular box of 250 cu. in., max. length of box less than 14 inches	Specification met, 242 cu. in., 11 in. long
Sterilization condition	Non-operating: 3 cycles consisting of 145° C storage for period of 36 hours	Specification met
Critical Environments: **		
Temperature	-10° C to $+75^o$ C	Specification met
High Impact	3 planes, 10,000 G, 1 ms duration	To be evaluated at JPL. Engr. model TWT tested to 9500 G with little change in performance. See Section III of this Report. Filter qualified to specification
Acceleration	$\pm$ 14 g, 3 axes, 5 min.	To be evaluated at JPL
Vibration		
Sine	$\pm$ 1.5 in., 1-4.4 cps 3 g peak from 4.4 to 15 cps	To be evaluated at JPL
Complex	14 g rms noise 18 sec. 5.0 g rms noise + 2.0 g rms sine, 15 – 40 cps 9.0 g rms sine, 40 – 2000 cps $\Big\rbrack$ 600 sec. 14 g rms noise 18 sec	To be evaluated at JPL

*   Jet Propulsion Laboratory Statement of Work, Contract 951287.

**   Per Jet Propulsion Laboratory Specification No. 30250B.
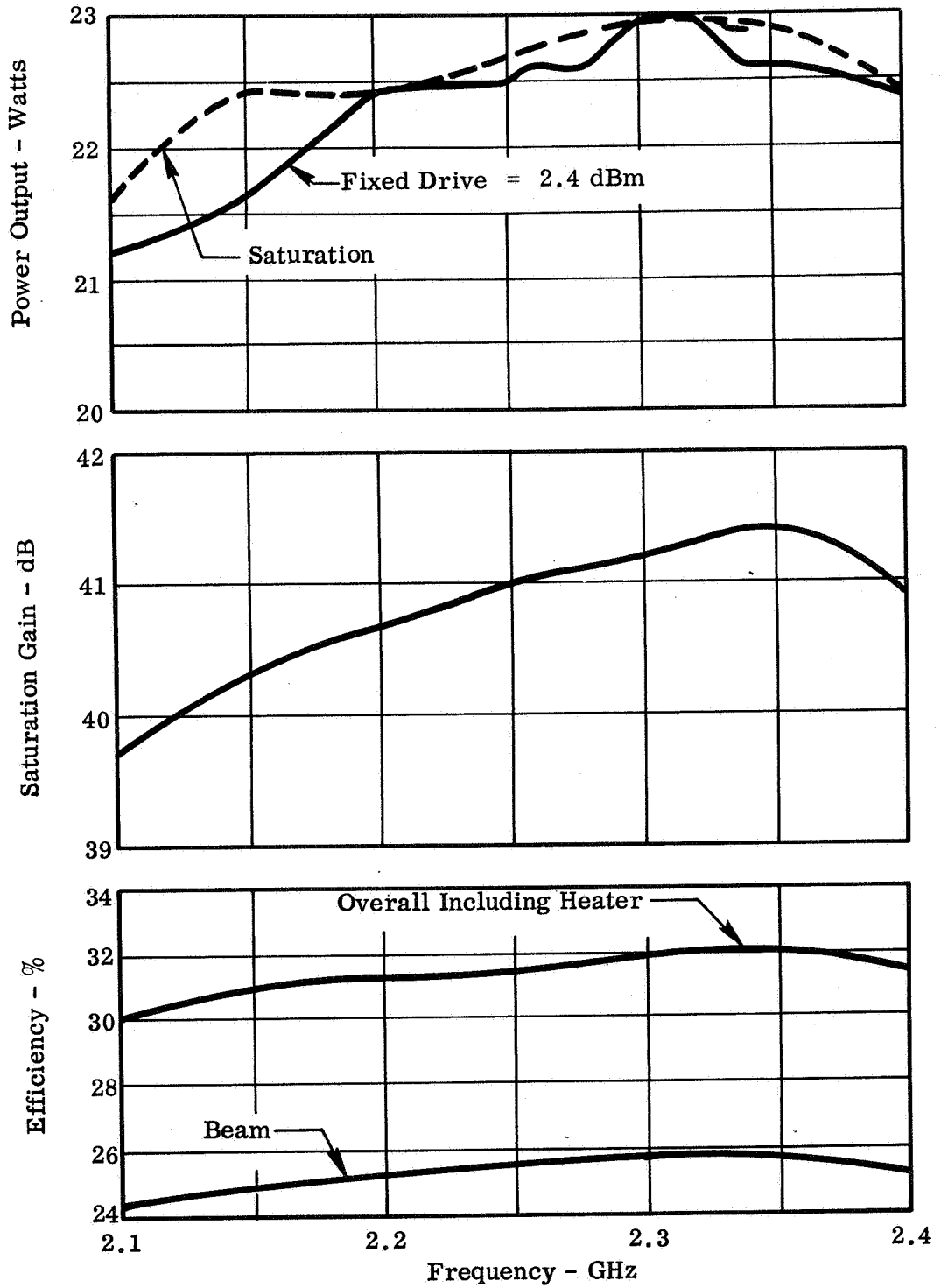
Fig. 3 –Performance characteristics of the WJ–398 S/N 4 traveling-wave tube.

21.6 watts over the frequency range from 2100 to 2400 MHz with 39.8 dB minimum gain and 30 percent minimum overall efficiency, including heater power. The beam efficiency is greater than 24 percent over the frequency range. Due to the mechanical design of the cathode structure for high impact capability, the heater power for this tube represents a significant percentage of the total primary power. Overall efficiency excluding heater power is 31.8 percent minimum.

The power transfer curve is shown in Fig. 4. It has the characteristic typical of a TWT operated in a high overvoltage condition where the saturation gain is greater than the small signal gain. The transfer characteristic has a broad plateau in power output with only a 0.5 dB decrease in power output for over 5.6 dB variation in drive level.

2. **TWT Design Parameters.** The parameters which describe the TWT design are listed in Table III.

3. **Physical Configuration.** A photograph of the encapsulated tube is shown in Fig. 1. The flying leads shown in Fig. 1 are the anode, cathode, heater, helix, and collector connections to the tube. RF terminals are OSM jack type connectors. The TWT is described in detail in the following paragraphs.

   a. **Mounting, Tube Capsule, and Encapsulation.** The outline drawing for the TWT is shown in Fig. 5. The outline shows the important external dimensions as well as the requirements for mounting the tube to the baseplate. The close fitting recess in the mounting plate provides the necessary support for the tube during impact in directions parallel to the baseplate. Impacts away from the mounting plate are provided for by the use of 14 high tensile strength 1/4 inch x 28 Titanium bolts. This mounting scheme does away with the need for matched machining of the baseplate and tube capsule – an intolerable situation from the standpoint of parts interchangeability.

   Fig. 6 shows a photograph of an encapsulated WJ-398 which has been machined in half to show the assembly details. The electron gun and RF input connector are shown on the right and beam collector and RF output on the left; not included in the photograph are the high voltage leads which thread through the capsule top at both ends.
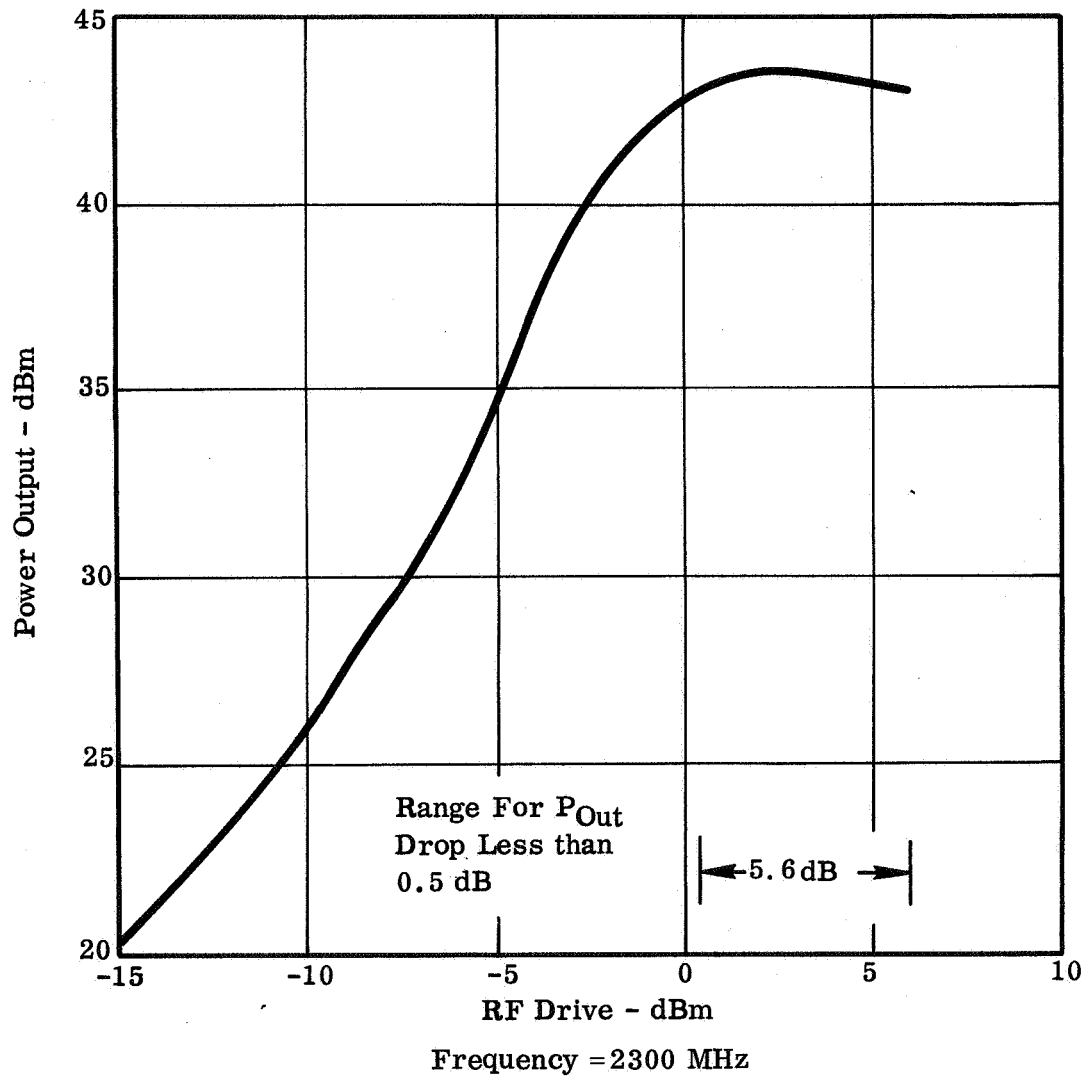
Fig. 4 - Transfer characteristics of the WJ-398 S/N 4 traveling-wave tube.

TABLE III

TABULATION OF TYPICAL WJ-398 DESIGN PARAMETERS

Frequency, f_o	2300 MHz
Normalized circuit phase velocity, v/c	0.0562
Helix pitch	60 TPI
Helix mean diameter, 2a	0.091 in.
Helix wire size	0.005 x 0.010 in. tape
Helix loss/wavelength, $L/\lambda g$	0.20 dB/wavelengths
Barrel I.D. to helix mean diameter ratio, c/a	1.76
Dielectric loading factor, DLF	0.766
Normalized helix radius, γa	0.99 radians
Beam to helix diameter ratio, b/a	0.41
Helix voltage, V_o	1487 volts
Cathode current, I_o	60 mA
Beam perveance, $\mathbb{P}_o$	1.05×10^{-6} pervs.
Beam current density, J_o	$8.5 A/cm^2$
Pierce gain parameter, C	0.122
Space charge parameter, QC	0.186
Interaction impedance, K	171.2 ohm
Velocity parameter, b	2.705

Electron Gun

Gun perveance, $\mathbb{P}$	0.69×10^{-6} pervs.
Cathode loading, J_c	$212 mA/cm^2$
Cathode diameter, $2r_c$	0.236 in.
Area convergence, A_c/A_b	13.5
Cathode half angle, θ	21°
Cathode radius of curvature, $\bar{r}_c$	0.329 in.

Focusing *

Magnet period, L	0.206 in.
Peak magnetic field, B_{pk}	980 gauss
r_1/L	0.449
r_2/r_1	1.95
R_1/L	0.49
R_2/R_1	2.06
d_1/L	0.208
d_2/L	0.403

*   J. E. Sterrett and H. Heffner, "The Design of Periodic Magnetic Focusing Structures," Trans. of PGED, vol. ED-5, no. 1, Jan., 1958, pp. 35-42.
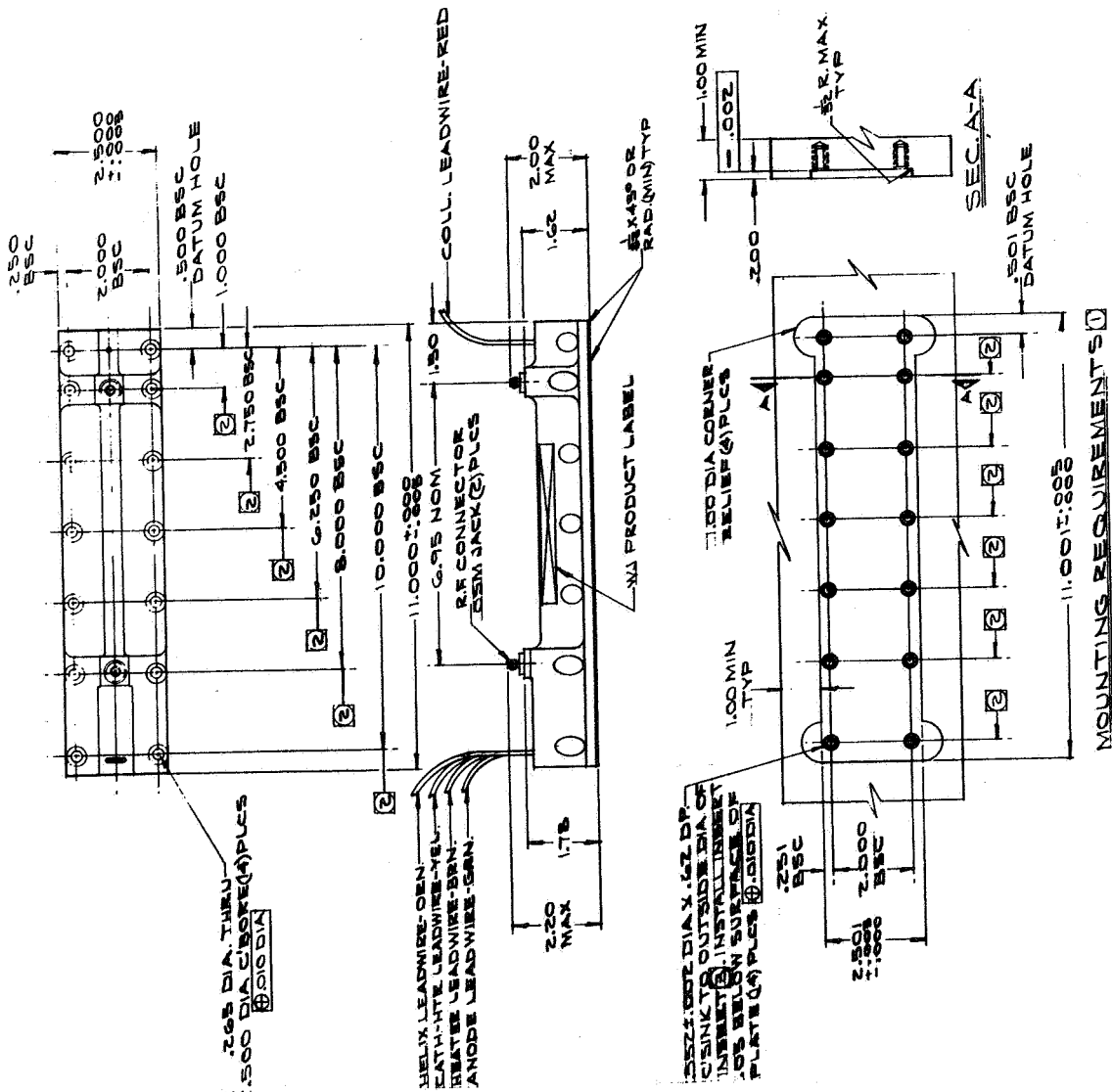
Fig. 5 – Outline drawing of the WJ-398 traveling-wave tube.
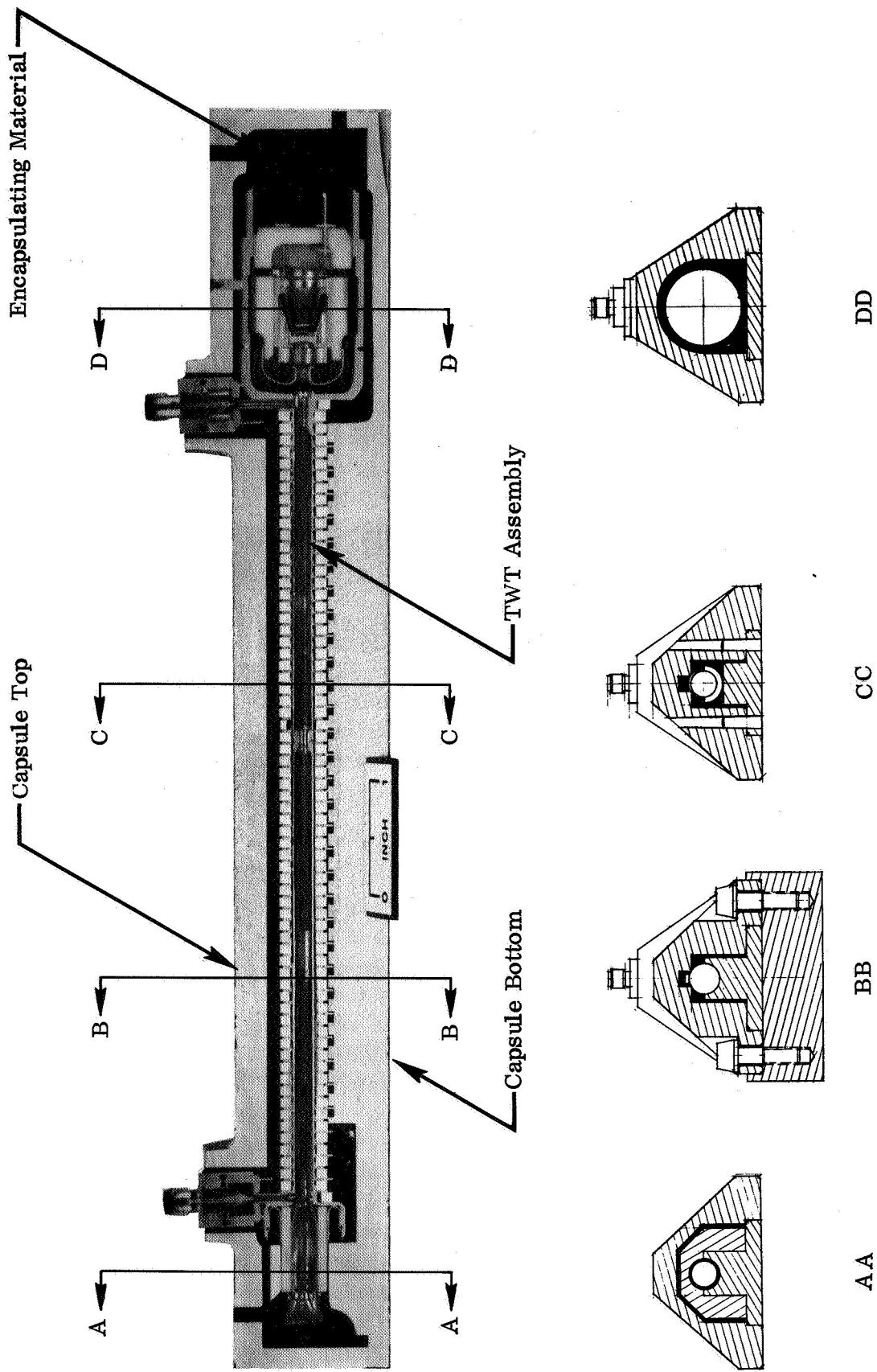
Fig. 6 – Photograph of an encapsulated WJ-398 TWT which has been machined in half to show assembly details. Also shown are section views of the assembly.

The tube is supported between the capsule halves with all gaps and voids filled with Stycast 2850GT, an epoxy casting resin. This material can fill voids and gaps as small as a few thousandths of an inch. The potting material has a low shear and tensile strength; however, its compression strength is high. The tube assembly is uniformly supported by the capsule and the potting material.

The magnets used to focus the electron beam are made from platinum cobalt magnetic material – a very dense material. Ordinarily if the TWT were impacted in the axial direction of the assembly, the combined weight of the magnets would be placed on the end pole piece. Such a stress could not be supported without damage to the tube. This difficulty is overcome by a series of ring shaped inserts which fit between the magnets and interlocking recesses in the capsule bottom. When the voids are potted with Stycast resin, the weight of the magnets is evenly distributed to the capsule.

A number of section views are also shown in Fig. 6. Section AA shows the encapsulation detail in the collector region. The TWT collector is mounted between the capsule bottom and an enclosing cap. The gap between the collector and capsule parts (a few mils) is potted with Dow Corning 850 silicone rubber. This material provides the needed heat transfer path and allows for any misalignment of capsule and tube parts due to machine tolerances.

Section BB shows the encapsulation detail of the TWT body. For clarity the mounting plate and tie down bolts have been included to show the support given to the assembly in all planes of shock. Note how the body of the TWT assembly is supported about its diameter – over the bottom half by the capsule, and over the top half by the capsule along two line contacts with the potting material completing the enclosure. The body cannot be supported directly by the capsule over the entire circumference due to the need for placing "magnet trimming shunts" along the focusing structure.

Section CC shows the details of the interlocking mechanism used to support the TWT focusing magnets. Also shown in Section CC are the taper pins used to unite the capsule halves. There are a total of 22 pins which are fitted in accurately matched machined holes in the capsule halves. This interlocking scheme prevents relative movement between the capsule halves. The taper pin method provides assurance of support about the entire diameter of the pin.

Section DD shows the detail about the electron gun area of the assembly.

A photograph of the capsule parts is shown in Fig. 7. Also shown in the photograph are samples of the mounting bolts, taper pins, and magnet support sleeves. The capsule parts are machined from 7075-T651 aluminum material which has been thermally stress relieved during machining. This material combines high strength and elongation with low density.

Fig. 8 shows a photograph of the TWT assembly, with magnets, mounted to the capsule bottom. The magnet support sleeves have not been mounted. In the foreground of Fig. 8 is the tube assembly as it appears prior to inserting magnets and encapsulation. The tube assembly is of all metal-ceramic construction and consists of the following three major regions: 1) Electron beam formation region, 2) interaction region including the RF coupling, slow wave, and beam focusing structure, and 3) the beam collecting region.

b.   Electron Gun. An expanded view of the electron gun of the tube is shown in Fig. 9. Also shown is the electron gun structure, the RF coupling and interaction geometry, and the PPM focusing array and details of the interlocking support scheme.

The electron gun consists of the cathode and its supporting structure, focusing electrode, and anode structure. The header provides the vacuum seal and high voltage lead throughs. Individual subassemblies of the electron gun are packaged as a series of tightly fitted concentric cylinders for support in the radial direction. The cathode structure is brazed to the inner diameter of the focus electrode which in turn fits tightly within the inner diameter of the anode supporting ceramic. The combination fits tightly within the inner diameter of the outer shell.

The structure is supported in the axial direction by a number of stepped bearing surfaces. The anode structure is held between the shoulders in the outer shell; and the focus electrode with the cathode structure brazed in place is inserted into the anode structure with the header assembly, which is seated against the back side of the focus electrode, completing the support.

With the exception of the supporting cones, the materials used throughout the gun structure are quite common to the vacuum tube industry. The cathode supporting cone is made from 0.003 inch Inconel 625 material, drawn into a frustrum of a cone. The heater lead cone is made from 0.002 inch Hastelloy alloy B material, also drawn into a frustrum of a cone.
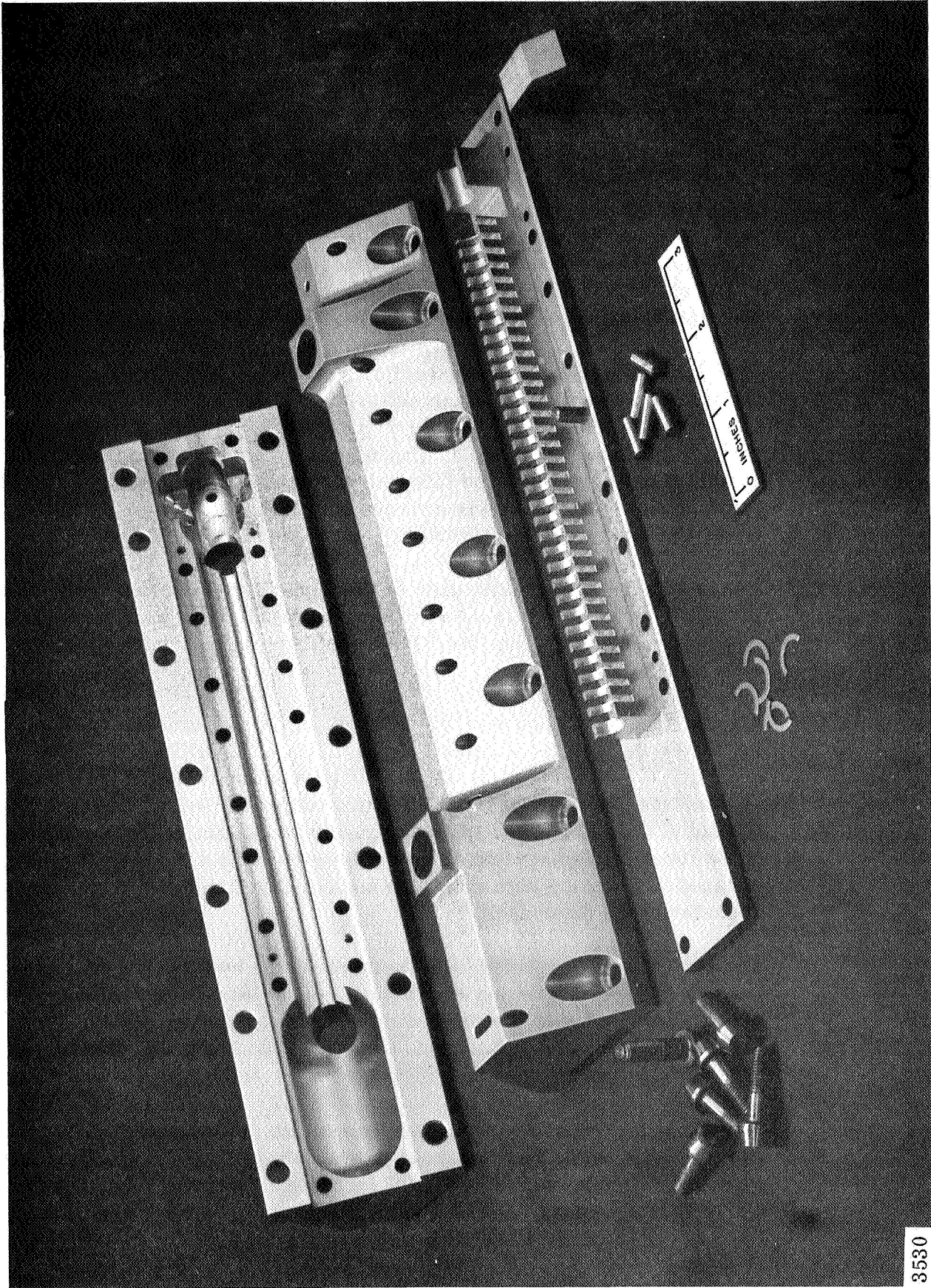
Fig. 7 – WJ-398 capsule parts. Also shown are samples of the Titanium mounting bolts, taper pins, and magnet support sleeves.

3530
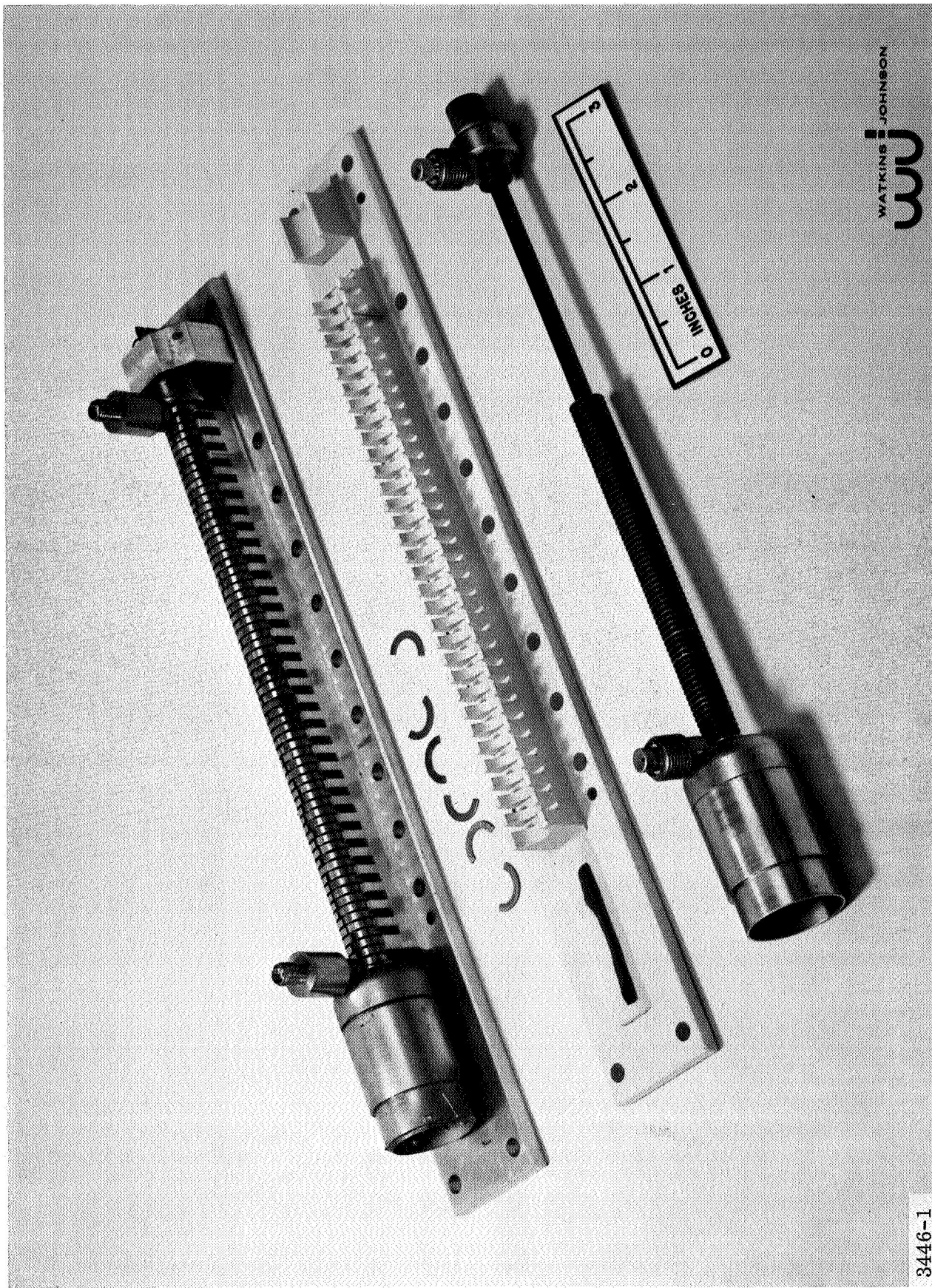
Fig. 8 – Photograph of the WJ-398 tube assembly mounted to the capsule bottom. In the foreground is the tube assembly without magnets.
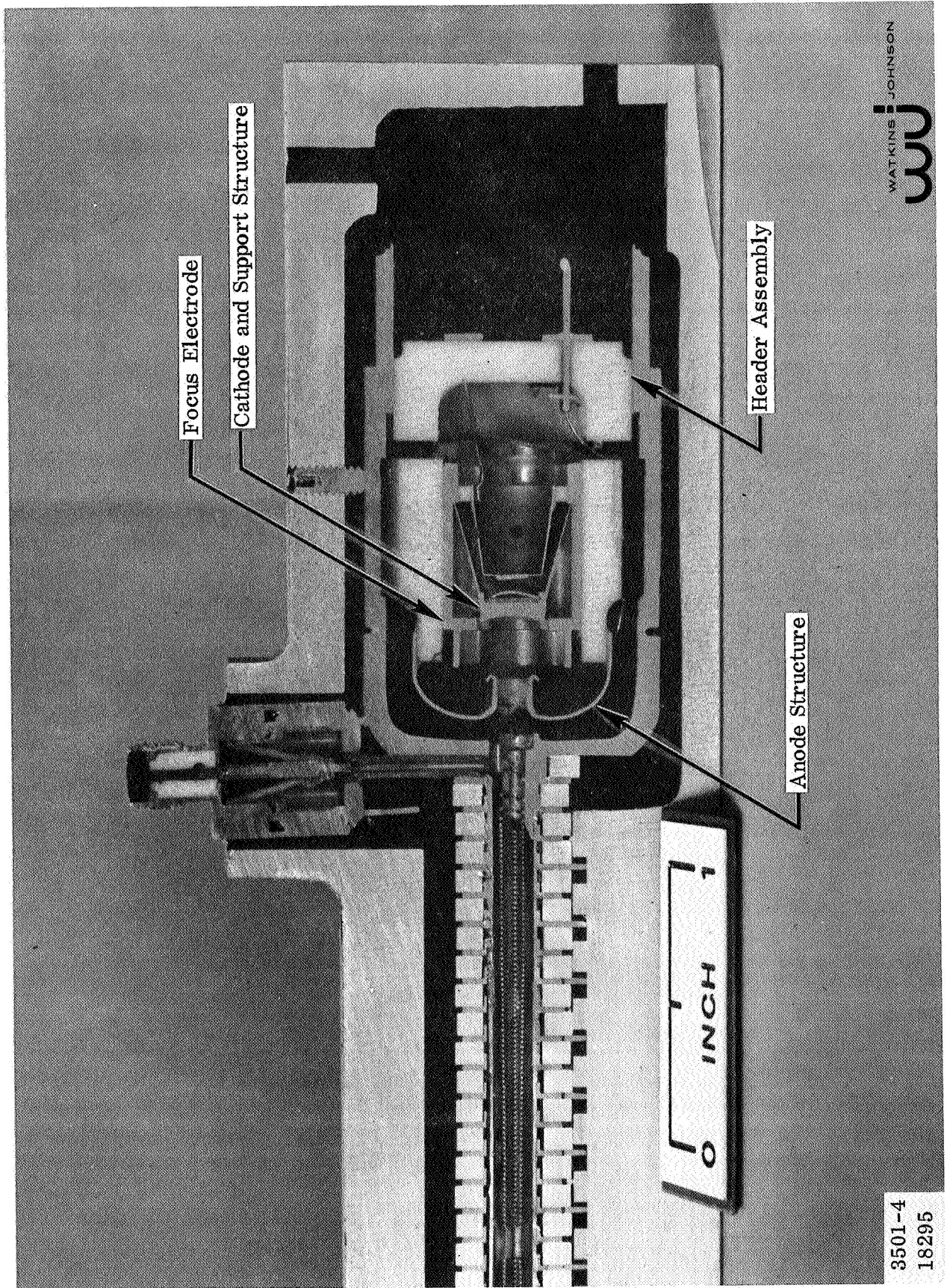
Fig. 9 – Photograph of a WJ-398 TWT machined apart to show the assembly details in the region of the electron gun.

Fig. 10 is an exploded view of the electron gun structure showing some of the individual piece parts and the major subassemblies. Notice the two flat surfaces on the anode ceramic. These flats are what are shown in section view in Fig. 9. A section view located 90 degrees from these flats would better show the enclosure of the ceramic by the shoulders in the outer shell. The anode electrode is made from relatively thin sheet material drawn to the dome shape shown in Fig. 10.

Fig. 11 shows the individual piece parts which make up the cathode and focus electrode assemblies.

The uncoated surface of the oxide coated cathode has been roughened by having fine nickel powder sintered to the surface. This "nickelated surface" is required for adherence of the coating during high impact loading.

c. TWT Body Assembly. The TWT Body Assembly houses the helix interaction circuit, the RF input and output couplers, and the beam focusing pole pieces. Fig. 12 is a sketch of the body assembly. Fig. 13 shows a breakdown of the body assembly with its component parts.

The input and output helix assemblies are made with 0.005 x 0.010 inch molybdenum tape which is glazed, turn by turn, to three beryllium oxide wedge shaped ceramic supports. After applying the attenuator coating to the severed ends of the helices, the helices are inserted into the body tubing, which has been deformed in a triangular manner to accept the larger helix assembly. The tubing is made from Hastelloy alloy C material, which retains its high strength at elevated temperatures, thus assuring the compressive forces on the helix assembly do not relax during the tube bakeout cycle.

The body tubing with the assembled circuits are brazed to their interfacing pole piece assembly, and the RF window and transmission line assemblies are brazed in place. The window-stripline subassembly can be seen in Fig. 13 just above the gun pole piece assembly. This assembly brazes directly into the threaded window cups, and the end of the stripline is spot-welded onto the end of the helix tape.

The RF stripline is supported by an outer conductor made from rectangular waveguide, which has been broached down its small side to accommodate the stripline ceramic supports. This geometry provides the needed transverse support for high impact.
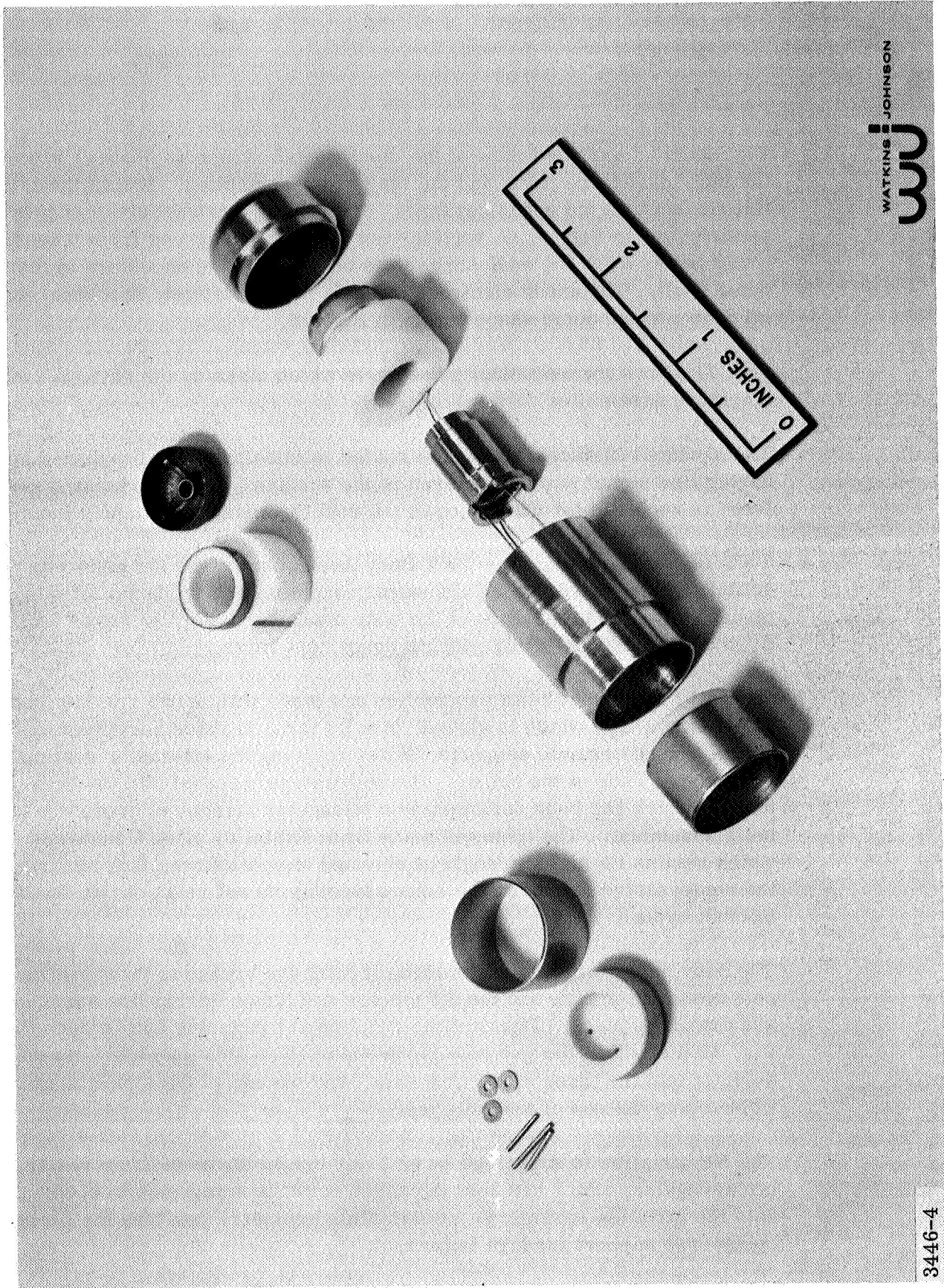
Fig. 10 – Photograph of the piece parts and subassemblies which make up the electron gun structure.

3446-4
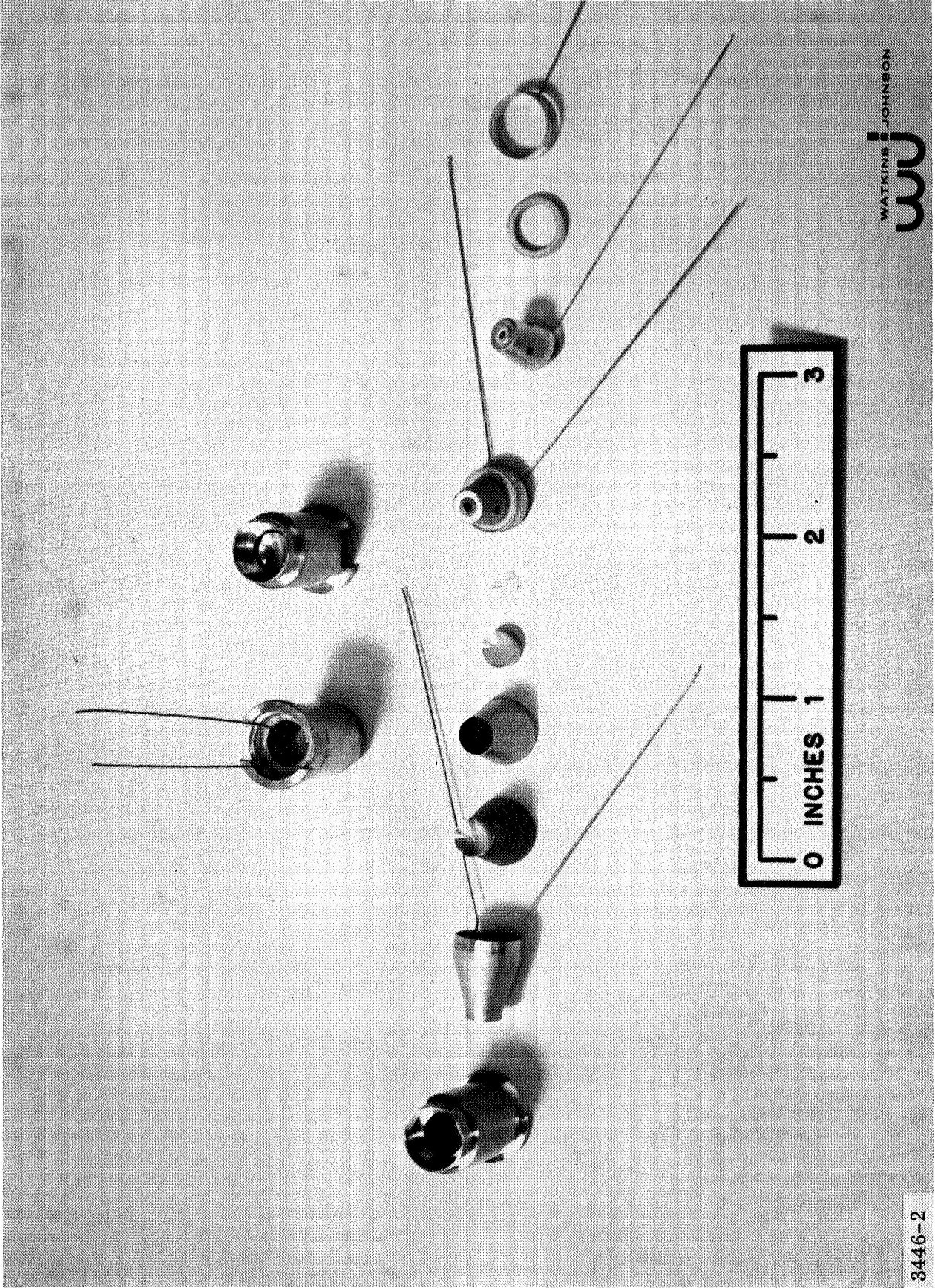
- 22 -

Fig. 11 - Photograph of the piece parts and subassemblies which make up the focus electrode assembly. In the back-ground is the completed focus electrode assembly. In the foreground, from right to left, the parts/assemblies are: the cathode - heater return, heater insulating ceramic, heater lead cone, completed heater lead assembly, heater, cathode, cathode support cone, cathode assembly, cathode support assembly, and focus electrode.
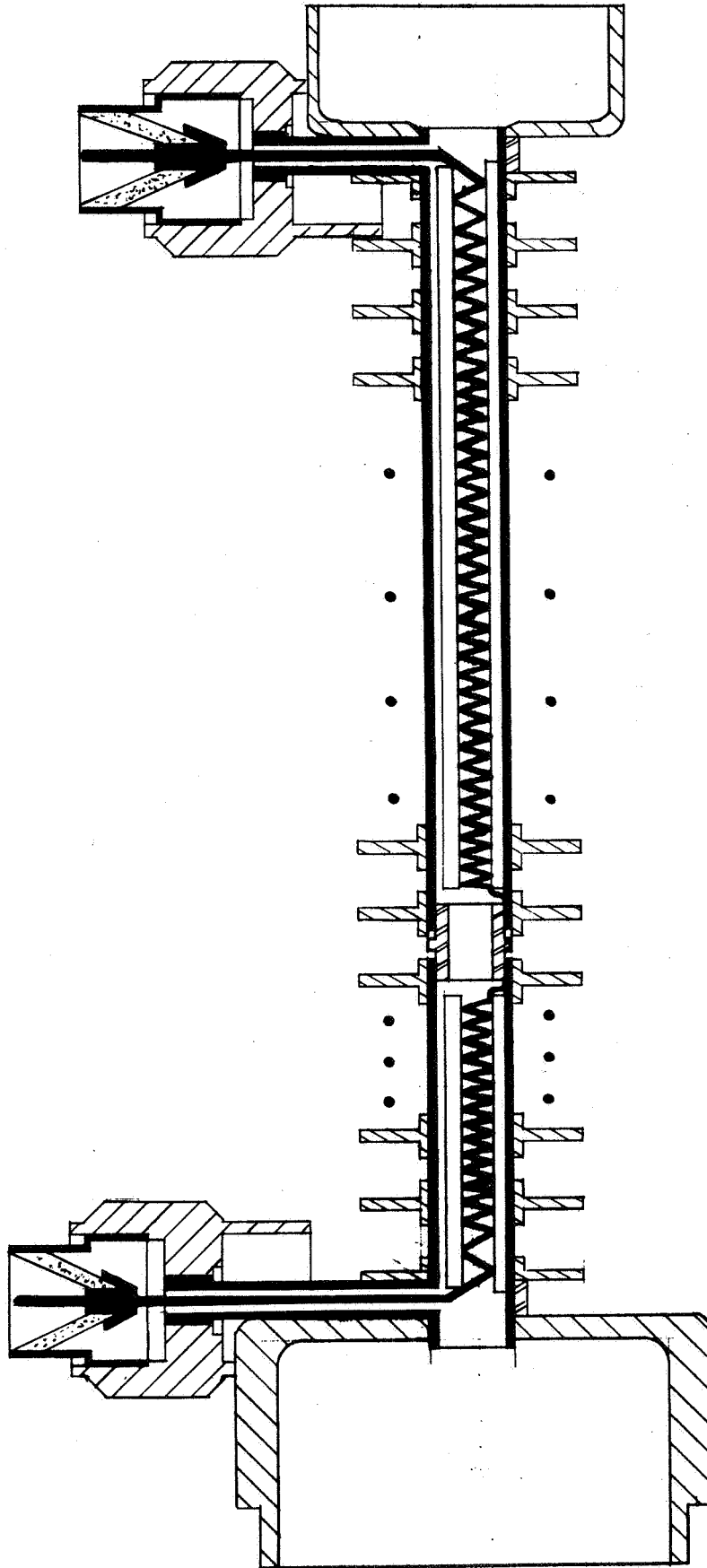
Fig. 12 – Sketch of the body assembly for the WJ-398 traveling-wave tube. From left to right are shown the interfacing gun pole piece, input RF coupler, input and output helix circuits with enclosing body and pole pieces, RF output coupler, and interfacing collector pole piece.

16654
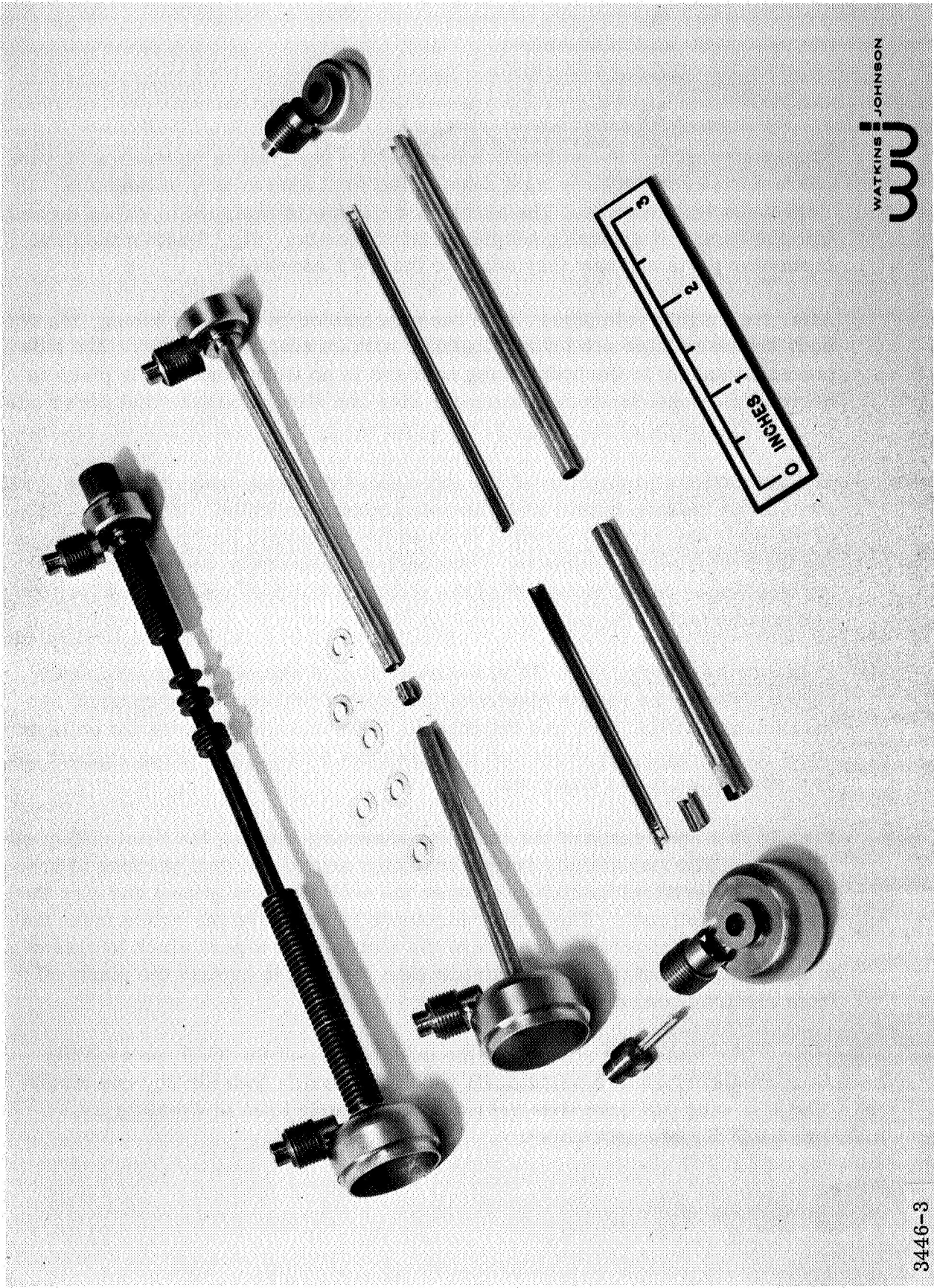
Fig. 13 – Photograph showing the body assembly and its component parts including strip transmission line and vacuum window. The helix is a glazed structure using three beryllium oxide wedges for dielectric support.

3446-3

The window-stripline combination is carefully designed to maintain a 50 ohm characteristic impedance right down to the first spread turn of the helix impedance transformer. The assembled window is designed to screw directly into the back of a specially adapted OSM connector. Fig. 9 shows the OSM connector parts and how they adapt to the TWT assembly.

After the magnet pole pieces have been assembled on the body tubing, the two body subassemblies are brazed together with an adapter cylinder. The pole pieces fit snugly to the body tubing so there is no tilting of the pole piece to degrade the beam focusing; however, they can slide to assure that the greater part of the weight of the magnets is supported by the capsule and not the tube.

Fig. 14 shows a photograph of the end view of the helix wedge assembly mounted in the tube barrel with the pole pieces assembled. The wedge shape of the helix supporting ceramics reduces the dielectric loading without degrading the heat transfer capability. The back surface of the wedge is a curved surface whose radius is less than the radius of the body tubing, thus insuring uniform contact to the tubing.

d. Collector Assembly. Fig. 15 is a view of Fig. 6 expanded in the collector region showing the copper electrode, the cylindrical insulating ceramic and the interface to the TWT and the capsule. The capsule encloses the collector about its diameter, as described in a previous section, providing support and heat conduction to the baseplate.

Fig. 16 is a photograph of the collector assembly showing the relationship of its parts. The metallized ceramic insulator serves the dual purpose of providing the electrical insulation between the collector and ground and also the heat conduction path. The copper electrode is brazed to the entire inner diameter of the ceramic. At the left of the electrode is a part which is brazed to the inner diameter of the electrode (See Fig. 15) to protect the pinch-off from electron bombardment.

4. Materials. The materials chosen for the manufacture of the TWT necessarily have to meet a number of requirements which are rarely found in any one material. The following list describes the principal criteria used in choosing the material (in order of importance):
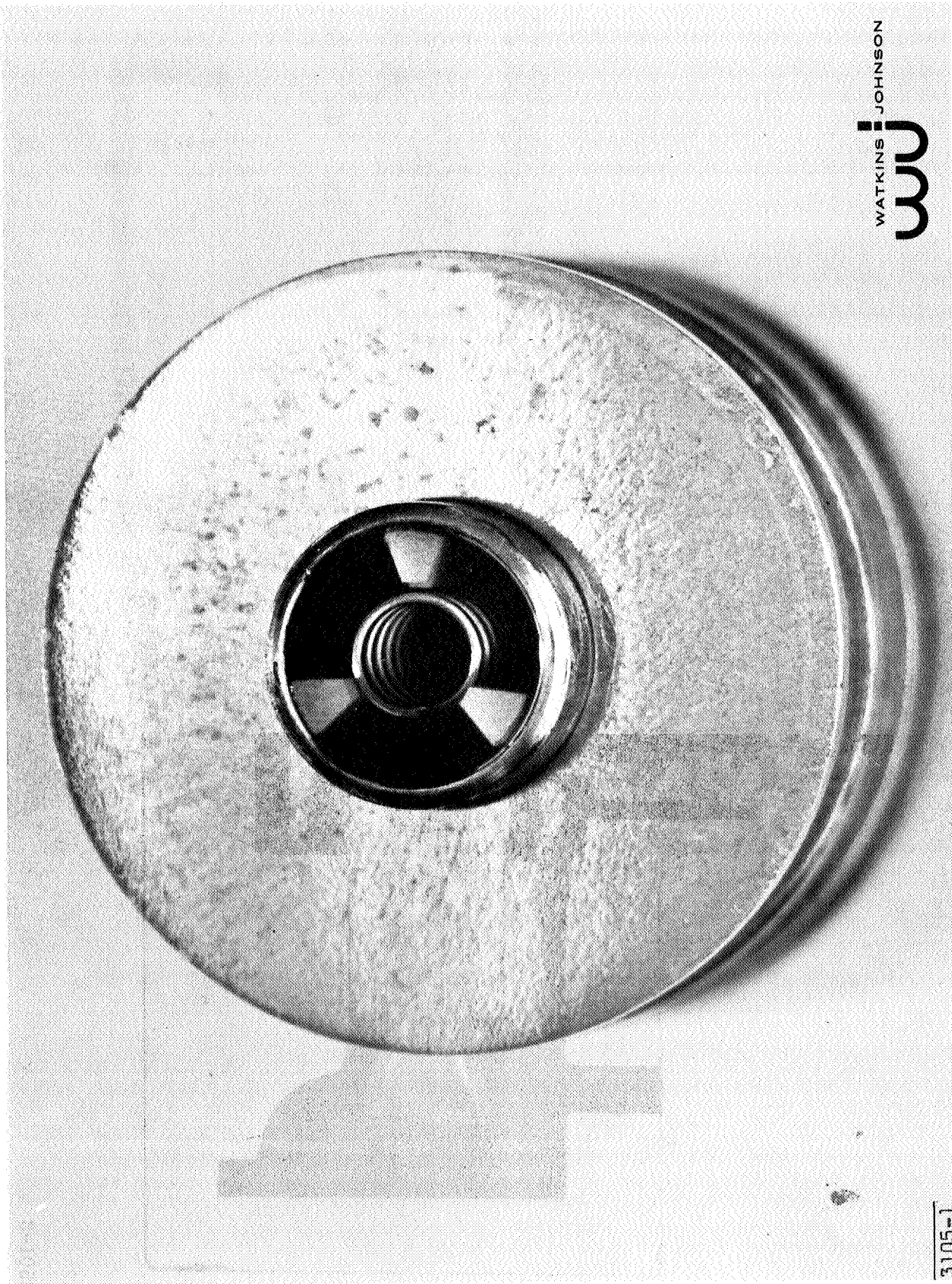
Fig. 14 – Photograph of end view of the helix-wedge assembly mounted in the tube barrel.

WATKINS–JOHNSON

3105–1
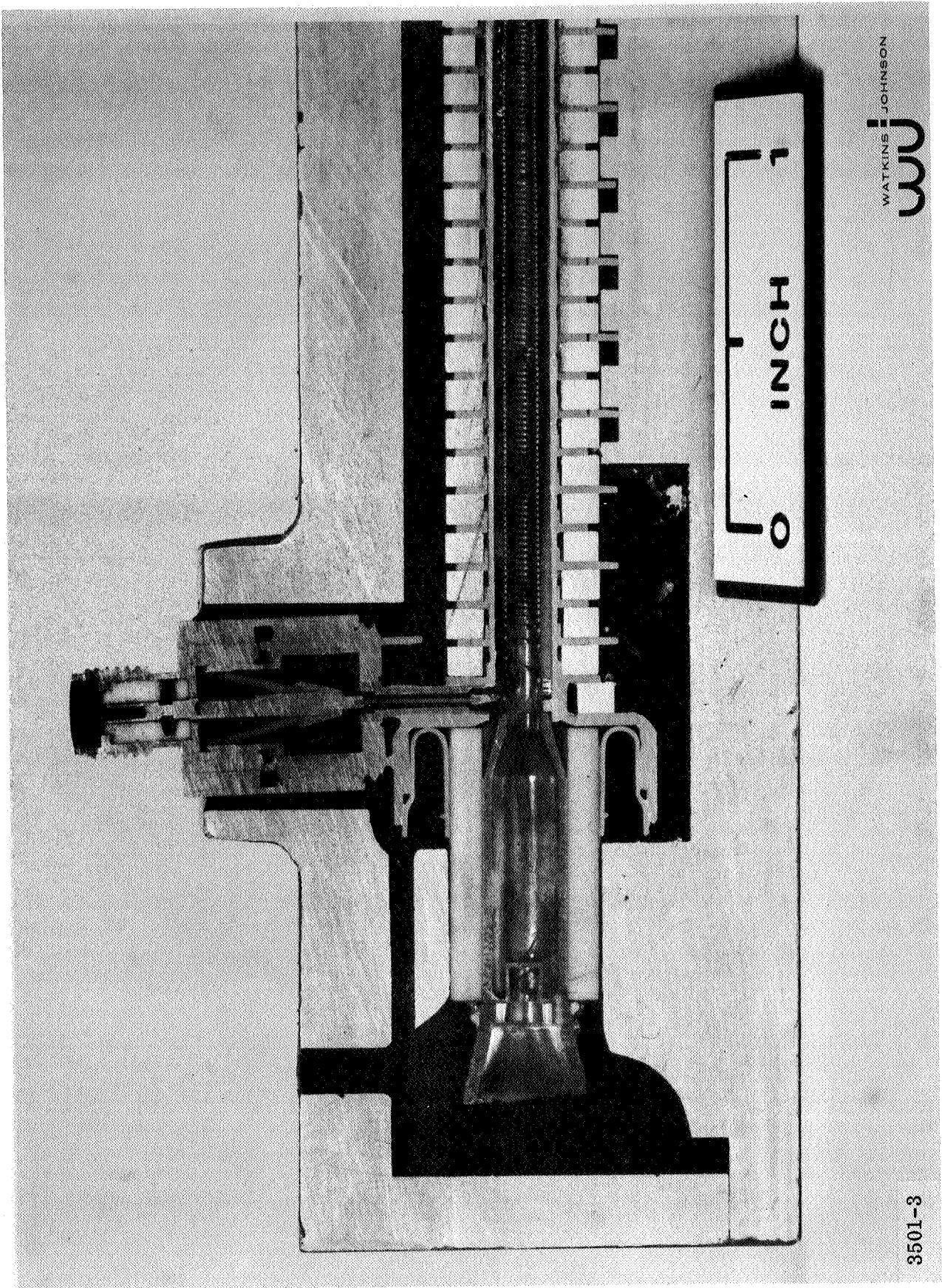
Fig. 15 – Photograph of a WJ–398 TWT cutaway model showing the assembly details in the region of the collector.

3501-3
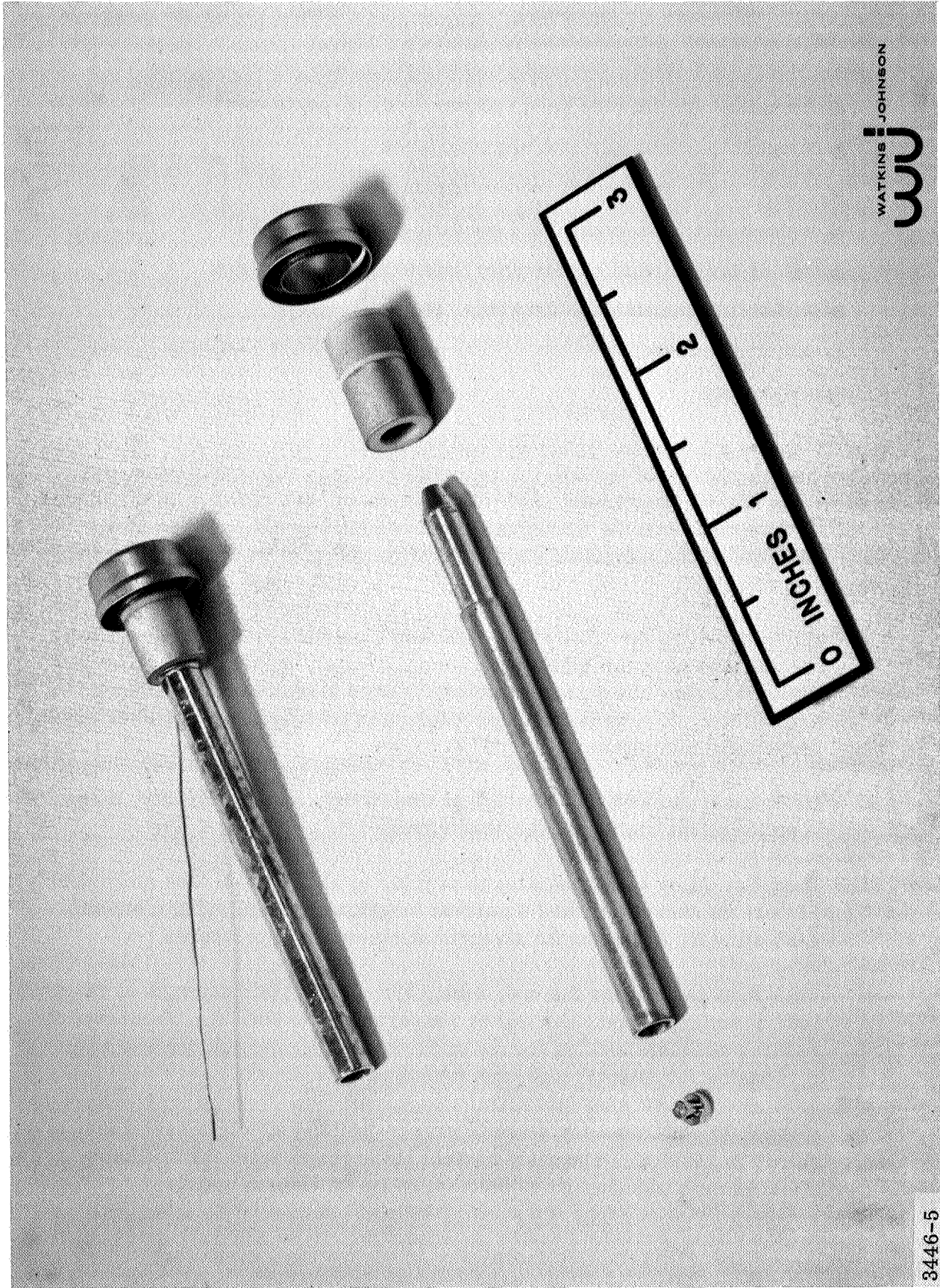
Fig. 16 – Photograph of the collector assembly and its component parts.

3446-5

- compatibility with tube hard vacuum (internal parts only)

- compatibility with surrounding interfaces

- high strength and impact loading capability

- compatibility with other TWT operating environments

- high or low thermal conductivity depending on application

- workability (machining, drawings etc.)

- cost and availability

- low density

Table IV shows a list of the materials used to manufacture the TWT. Also noted are the manufacturers of the special materials labeled. Materials used in the construction of the vacuum tube, with few exceptions, are common to the industry. The exceptions are the Hastelloy alloys and Inconel 625. These alloys along with a few of the materials used external to the tube warrant further discussion.

a. Hastelloy Alloy B. This alloy, which is used for the heater cone, is a nickel-base material alloyed with approximately 30 percent molybdenum, 5 percent iron, and 2 percent cobalt. Other elements include chromium and silicon. It retains a high percentage of its tensile and yield strength at elevated temperatures to 700° C.

Its thermal conductivity, electrical resistivity, and drawability, make it an excellent choice for the heater cone.

b. Hastelloy Alloy C. This alloy is similar to alloy B with less molybdenum, 15 percent chromium, and 4 percent tungsten as the alloying elements. Like alloy B, it retains its strength at elevated temperatures.

This alloy is used for the body tubing where high yield strength is required both at ambient conditions and at temperatures to 600° C. This property assures adequate locking forces on the helix assembly during and after processing the tube through high temperature bakeout.

c. Inconel 625. This alloy exhibits great strength and toughness at temperatures to 1100º C. The alloy derives its strength from the stiffening effect of molybdenum and columbium on its chromium matrix.

TABLE IV

SUMMARY OF RAW MATERIALS USED IN THE WJ-398 TRAVELING-WAVE TUBE

Internal to the Vacuum Wall

Aluminum Oxide Ceramic, 94 and 98 percent Al_2O_3
Beryllium Oxide Ceramic, 96 percent BeO
Braze Alloys: (OFHC Copper, Gold, Nickel, Silver)
Hastelloy Alloy B (1)
Hastelloy Alloy C (1)
Inconel Alloy 625 (2)
Kovar
Molybdenum
Monel, 404
Nickel
OFHC Copper
Platinum
Stainless Steel, 305
Tungsten / 3 percent Rhenium Alloy

External to the Vacuum Wall

Aluminum: 6061 T6
           7075 T651

Braze Alloys
Beryllium Copper
Copper, OFHC
Epoxy, 220
Hyperco 27 (3)
Kovar
Leadwire: (4) Tin Coated Copper
                Radiation crosslinked Polyalkene and
                radiation crosslinked Polyvinylidene Fluoride
                covering

Molybdenum
Monel, 404
Nickel, Grade A
Platinum-Cobalt Alloy
Shrink Tubing
Silastic, 850 RTV Silicone Rubber (5)
Solder, SnPb 60/40
Stainless Steel, 300 Series
Stycast 2850 GT (6)
Teflon

NOTES:

(1) Nickel-base molybdenum/iron and molybdenum/chromium alloys manufactured by the Stellite Division of Union
     Carbide Corporation, Kokomo, Indiana.

(2) Nickel-base molybdenum/chromium alloy manufactured by Huntington Alloy Products Division of International
     Nickel Company, Inc., Huntington, West Virginia.

(3) Iron-base, cobalt alloy magnetic material manufactured by Materials Manufacturing Division of Westinghouse
     Electric Corporation, Blairsville, Pennsylvania.

(4) High voltage lead wire for space use manufactured by Raychem Corporation, Redwood City, California.

(5) Silicone rubber encapsulant manufactured by Engineering Products Division of Dow Corning Corp., Midland, Michigan.

(6) Epoxy casting resin manufactured by Emerson and Cumming, Incorporated, Gardena, California.

Like the Hastelloy alloys, Inconel 625 retains its strength at elevated temperatures; however, it is not an age hardenable material like the Hastelloys. This means it can retain its high temperature strength after thousands of hours at temperature. Age hardenable materials initially increase their strength properties with time at temperature. However, after 50 to 100 hours the strength may peak and begin to degrade.

Inconel 625 has a slightly lower thermal conductivity than the Hastelloys, thus adding to its preferred use for the cathode support cone.

d. **D. C. 850 Silastic Rubber.** D. C. 850 is a low viscosity material which has good dielectric properties, use temperature to 250° C, and has very little shrinkage during curing.

The material meets the requirements of its application as the encapsulant used in the TWT collector area.

e. **Stycast 2850 GT.** This casting resin has excellent high temperature properties, high thermal conductivity, good adhesion to a wide range of materials, low thermal expansion coefficient, and low shrinkage during cure. In addition, it provides excellent rigidity and strength. Stycast 2850 GT is an excellent material for the varied requirements of a high impact TWT.

D. DESCRIPTION OF THE FILTER

1. Procurement. Watkins-Johnson Company subcontracted the development program to the Rantec Corporation for the output filter. They had previously developed a filter that met similar performance requirements but which had not been designed to meet the shock requirements. The filter development program consisted of an electrical and mechanical redesign, so that an insertion loss of 0.5 dB or less could be maintained while meeting the 10,000 G shock requirement.

   The subcontract Specification and Statement of Work are shown in Appendix II.

2. Performance of the Filter. The unit delivered to Watkins-Johnson Company was the FS-607 S/N 11 filter. Prior to shipment to Watkins-Johnson Company, the filter was shock tested at the Jet Propulsion Laboratory to the qualification level of 10,000 G. Fig. 2 shows a photograph of the unit after qualification tests.

Fig. 17 shows the post shock test VSWR, insertion loss, and stop band atten-
uation data for the filter. Fig. 18 shows the fine spectrum response for the
item.

The complete Rantec Corporation Final Report, including Acceptance and
Qualification Test results, is shown in Appendix III.

3. Physical Configuration and General Design Aspects of the Filter. Fig. 19
   shows an outline drawing of the filter. The unit weighs less than 0.53 pounds
   and has a containment volume of less than 12.7 sq. in. As shown in Fig. 19,
   the mounting method and requirements are similar to those of the TWT.

   The filter is a combined low pass and band reject filter. The equivalent cir-
   cuit for the combined filter is shown in Fig. 20. It has seven (7) low pass
   π sections and six (6) rejection resonators. Fig. 21 shows a radiograph of
   the unit showing the physical configuration of the low pass sections and the
   rejection resonators. Lockable tuning screws are used to optimize the per-
   formance.

4. Materials. A summary of the raw materials used in the manufacture of the
   filter is shown in Table V. The materials used differ little from those listed
   for the TWT.

PERFORMANCE TEST REPORT

FOR THE FS-607

HIGH IMPACT BAND REJECT HARMONIC FILTER

Post Qual. Test

Rantec Model No. FS-607

Customer Watkins Johnson

Customer Part No. _____

Project No. 66245

Serial No. 11

Specification No. 120090

NAME OF TEST	FREQUENCY IN MC											
	2103.0	2118.0	2128.0	2290.0	2295.0	2300.0	4580.0	4600.0	6870.0	6900.0	9160.0	10,000.0 *9,200 mc*
VSWR 1.2:1 Max.				1.06:1	1.06:1	1.06:1						
INSERTION LOSS 0.5 db Max				0.25	0.25	0.25						
STOP BAND ATTENUATION	86db min >95	86db min >95	86db min >95				20db min >30	20db min >30	12db min >20	12db min >20	5db min >20	5db min >20

TESTED BY _[signature]_   QC STAMP _[signature]_   DATE 10-26-66

RANTEC CORPORATION
CALABASAS, CALIFORNIA

TR-3

Fig. 17 – Reproduction of the Rantec Corp. qualification performance test results.

- 34 -

FS-607 SPECTRUM RESPONSE
S/N 11

Frequency-GHz	Insertion Loss db	Frequency-GHz	Insertion Loss db
2.000	20	3.160	40
2.075	86	3.280	50
2.148	86	3.540	60
2.180	30	3.580	80
2.187	20	3.730	70
2.192	10	3.800	80
2.236	1.0	5.400	80
2.270	0.5	5.480	50
2.290	0.25	5.625	25
2.300	0.25	5.660	50
2.397	0.5	5.670	80
2.420	0.6	6.950	80
2.465	0.3	6.970	50
2.520	0.7	7.060	10.5
2.580	0.3	7.160	50
2.680	2.7	7.280	80
2.760	0.4	9.280	80
2.790	3.0	9.500	8.0
2.815	10	10.500	8.0
2.910	20	11.000	80
3.010	30		

Fig. 18 - Reproduction of the Rantec Corp. qualification spectrum response test results.

TR-11

Fig. 19 – Outline drawing of the Rantec Corp. FS–607 low pass and band reject filter.

Seven Low Pass π Section

Six Rejection Resonators
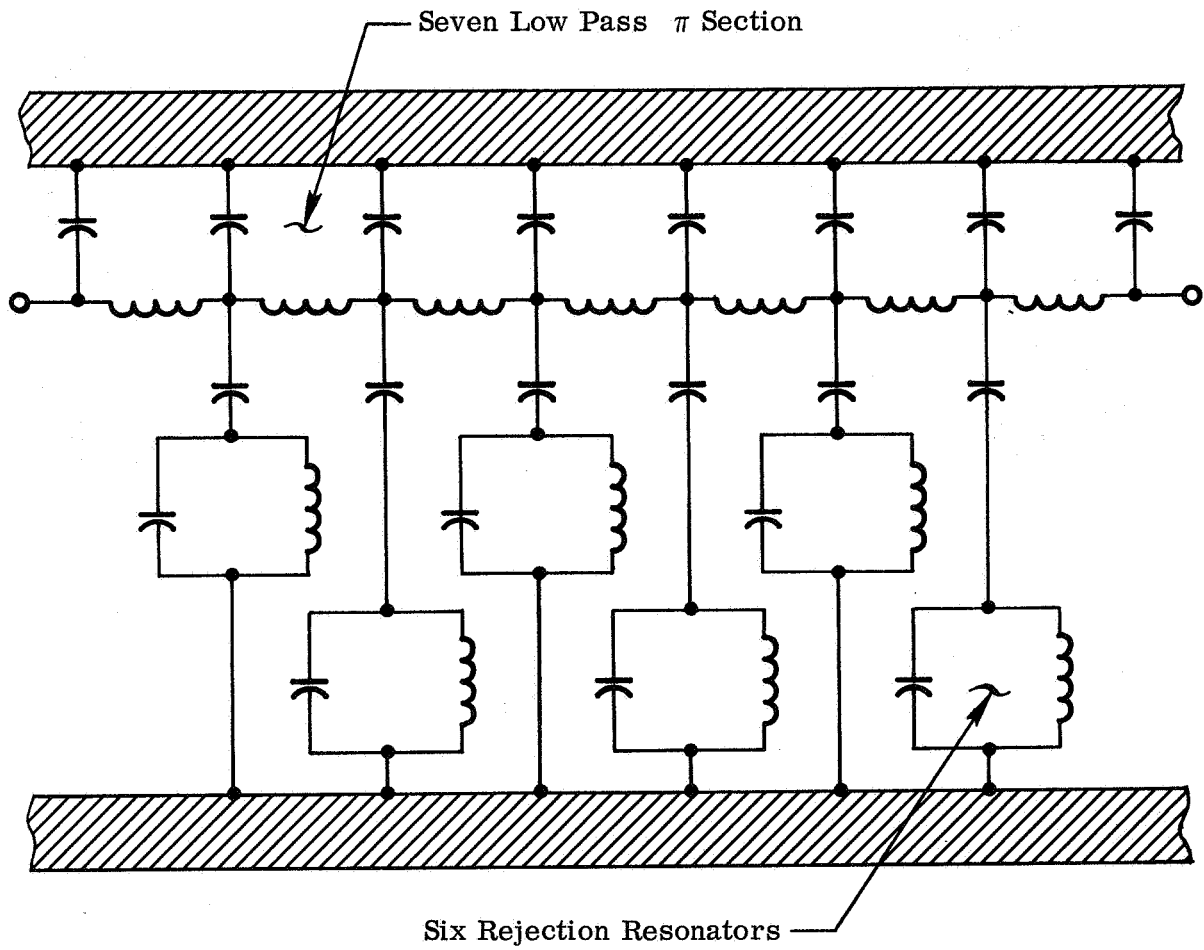
Fig. 20 - Equivalent circuit for the FS-607 low pass and band reject filter.

a) Side View
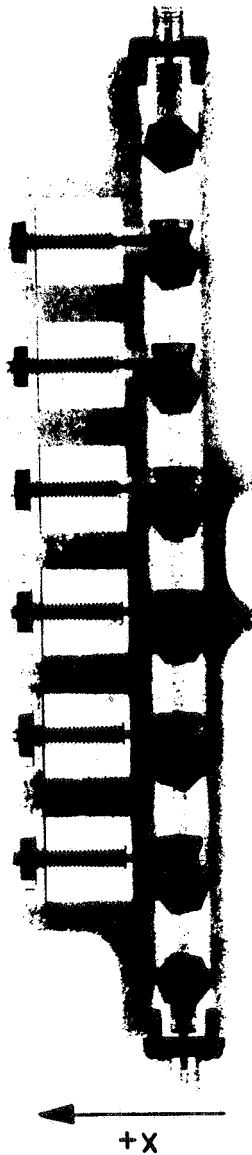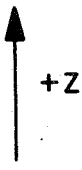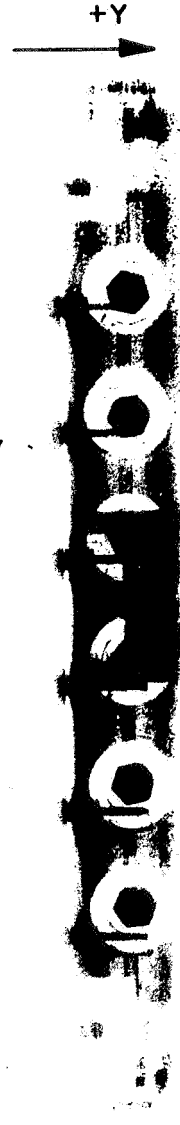
b) Top View

Rantec FS-607 Filter Qualification Model
After High Impact - 25 October 1966

CALABASAS, CALIFORNIA

TR-9

Fig. 21 - Radiograph of the filter.

TABLE V

SUMMARY OF RAW MATERIALS USED FOR THE RF FILTER

Aluminum

Beryllium Copper

Epoxy (Ecco Bond 55)

Gold

Silver

Stainless Steel (300 series)

Stainless Steel (420)

Teflon
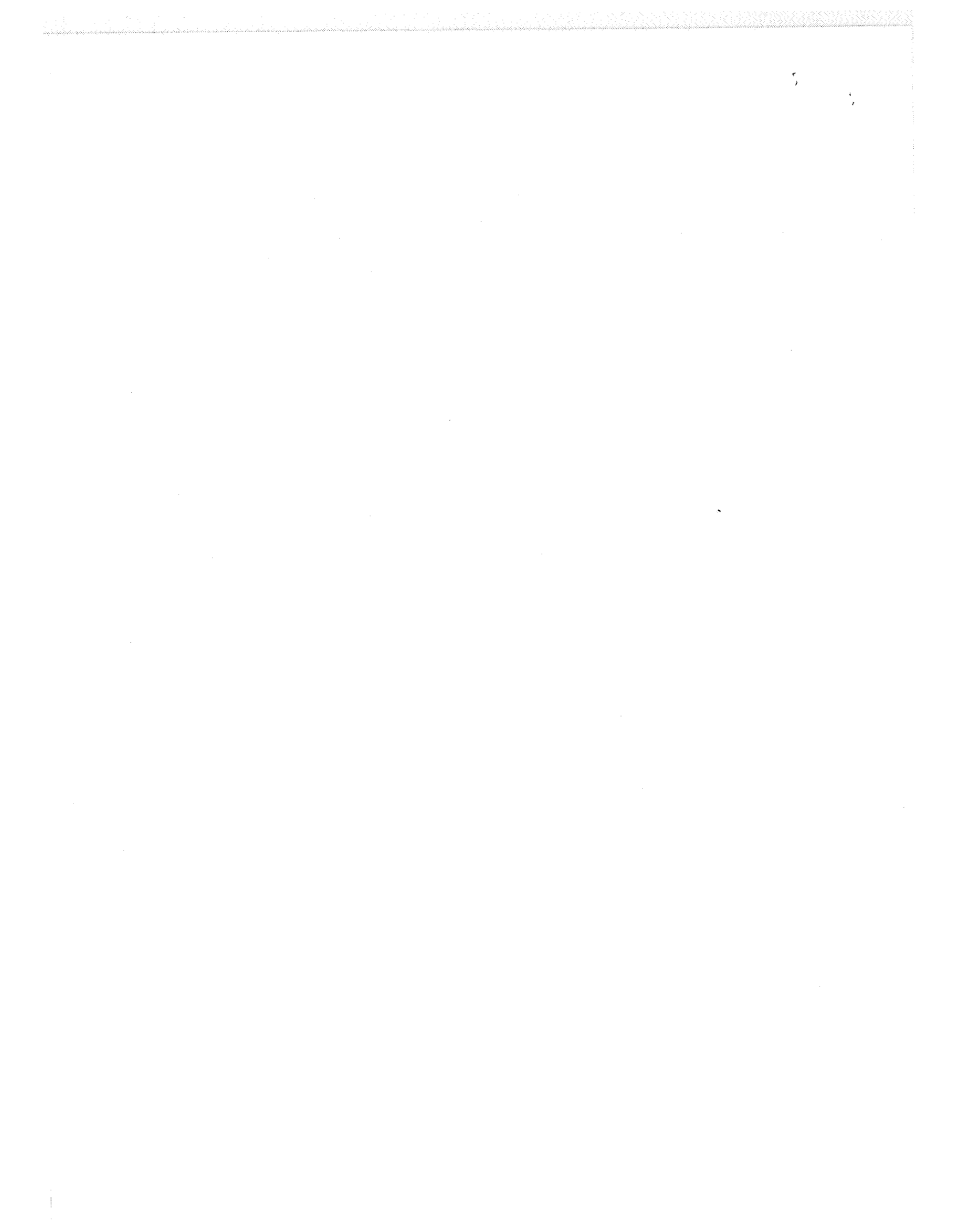
SECTION III

ENGINEERING MODEL TWT DEVELOPMENT

A. EVALUATION, INITIAL DESIGN AND APPROACH

The initial evaluation of the development effort, preliminary design, and development approach taken are noted below. A clearer picture of the end item can be obtained it the development effort is understood in view of the initial evaluation and design.

The critical electrical characteristics of the components can be determined by an analysis of the system efficiency requirement. Specifications of 20 watts minimum power output from the filter with a limitation of 60 watts dc power input to the TWT under worst case conditions imposes very tight requirements on the total unit performance. Filter requirements which place a stop-band 162 MHz away from the pass band make a low pass band insertion loss difficult to obtain. Consultation with the Rantec Corporation, which manufactured a filter for JPL with identical electrical characteristics, showed that they were able to build units with 0. 5 dB insertion loss in the pass band   for   normally   encountered shock environments.   They could not make an accurate estimate as to the pass band insertion loss when the unit was ruggedized for 10, 000 G shock. Their best estimate was that it would be less than 1. 0 dB, unless an electrical redesign were undertaken. Table VI illustrates the efficiency requirements for the TWT based upon filter losses of 0. 5 dB and 1. 0 dB. In terms of TWT results achieved at the time the program began, the 42. 0 percent efficiency required for the case of the 1. 0 dB filter loss was beyond the state-of-the-art. The 37. 4 percent efficiency required for the case of the 0. 5 dB filter loss was barely within the state-of-the-art. This meant that as much effort as possible had to be made to further develop the filter to simultaneously provide no more than 0. 5 dB insertion loss and 10, 000 G shock capability.

The general design of the WJ-398 was chosen from an existing tube, the WJ-274, which was developed for NASA, Langley Research Center, under Contract No. NAS1-3766. The WJ-274 is a 20 watt, S-band, lightweight, PPM focused tube with an overall efficiency in the range from 35 to 41 percent with the collector depressed below helix potential. The Final Report* of the NASA contract gives the design details and performance of the tube. For clarity, Fig. 22 through Fig. 25 have been included to show the physical configuration of the WJ-274.

*   Roberts, Lester A., "The Design and Performance of a High Efficiency Traveling-Wave Tube, The WJ-274." Final Report on Contract No. NAS1-3766, Watkins-Johnson Company.

PRECEDING PAGE BLANK NOT FILMED.

TABLE VI

DETERMINATION OF SYSTEM EFFICIENCY REQUIREMENTS

	Filter Loss	
	1.0 dB	0.5 dB
1. Maximum dc power input to tube	60 watts	60 watts
2. Minimum RF power out of filter	20 watts	20 watts
3. Minimum RF power out of tube into filter	25.2 watts	22.4 watts
4. Required minimum tube efficiency (3/1)	42.0%	37.4%
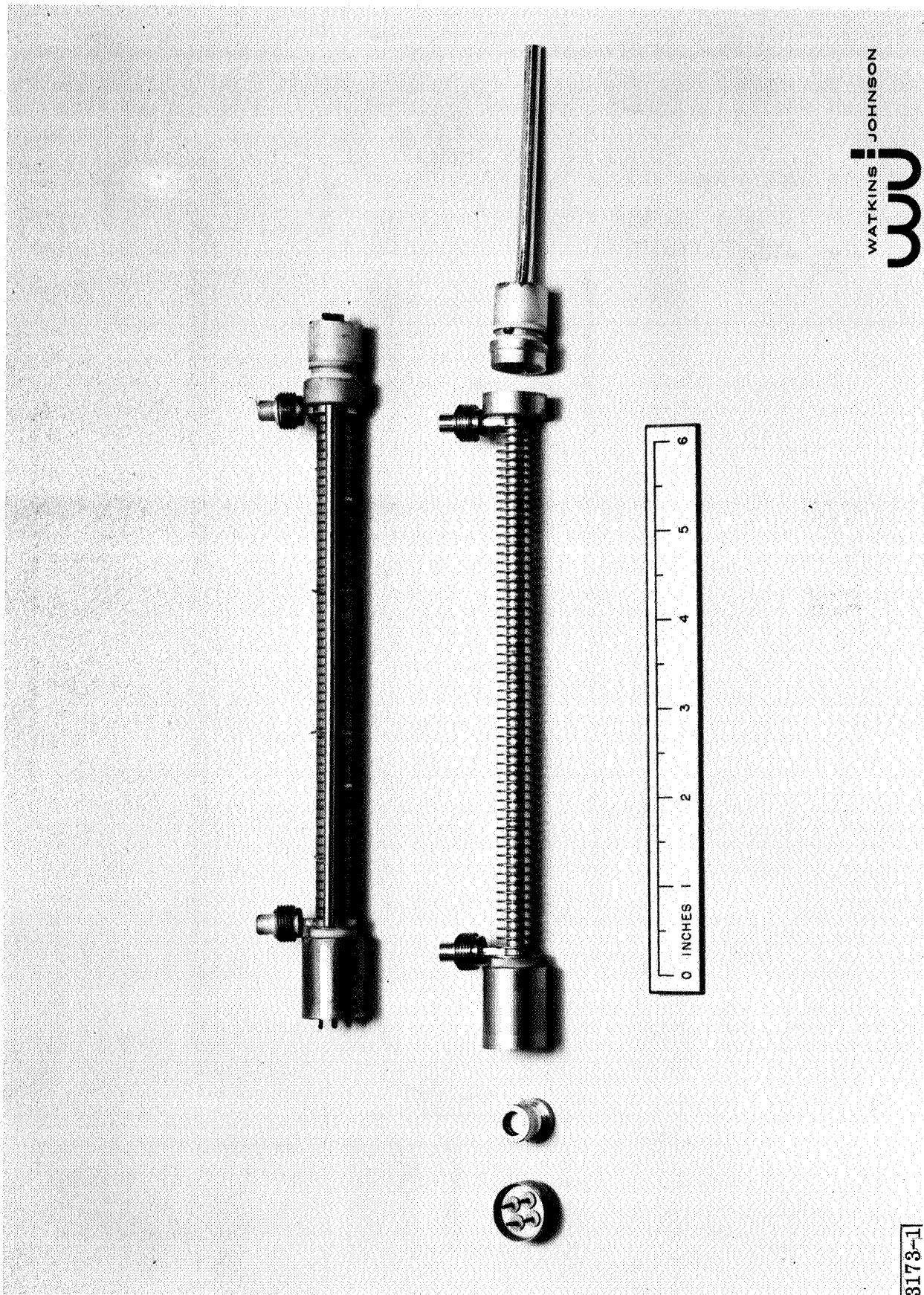
Fig. 22 – Photograph of the WJ-274 showing a completed tube with magnets in place (above) and a completed body with cathode and header subassemblies to the left and collector subassembly to the right (below).

3173-1
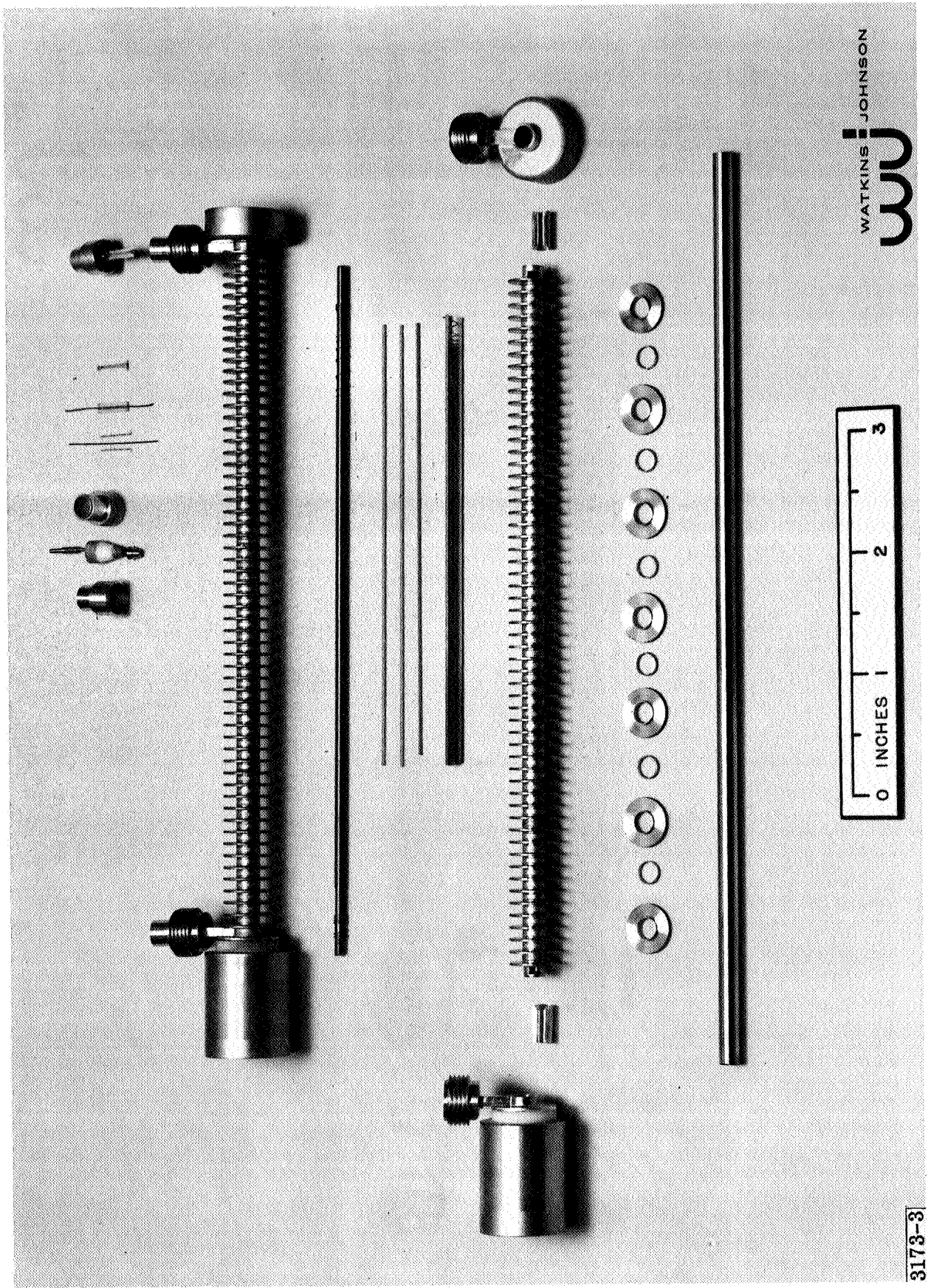
Fig. 23 – Photograph showing the WJ-274 body subassembly and its component parts including strip transmission line vacuum window. The helix is a glazed structure using three beryllium oxide wedges for dielectric support.

Fig. 24 – Photograph of the electron gun and input stripline subassembly and component parts. The lower row shows the header components (at left), the cathode subassembly, cathode insulating ceramic and anode subassembly. The upper row shows the parts which make up the anode subassembly.

3173
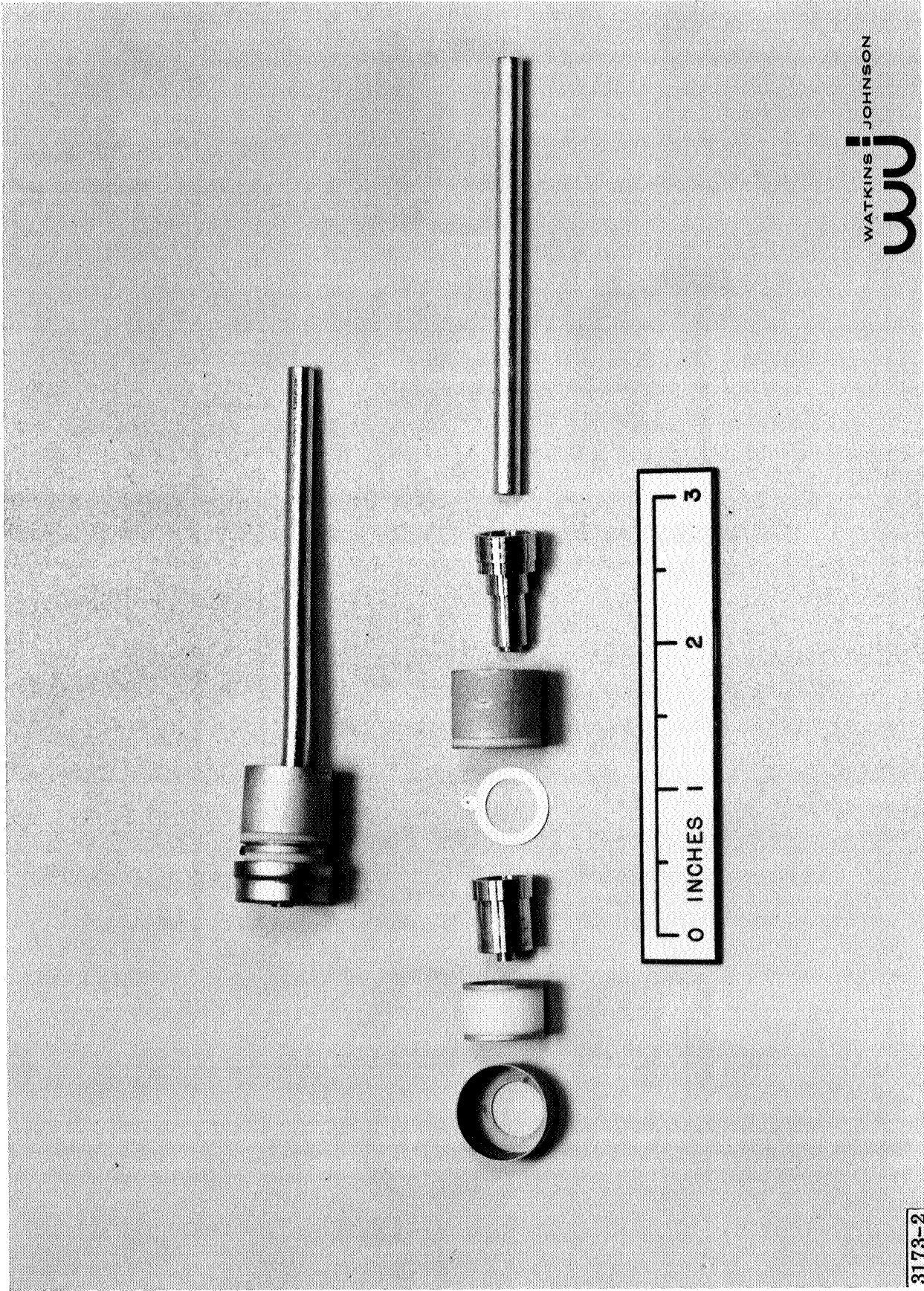
Fig. 25 – Photograph of the collector subassembly and its component parts. This is a complete two stage collector assembly including the metallized ceramic insulator which serves to insulate and also conduct heat from the two stages

Several areas of the basic WJ-274 design had to be modified to meet the high shock requirement. The effects on these areas will be briefly pointed out below.

1. <u>Cathode Support and Electron Gun.</u> Two factors influence the choice of the cathode support design. These lead to conflicting requirements - adequate mechanical support under impact conditions, and low heater power. A rigidly fixed cathode position with respect to the surrounding electrodes is very important to the proper functioning of the tube. However, stiffening the cathode support results in increased heat loss from the cathode. Since the heater power degrades the overall efficiency, it is desirable to keep the heater power to an absolute minimum. Table VII shows the requirements on the depressed efficiency of the tube for various values of heater power. Heater power requirements greater than 4 to 5 watts place a severe requirement on the tube performance.

   Several support schemes common to the tube industry include crossed insulating rod support, "milk stool" platform, wire suspension, and cylindrical support. However, each of these schemes is deficient in one or both of the requirements of high impact capability and low thermal loss. A support in the form of a truncated segment was chosen for the cathode supporting structure. This configuration has high geometrical strength. In addition, through proper choice of materials the thermal conduction loss can be minimized. The coated heater, like in the WJ-274, is a flat "pancake" design, and is potted in place with sintered nickel powder, thereby assuring adequate support to the heater. A truncated cone was also chosen for the heater lead return to minimize any differential movement between the heater returns.

   The electron gun envelope was altered to provide a metal enclosure which rigidly supports the internal gun assembly. The metal envelope allows the outside of structure to be held at ground potential so that it can be directly supported by the surrounding capsule.

2. <u>Helix.</u> In modifying the helix design for high impact conditions, an attempt was made to minimize any degradation in interaction impedance, and heat dissipating properties of the helix.

   It is important to retain a high helix interaction impedance so that the design value of the gain parameter, C, can be achieved with a low beam admittance, I_0/V_0, since a low beam admittance makes beam focusing easier.

TABLE VII

DEPRESSED TUBE EFFICIENCY
REQUIREMENT AS A FUNCTION OF HEATER POWER

$$P_{rf} = 22.4 \text{ Watts}$$

$$P_{dc} \quad \text{(Including heater)} = 60 \text{ Watts}$$

P_{Htr}	P_{dc} (excluding heater)	Required Depressed Efficiency
3.0 Watts	57.0 Watts	39.3 Percent
4.0	56.0	40.0
5.0	55.0	40.7
6.0	54.0	41.5
7.0	53.0	42.3
8.0	52.0	43.1

The high interaction impedance of the WJ-274 design is achieved by using a band center γa of 0.95 and a dielectric loading factor (DLF) of 0.79. This relatively high DLF is obtained by using beryllium oxide wedges for the helix support. The lower dielectric constant of beryllia ceramic compared to the higher value of the more commonly used alumina ceramic leads to a considerable improvement in the DLF. It also performs an excellent job in cooling the helix by its high thermal conductivity. The wedge shaped support rods further reduce the amount of dielectric material in close proximity to the helix, and thus helping to improve the DLF.

There are three sources of helix heating in a tube design such as this:

    a.   RF losses in the output section,

    b.   Current interception due to beam defocusing caused by beam expansion and velocity spread under saturated output conditions, and

    c.   Reflected electrons from the collector which is operated at a lower potential than the helix.

It is very important in a high efficiency tube to provide a high thermal conductance from the helix so that it does not rise to excessive temperatures. Heating increases both the skin effect loss of the helix and the dielectric loss of the helix support and leads to power fade and loss of efficiency. The beryllium oxide helix support, because of its high thermal conductivity, leads to a lower temperature difference between the helix and the vacuum envelope. Even more important is to provide a low thermal impedance across the interface between the back of the wedge and the body wall. This is accomplished by providing superior surface contact between the wedge and the body. Accurate machined fits are used, and strong forces are applied across this interface.

The helix support chosen must properly support the helix in order to prevent any relative motion between the helix and its support. Any motion would give local variation in helix pitch and could seriously degrade both the power output and tube efficiency. Furthermore, the dielectric support must not fracture since this leads to discontinuities which will cause regenerative effects.

A more rugged helix configuration than the glazed, beryllium oxide (BeO) wedge supported structure was considered necessary. Several possible alternatives were considered including heavier BeO wedges or rods, aluminum oxide material rather than BeO, or a ceramic support which is metallized and brazed to the helix turns.

Since each of the alternative methods listed degrade the interaction impedance and/or heat dissipation properties, it was important to thoroughly investigate these in order to minimize the adverse affects while providing the necessary high impact capability.

3. RF Windows and Stripline. The capability of the RF window and the transmission line between the window and the helix to withstand high impacts was considered to be very good. The actual window is a conical ceramic which is metallized on the outside at the large diameter end and also on the outside at the tip. This type of window is superior to the coaxial bead type in the method of sealing to the center conductor. The coaxial bead develops stresses in the ceramic around the center conductor which create a tensile failure probability in the weak ceramic. In the conical window, the sealing metal is on the outside of the cone (refer to Fig. 9) placing the ceramic under compression where it is strong.

The transmission line consists of a stripline supported within a rectangular metal outer conductor. This is a very lightweight and strong mechanical support. Since the stripline is supported along its entire length, there is no possibility of the center conductor moving under high impact shock.

4. Ceramics. Various metallized ceramic parts are used on the tube to provide electrical insulation. If the impact stresses which are placed on the ceramics lead to large shear or tensile forces, shattering or cracking of the ceramic could take place. To prevent this, the surrounding capsule of the tube must be made heavier and less flexible and the fit between the tube parts and the capsule made very close so that relative motion cannot take place.

5. The Effect of Shock on the Magnets. There was no actual data of the effect of the high impact shock on permanent magnets of this type. All conclusions were based upon speculation. The effect of shock is a re-ordering of the magnetic domains of the material and it may be assumed that demagnetization due to shock could be akin to the difficulty of demagnetizing the material by applying a reverse magnetic field. In this case, cobalt-platinum is the most difficult material to demagnetize because its coercive force is the highest of any permanent magnet material known. It has a coercive force twice that of oriented

barium ferrite material which is the next best material. Based upon this reasoning, it was felt that the cobalt-platinum material would be the least sensitive to demagnetization by shock of any of the permanent magnet materials.

Meeting the required impact test level was the major area of effort in the program. A thorough mathematical analysis of the dynamics of a 10,000 G shock pulse is impractical for such a device as a TWT. Such an analysis would have to consider the frequency domain response of the pulse and the corresponding response of the assembly under test. However, it is reasonable to assume since the peak loading is at $\omega = 0$, a static analysis is quite appropriate with firm consideration given to the lower resonant frequencies. Using this approach for the initial design, parts, materials, and interfaces were designed to withstand the forces experienced during a constant deceleration of 10,000 G, with allowance for adequate safety margin.

With the initial design, key units, such as the cathode support structure, were tested under statically loaded conditions to check the calculations. However, at that point, further design changes were principally determined by the empirical approach based on high impact tests.

The development effort progressed from key parts, to minor subassemblies to major subassemblies, to the completed tube. Using this approach, the design of progressively larger elements of the TWT could be certified as acceptable. In this manner, the specific damage could be analyzed in order to isolate the cause of the failure whether materials, interface design, or geometry. If complete assemblies were tested at high levels at the start of the program, the problems/failures could not be adequately separated, identified, and corrected.

B. HIGH IMPACT INVESTIGATION

1. Impact Facility and Testing. The impact facility and the test methods used are pertinent to this report since they had a large influence on the design and development effort. The high impact facility and testing was provided by Section 355, Lunar Spacecraft Development Section, of the Jet Propulsion Laboratory.

   Fig. 26 is a diagram of one of the test machines capable of providing near 10,000 G impacts between 0.5 and 1.0 ms duration depending on the payload. This device in effect is a massive slingshot and operates in the same fashion.
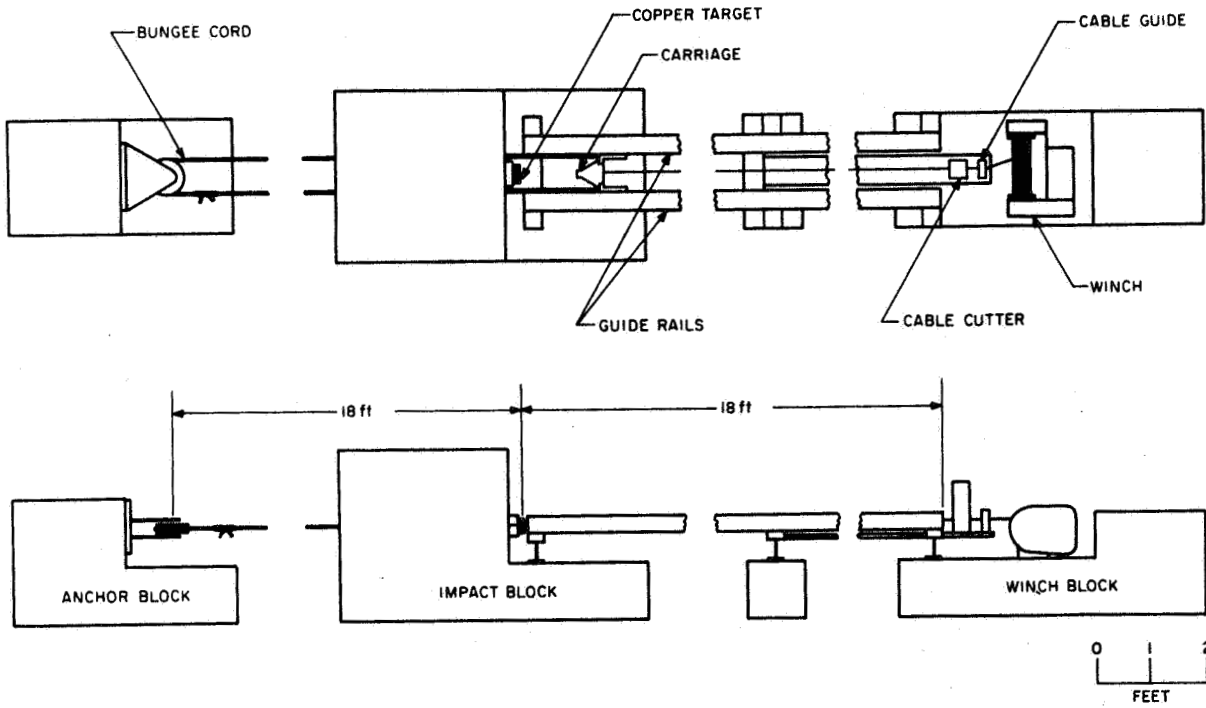
Fig. 26 – General configuration of the JPL horizontal shock test machine (reproduced by permission of the contracting agency).
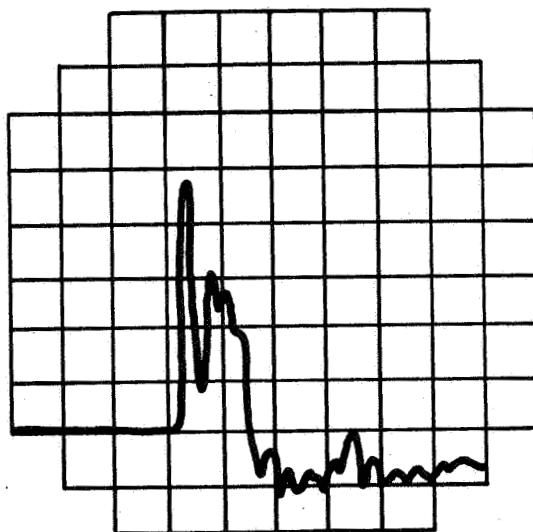
Calibration:

Vertical – 4,000 g's/div.
Horizontal – 0.5 ms/div.

Fig. 27 – Typical shock test deceleration – time history for the shock test machine.

After mounting the payload to the sled, the winch stretches the bungee cord to the required length; then the holding cable is severed releasing the sled. Impact magnitude, shape, and duration are determined by the combination of impact velocity (payload and pull back distance), payload weight, penetrating tool diameter, and absorbing material. Typical examples of impacts are 8500 G, for a 15 pound payload, with an impact velocity of 162 ft/sec(110 miles/hr) and a deceleration distance of 0.575 inch; or 12,940 G, for a 2.5 pound payload, with an impact velocity of 175 ft/sec (120 miles/hr) and a deceleration distance of 0.441 inch. Fig. 27 shows an oscilloscope trace of a typical shock pulse. Notice while the average level is 9300 G, there can be peaks as high as 18,000 G.

The level of the shock pulse is determined by two methods, one providing a check for the other. The actual pulse is displayed on an oscilloscope using an accelerometer mounted on the assembly from which the average level of the pulse is determined. The second method is a theoretical computation using the measured impact velocity and the deceleration distance (depth of cavity in copper block). The average level is computed using the expression

$$\text{Impact Level} = \frac{v^2}{5.36\,x} \quad (\text{G's})$$

v = impact velocity (ft/sec.)

x = deceleration distance (inch)

This expression assumes a constant deceleration (i.e., a perfect rectangular pulse). Whenever the impact level is discussed in this report, it is the average level found by averaging the peaks and valleys of the scope trace or the computation. It does not refer to the peak level of the spikes in the pulse.

Fig. 28 and Fig. 29 show various photographs of the shock test facility.

To some extent the assembly mounting fixtures must be designed within the restrictions of the test machine on payload weight and dimensions. In designing the testing fixture for the various TWT subassemblies, efforts were made to minimize the influence of the fixture on the assembly during shock, that is, only the assembly was to be examined. It is important that the fixture does not have any weaknesses which could in turn damage the assembly under test.

The approach taken for the TWT subassembly evaluations was to build test fixtures which were in themselves very strong and free from deformation. The subassembly is rigidly potted with an epoxy material in a cavity machined deep within a block of aluminum. The fixtures were symmetrically designed so the principal planes of the assembly could be shock tested. For the case of the TWT assembly fixture, this rigidly potted philosophy could not be used since the TWT had to be evaluated mounted to a single surface. Since often there is a secondary impact directly to the fixture due to the wild whipping of the bungee cord after initial impact, it was important that all surfaces of the test assembly be enclosed or protected.
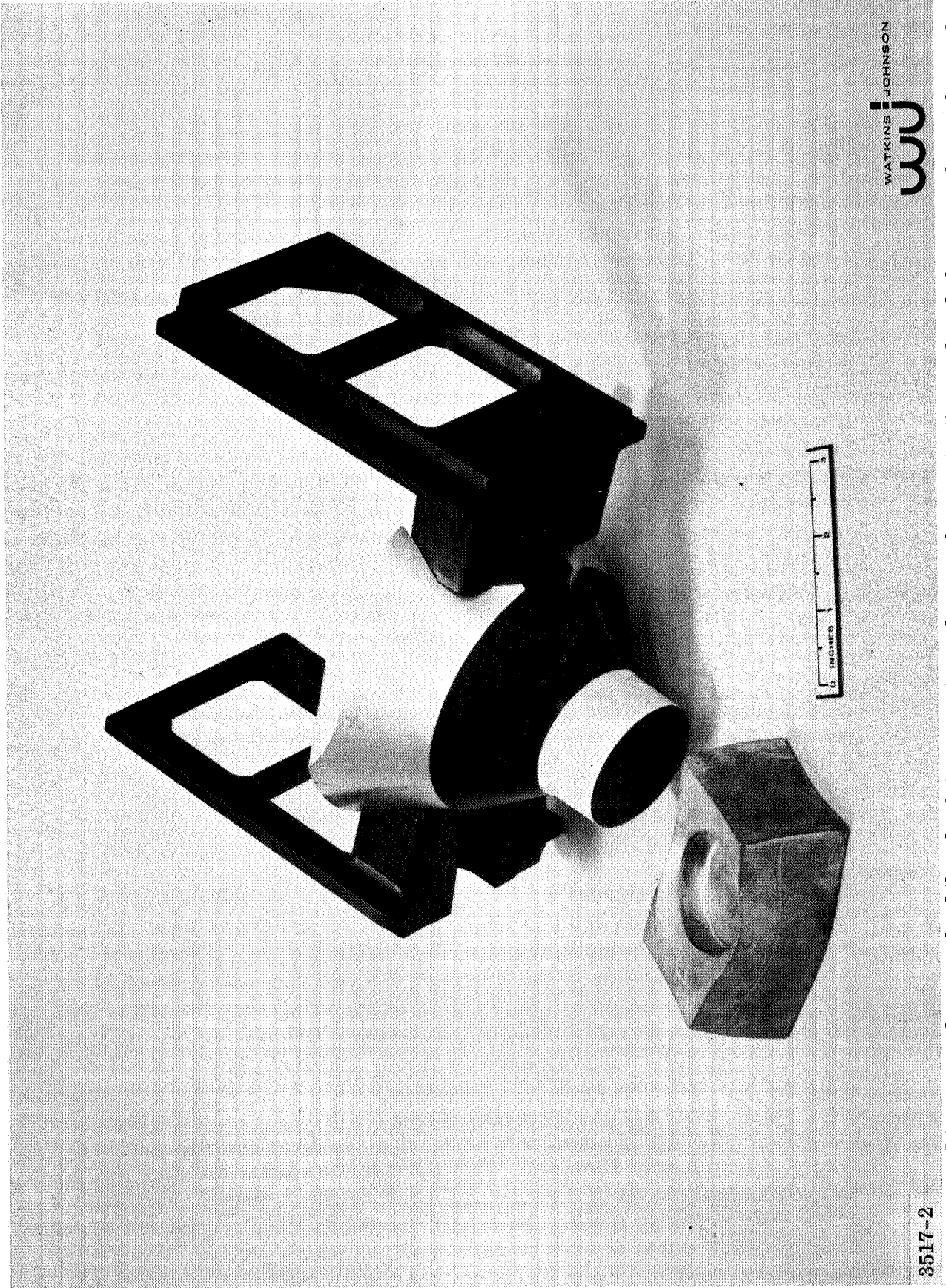
Fig. 28 – Photograph of the shock test carriage showing the penetrating tool and plastic guides. The guides are expended during each shock. Also shown is the copper target after deformed by the impact.

3517-2

Shock Machine
View From Anchor Block
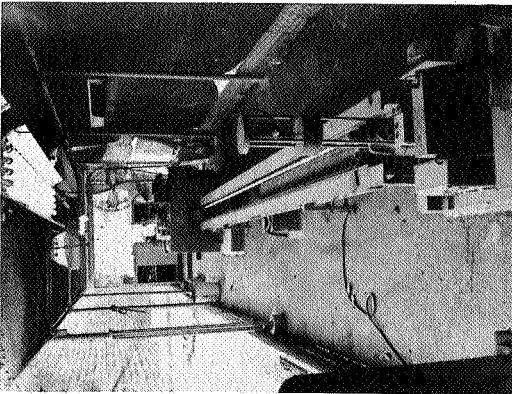
Shock Machine
View From Winch Block

Impact Block
TWT Test

Impact Block
TWT Test
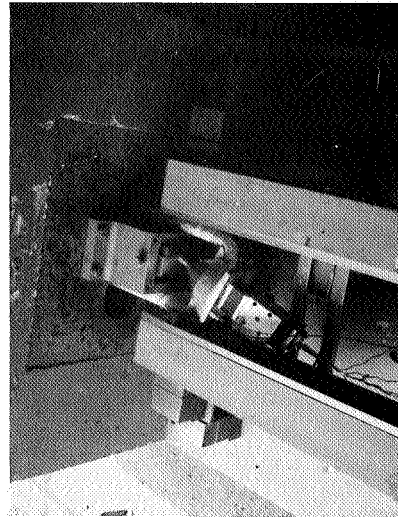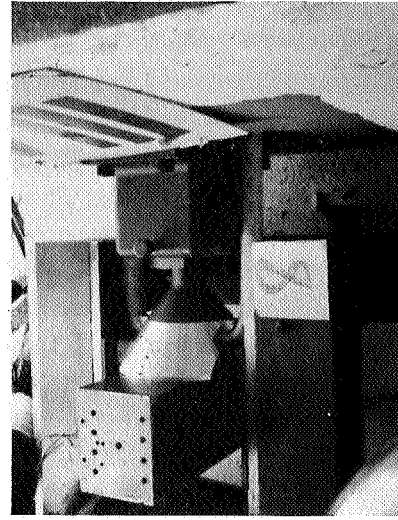
Impact Block
TWT Sub-Assembly Test

Fig. 29 – Various photographs showing the shock test machine and the details of the impact block.

18258

Fig. 30 shows a photograph of various test fixtures used for the TWT development. Fig. 31 shows the fixture for the TWT with the tube mounted for impact. Note how all of the fixtures completely surround and protect the specimen.

The method used to analyze the results of the shock test is one of the difficult procedures to determine. It is important to use, when practical, non-destructive tests so as not to confuse impact damage with the damage caused by dissecting and analyzing the assembly. Almost without exception, specimens were tested at increasingly higher levels successively checking the principal planes of orientation at each level. Before and after a series of impacts on an assembly, a complete set of diagnostic measurements were made on the specimen. Between each impact, the specimen was examined and measurements made of a limited number of key parameters. Table VIII gives a summary list of the investigative tools and measurements used on the principal impact tests.

The type of examination and measurement included visual, dimensional, radiographic (X-ray), electrical, and RF checks. As specimens were being manufactured, careful records were kept of inprocess inspections and measurements in order to compare with post test examinations.

2. <u>High Impact Development Tests.</u> Impact investigations were made on the following assemblies:

        a. Helix Assembly and Body Assembly Segments,

        b. Complete Body Assemblies,

        c. Electron Gun Assemblies (diodes),

        d. Collector Assembly, and

        e. Encapsulated TWT.

Results of these investigations are described in the following paragraphs.

a. <u>Helix Assembly and Body Assembly Segments.</u> Adequate support of the slow-wave circuit is dependent on the materials and the interface between the helix wire and the ceramic supports, as well as between the helix assembly and the vacuum envelope. Two experiments were formulated to determine first an acceptable helix assembly, and second an acceptable helix assembly enclosure.
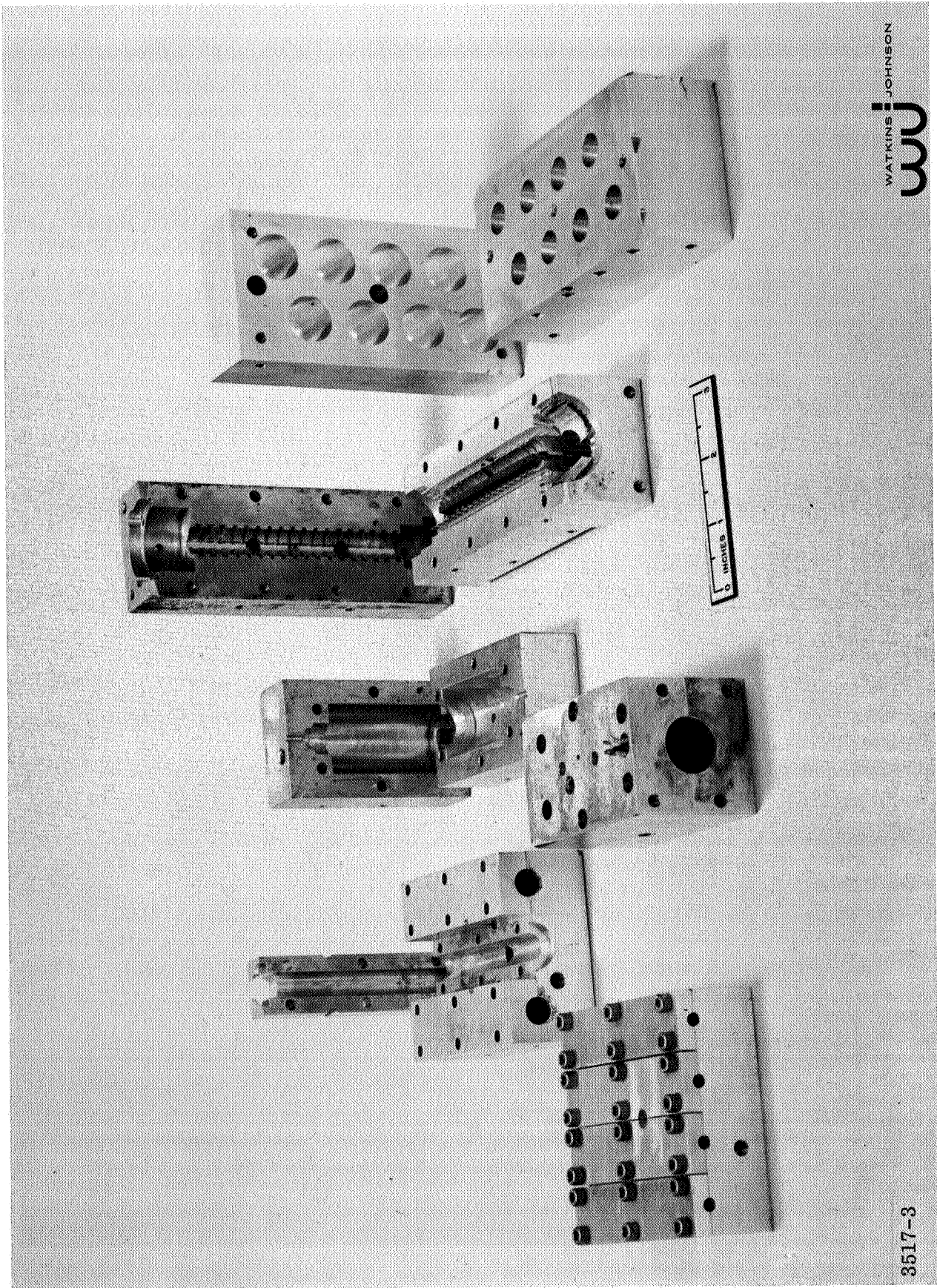
Fig. 30 – Photograph showing samples of the various test fixtures used for the TWT development. From left to right are the fixtures for the helix assemblies, body segments, collector assembly, gun assembly, body assembly, and cathode support structure.

3517-3

- 55 -
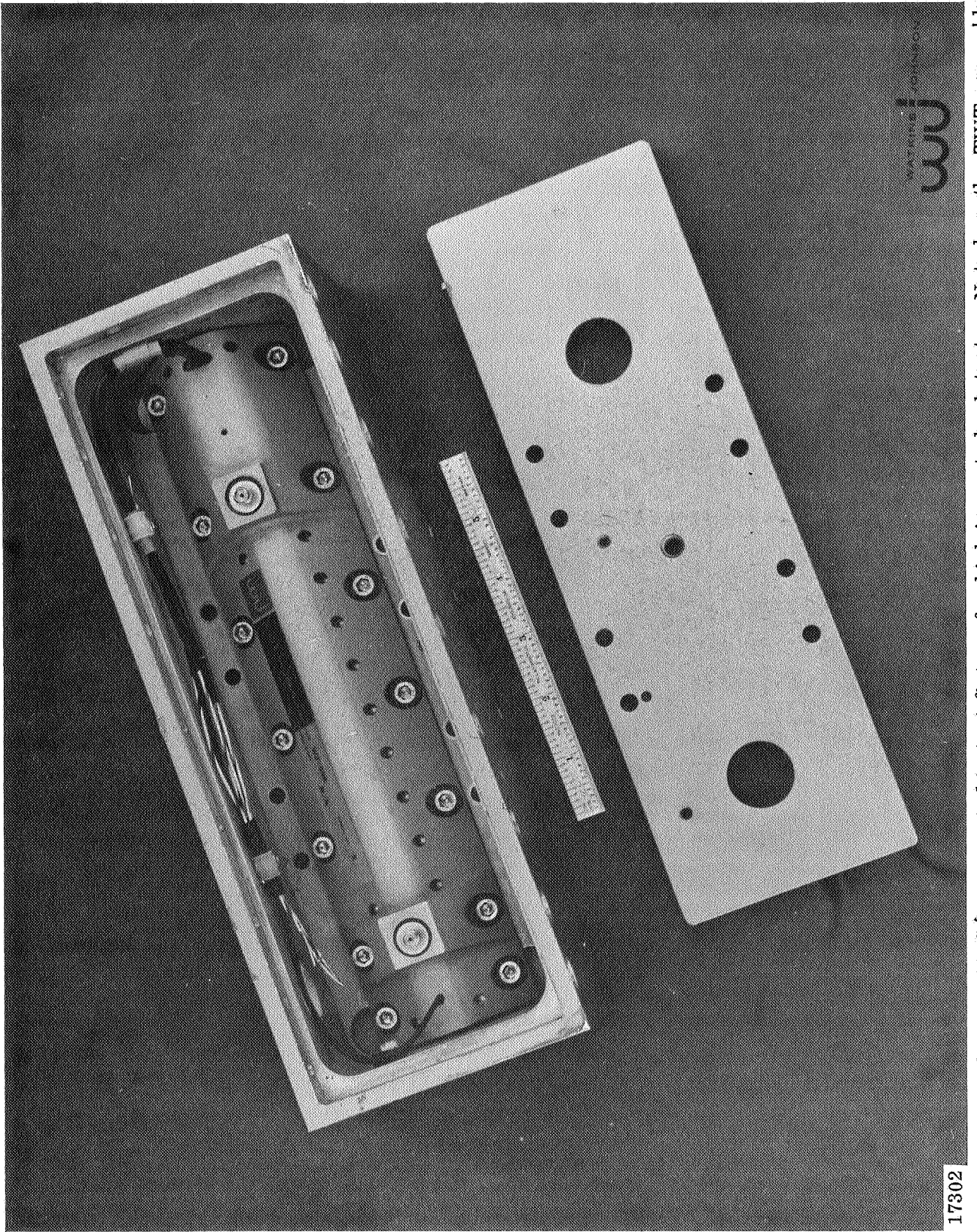
Fig. 31 - The WJ-398 S/N 3 mounted in test fixture for high impact shock tests. Note how the TWT assembly is completely enclosed and protected by the fixture.

TABLE VIII

SUMMARY LIST OF DIAGNOSTIC TOOLS AND MEASUREMENTS USED FOR IMPACT TESTS

Analysis Tools/Measurements	IMPACT TEST						
	Cathode Support Structure	Helix Structures	TWT Body Segments with Magnets with Helix	Gun Assy (Diode)	Collector Assy	Complete TWT Body Assy	TWT
Visual Inspection							
In Process	X	X	X	X	X	X	X
Microscopic (aided eye)	X	X	X	X	X	X	X
X-ray Photographs	X		X	X	X	X	X
Mechanical							
Dimensional	X	X	X	X	X	X	X
Dissection		X	X	X		X	X
Plastic Potted Machine Section	X						X
Vacuum Check			X	X	X	X	X
Electrical/Magnetic							
Heater V, I Characteristics				X			X
Heater Resistance				X			X
Helix Resistance						X	X
Isolation Resistance				X	X		X
Interception Currents				X			X
Gun Perveance			X	X			X
PPM Magnet Field Check							
RF							
VSWR			X		X		X
Circuit Phase Velocity			X		X		X
Power Output vs Input							X
Power Output, Sat. Gain, SS Gain,							
Efficiency vs Frequency							X
Depression Characteristics							X

Four helix assemblies and three body assembly segments were tested. Fig. 32 shows the basic configuration of the segments. Two of the test samples were similar with the exception of the helix assemblies used. The third sample was a more complete body assembly taken from a WJ-274 tube. This assembly included the RF coupler assembly with the ceramic window, transmission line and helix matching transformer. All helix assemblies were locked in the body assembly using the braze flow technique. The assembled helix and barrel is heated to alloy melting temperature allowing the material to flow between the barrel and the helix assembly. When cooled, the larger contraction rate of the metal barrel compresses the helix assembly providing the helix lock-in.

Test results of the impact investigation on these assemblies and the conclusions reached are summarized in Table IX. Fig. 33 shows a radiograph of the body segments after the test series showing the damage experienced during shock.

b. __Body Assembly.__ Impact studies were performed on two assembly designs. Fig. 12 shows the general geometry of the body assembly. Not shown in Fig. 12 are the RF connector adapters which were included in the tests. Encapsulation details of the assembly showing the method used to support the magnets is shown in Fig. 34.

A summary of the results for the assemblies tested and the conclusions reached are shown in Table X.

Fig. 35 presents radiographs of designs No. 1 and No. 2 after the test series showing the resultant damage. Design No. 2, with only minor changes, was later shown to be adequate for the high impact requirements. A detailed description of this design can be found in the section describing the End Item TWT.

c. __Electron Gun.__ Prior to impact tests on the electron gun assembly, a number of static loading tests were performed on the cathode support cone. Results of the tests led to the use of a cone segment made from 0.002 inch Hastelloy alloy B sheet drawn into the cone shape.

Three diode designs were evaluated under impact conditions. With the exception of a few specific details such as cone material and parts configuration, the designs are similar to that described in the section on the

Test Fixture (or tube capsule)

Magnets

Hard Potting Material

Body Tubing

Helix Assembly

Pole Piece

P. P. Spacer
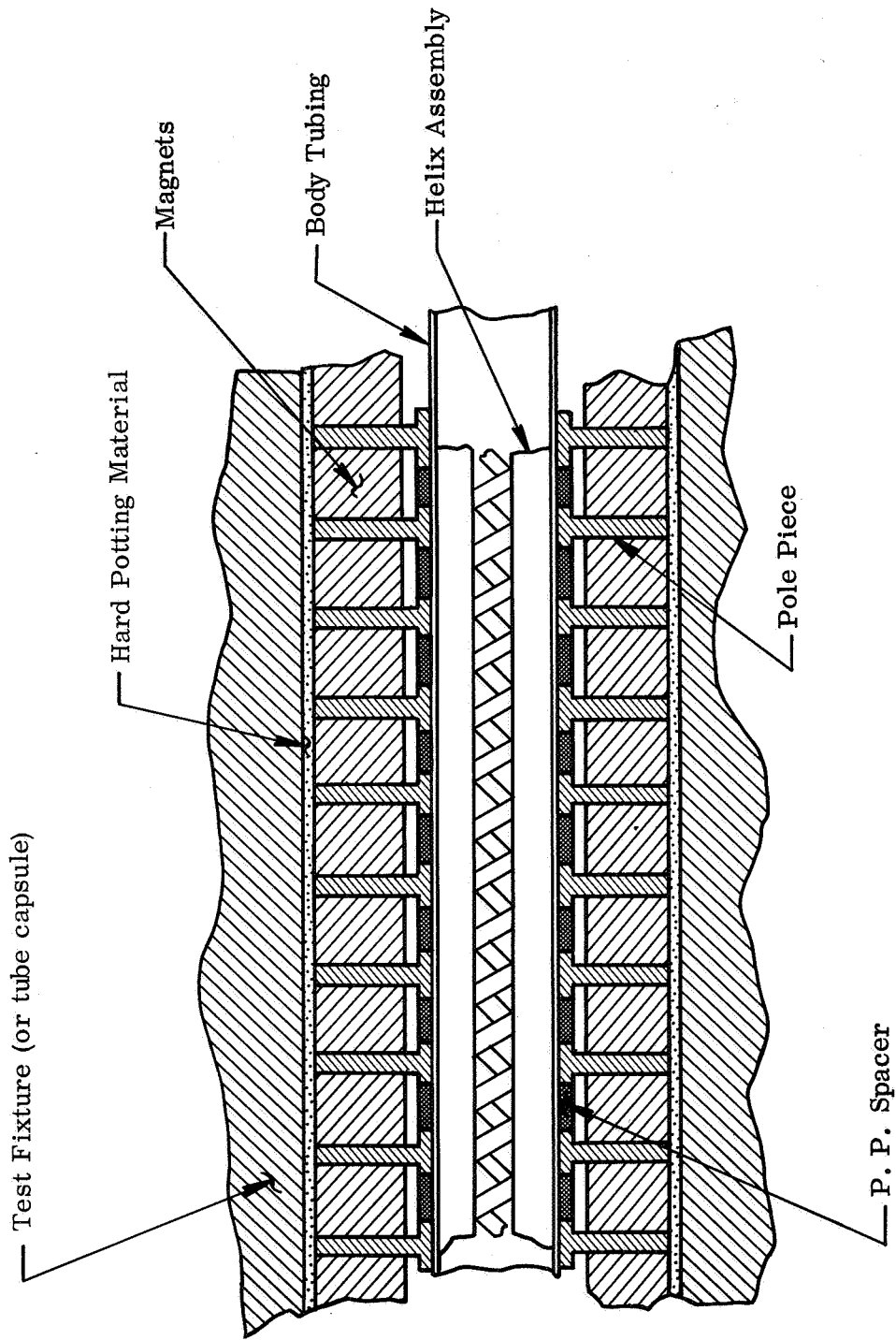
Fig. 32 — Basic configuration of body assembly segments. Helix assembly lock-in uses alloy technique.

- 59 -

15505

TABLE IX

HELIX AND BODY SEGMENT SHOCK TEST RESULTS

Test Sample	Failure Level	Highest Level Before Failure	Failure Mode/Remarks
Helix Assembly Samples			
1. Alumina ceramic wedges glazed to a tape helix.	13,250 G (Transverse)	9,350 G (Transverse)	Helix turns and glaze fillets undamaged except near ends and few isolated spots.
2. Alumina ceramic wedges brazed to a tape helix.	13,250 G (Transverse)	9,350 G (Transverse)	Almost all turns broken free at ceramic land below metallized bond.
3. Alumina ceramic wedges glazed to a wire helix.	1,200 G (Transverse)	1,200 G (Transverse)	Damaged while being examined. Test inconclusive.
4. Beryllia ceramic wedges glazed to a wire helix.	1,200 G (Transverse)	1,200 G (Transverse)	Damaged by test fixture. Test inconclusive.
Body Segment Samples			
5. Basic configuration*, alumina ceramic wedges glazed to tape helix.	13,100 G (Axial)	14,100 G (Transverse)	Body shifted in fixture and impacted against end. Body tubing separated. Helix turns uniform in places.
6. WJ-274 assembly segment**(Beryllia wedges glazed to wire helix).	6,150 G (Axial)	6,050 G (Transverse)	Body shifted in fixture separating tubing at end pole piece interface. Helix turns uniform except at separated area.
7. Basic configuration, alumina ceramic wedges brazed to tape helix.	3,975 G (Axial)	3,800 G (Transverse)	Helix slid out of body. Lockin considered marginal.

* Refer to Fig. 32. Helix lockin uses thermal compression of helix assembly by braze flow between wedge and body wall.

** Includes RF coupling assembly. All else same as basic configuration.

CONCLUSIONS BASED ON TEST RESULTS

1. A glaze bond between the helix wire and the ceramic supports is stronger than a braze bond.
2. A tape helix provides better bonding area than a wire helix.
3. Choice of beryllia or alumina ceramic wedges cannot be determined from this test series.
4. The lockin technique may be satisfactory.
5. The focusing magnets must be supported by the capsule.
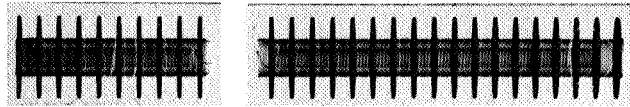
Sample 5
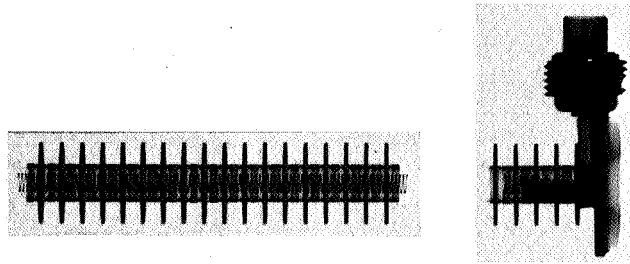
Sample 6
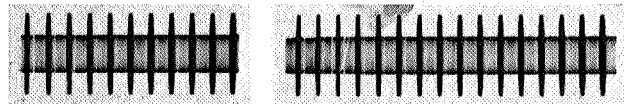
Sample 7

Fig. 33 – Radiograph of body assembly segments taken after impact tests (focusing magnets have been removed). When impacted in the axial direction, the helix assembly in sample 7 broke free of the assembly. All samples separated at the pole piece body tubing interface indicating the inadequacy of the body support scheme. Spread turns shown in the right segment of sample 6 are not a result of impact but are part of the impedance transformation to the helix.
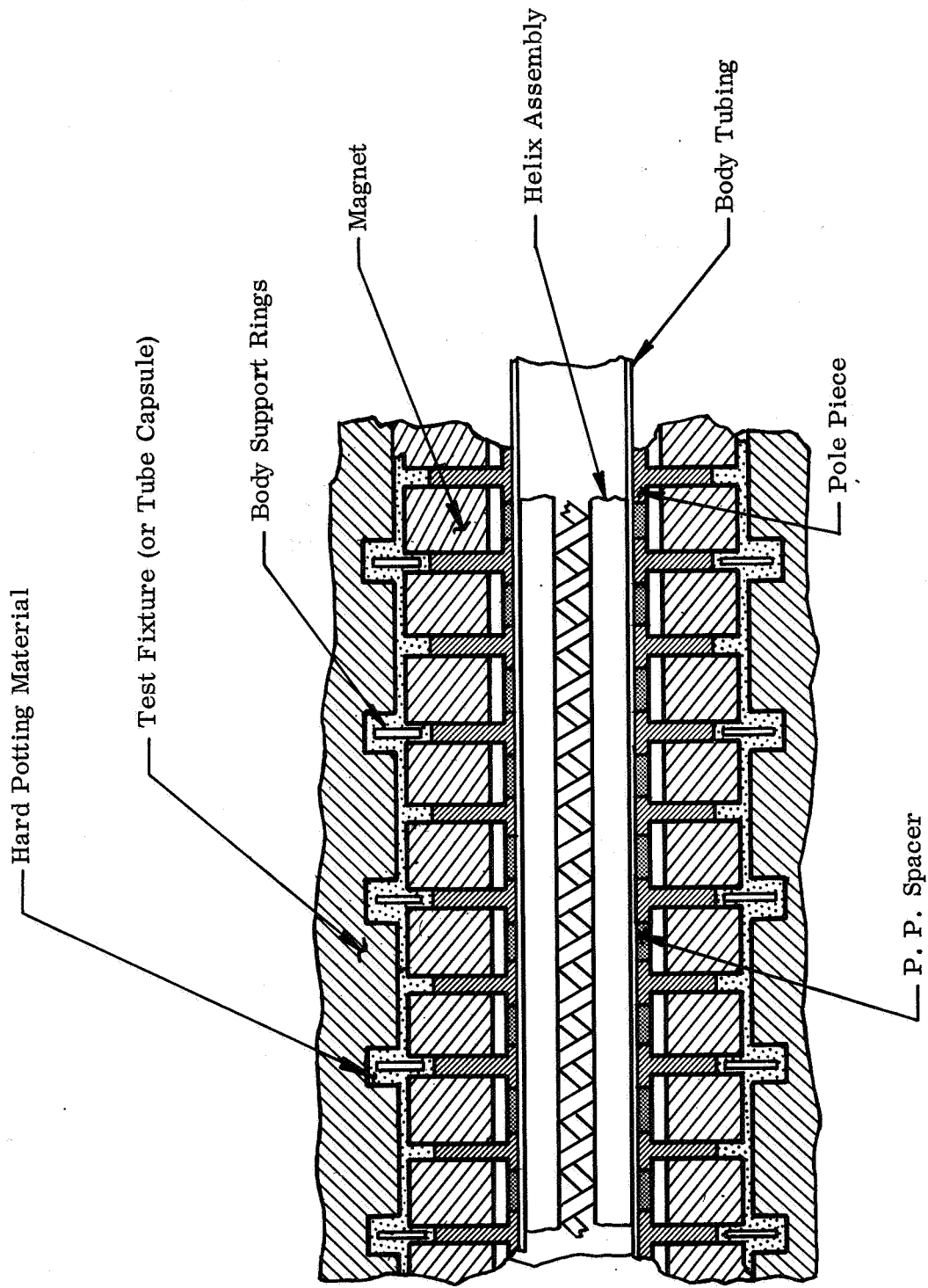
Fig. 34 – Encapsulation and support geometry for the TWT body. The body support rings are split rings which are inserted between the magnets and interlocking recesses in the capsule. When potted solid with epoxy material, the TWT body and magnets are rigidly held and supported by the capsule.

15504

TABLE X

BODY ASSEMBLY SHOCK TEST RESULTS

Description of Sample	Failure Level	Highest Level Before Damage	Failure Mode/Remarks
<u>Body Assembly - Design No. 1</u> Basic geometry represented in Fig. 12 with addition of RF connector adapters. Helix uses alumina ceramic wedges glazed to tape helix. Helix lockin by thermal compression using alloy flow between wedges and wall. Body/magnet support provided by method shown in Fig. 34.	11,000 G (Axial)	12,900 G (Transverse)	1. Assembly developed vacuum leak – considered associated with fixture deficiency. 2. Change in VSWR; physical deformation of connector parts. 3. Gross damage to helix due to inadequate lockin. 4. Damage to stripline caused by shifted helix. 5. Body support/encapsulation and window stripline geometries showed no adverse effects of shock. <u>Test Conclusion</u> 1. Lockin technique inadequate. 2. Connector parts need redesign using stronger material.
<u>Body Assembly - Design No. 2</u> Basic geometry represented in Fig. 12 with addition of RF connector adapters. Helix uses beryllia ceramic wedges (heavier design) glazed to tape helix. Helix lockin uses triangulated body technique. Pole pieces snug to body but not brazed to it. Body/magnet support as shown in Fig. 34.	12,220 G (Axial)	12,170 G (Transverse)	1. Non uniform turns in attenuator area. 2. Only second order changes to RF match and electrical resistance between helix assembly and body wall. These changes would not affect performance of the TWT. <u>Test Conclusion</u> Design No. 2 adequate for high impact requirement to 10,000 G with minor changes in manufacturing methods.
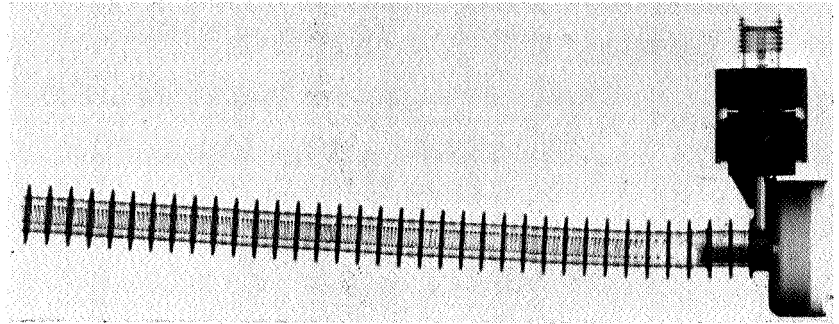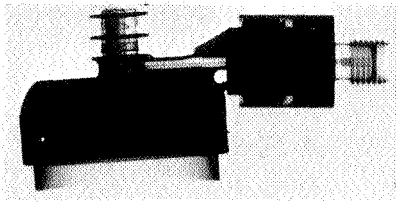
Design No. 1 – Damage included gross movement of the helix assembly indicating inadequacy of alloy lock-in technique and deformation of RF connector parts (non-detectable in radiograph). Separated body and deformed barrel resulted during removal from fixture, not as result of impact. Damage to stripline assembly on right caused by shifted helix. No adverse effects of shock were detected in the RF window-stripline area or to the body/magnet supporting configuration.
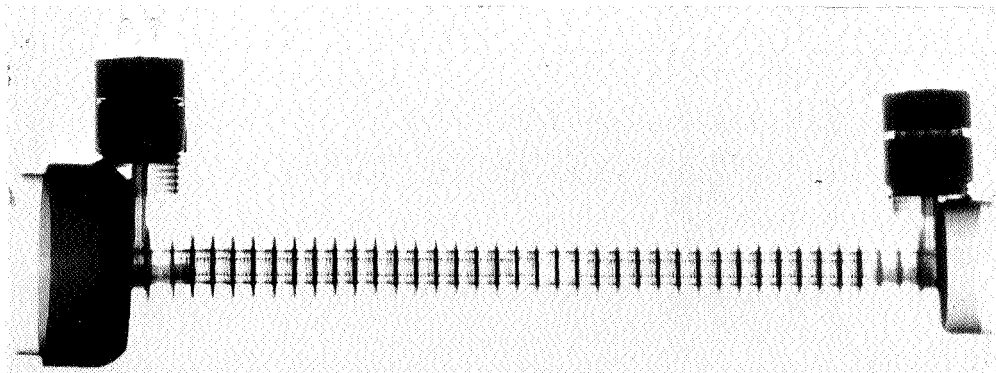
Design No. 2 – Damage occurred to helix turns in the attenuator area (center). Second order changes were observed to the RF matches and the electrical resistance between the helix and body wall.

Fig. 35 – Radiograph of body assemblies after impact tests. Focusing magnets have been removed.

18289

End Item TWT. Only the significant design differences will be presented here. Fig. 36 shows the physical configuration of Design No. 1 and Fig. 37 the configuration of Design No. 2 and Design No. 3. These latter two designs are the same with the exception of the method used to apply the cathode coating.

Table XI gives a summary of the tests and analyses of the resulting damage observed. Failure areas and remarks have been labeled for cross reference in Fig. 36 and Fig. 37. Radiographs of the three diodes after shock tests are shown in Fig. 38, Fig. 39 and Fig. 40 respectively.

The cathode cone design weakness was not detected until Designs No. 2 and No. 3 were tested. Previous static tests on the cones had been successful; however, these preliminary investigations were not equivalent to impact tests. Since the heater lead circuit of Design No. 1 was broken at a low impact level, the cathode was not at operating temperature when impacted at higher levels; thus, the inadequacy of the design was not determined during that test.

d. Collector Assembly. The collector configuration tested is shown in Fig. 41. This assembly was undamaged after a test series of 12,500 G in all planes. Details of the design are the same as described in the section on the End Item TWT.

e. Impact Effects on Magnets. As part of the Body Assembly tests, the axial magnetic field of the focusing magnet stack was carefully measured. The platinum cobalt magnets in the configuration tested show no adverse effects or degradation in field strength after impacts exceeding 13,000 G.

f. TWT. One of the engineering model tubes, S/N 3, was fully encapsulated and shock tested. This tube incorporated the design modifications determined from the subassembly shock tests discussed in previous paragraphs.

Details of the capsule design and encapsulation are similar to that described for the End Item TWT. Fig. 42 shows a photograph of the capsule parts used for the TWT. Capsule parts were made in cast form from aluminum alloy 357.

Collector, body, and gun assembly designs were the same as described in the previous paragraphs with little or no changes. The gun assembly
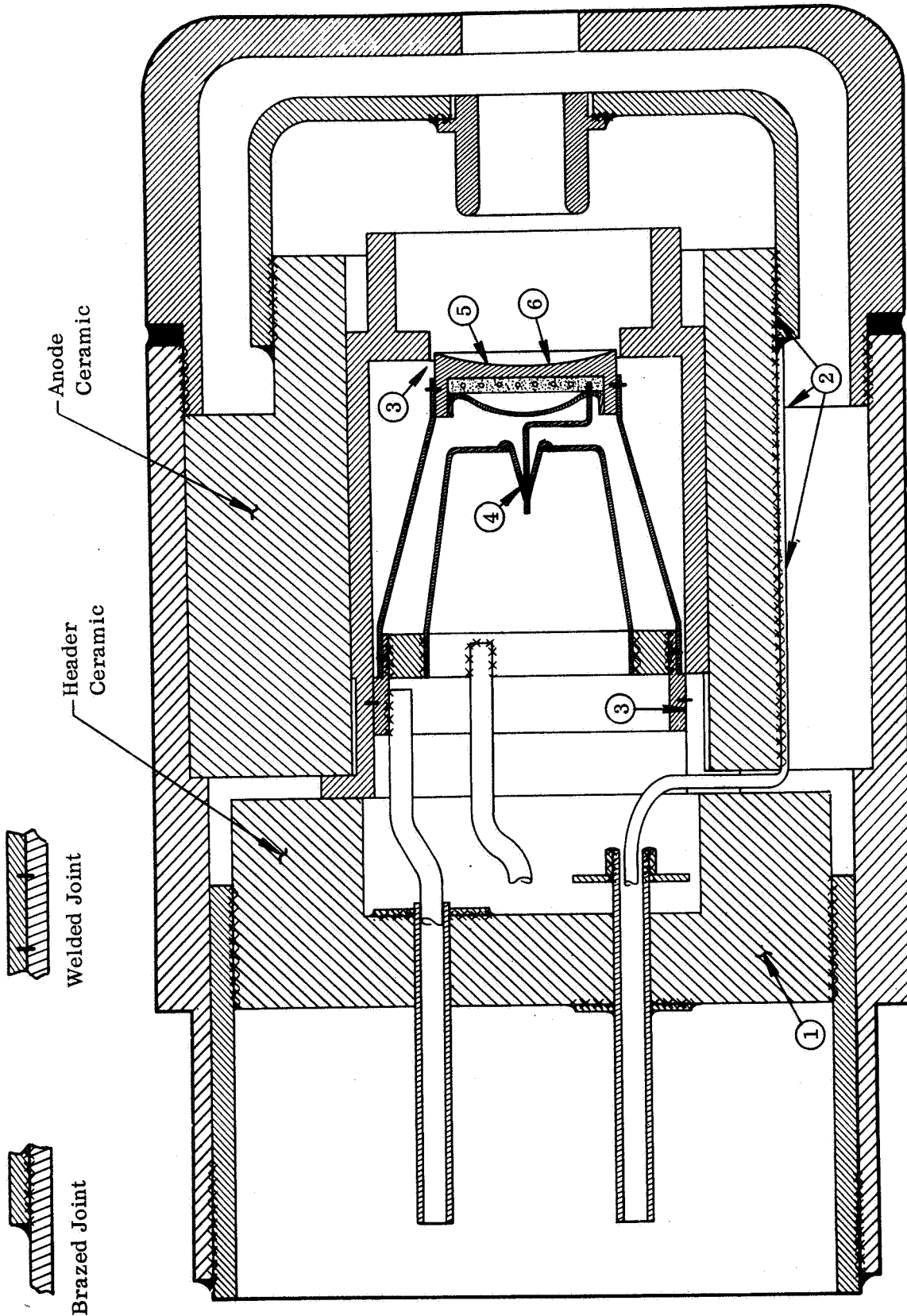
Fig. 36 – Physical configuration of Electron Gun Design No. 1. Labels refer to damaged areas after high impact tests, as follows: 1. Cracked ceramic causing vacuum leak, 2. Broken anode ceramic and displaced anode, 3. Displaced cathode assembly, 4. Heater lead circuit broken, 5. Loss of cathode coating, 6. Change in cathode radius of curvature.

15620
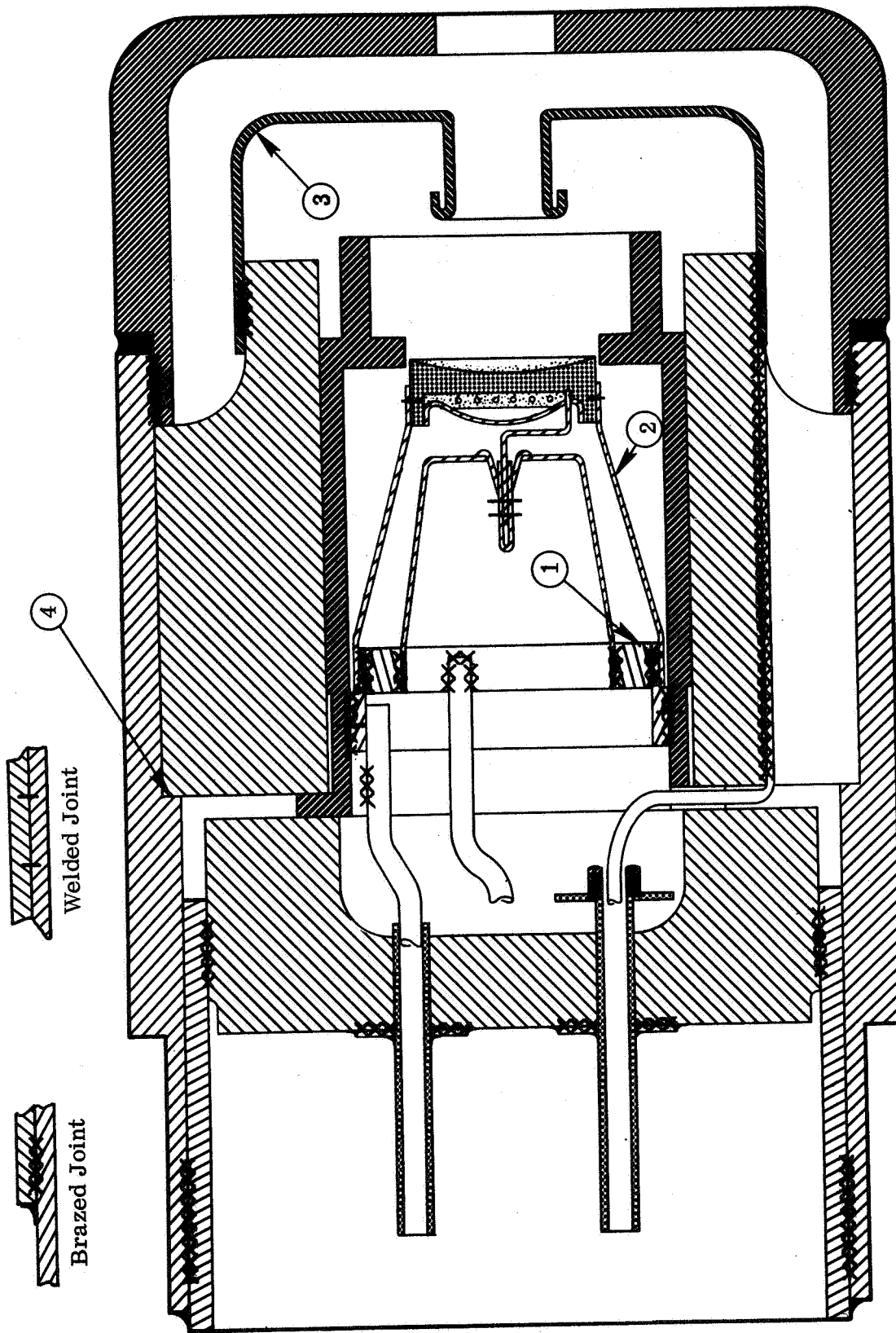
Fig. 37 – Physical configuration of Electron Gun Designs No. 2 and No. 3. The two designs differ only in the method used to apply the cathode coating. Labels refer to damaged areas after high impact tests, as follows: 1. Cracked heater ceramic, 2. Displaced cathode assembly, 3. Deformed anode electrode, 4. Chipped anode ceramic.

TABLE XI

ELECTRON GUN (DIODE) SHOCK TEST ASSEMBLIES

Design	No. 1	No. 2	No. 3
Physical Configuration	Per drawing of Fig. 36.	Per drawing of Fig. 37. Cathode coating applied using spray technique.	Same as No. 2 with cathode coating applied using brush technique.
Failure level or highest level tested	12,620 G (Axial)	9,000 G	13,020 G (Axial)
Highest level below failure	12,620 G	9,000 G	13,000 G (Transverse)
Failure mode/remarks	Reference labels in Fig. 36. 1. Cracked header ceramic–vacuum leak. 2. Broken anode ceramic. 3. Displaced cathode due to movement at base of cone. 4. Heater lead open circuit. 5. Loss of cathode coating. 6. Change in cathode radius of curvature.	Reference labels in Fig. 37. 1. Heater insulating ceramic cracked–tolerable. 2. Cathode support cone deformed changing gun perveance. 3. Anode electrode deformed changing gun perveance.	Reference labels in Fig. 37. 1. Heater insulating ceramic cracked – tolerable. 2. Cathode support cone deformed changing gun perveance. 4. Chipped anode ceramic.
Conclusions based on test results	1. Anode and header ceramics require redesign of geometry. 2. Base of cathode support requires enclosure about full circumference. 3. Heater weld to cone eyelet was marginal. 4. Cathode surface too smooth for adequate adherence of coating – roughen. 5. Thickness of cathode on axis must be increased. 6. Anode electrode too massive.	1. Cathode cone design inadequate. 2. Anode electrode requires redesign to remove "oil can" deforming. 3. Gun shell requires modification to remove sharp corners bearing on anode ceramic. 4. Both methods of applying cathode coating are adequate. Brush technique preferred for manufacturing reasons.	

- 68 -
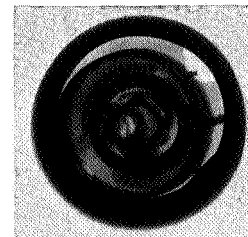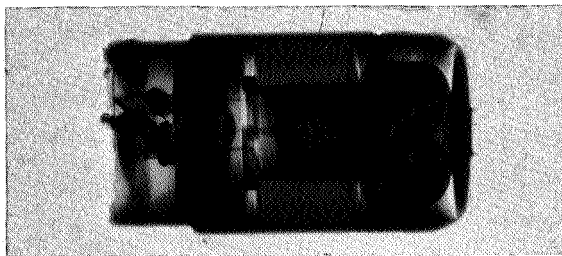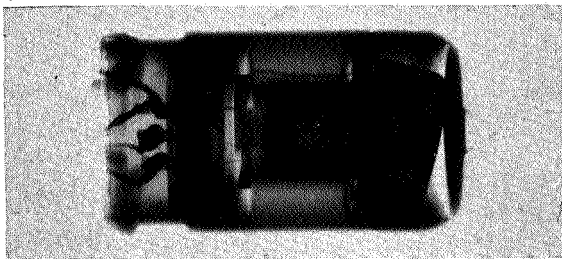
Fig. 38 – Radiograph of Electron Gun Design No. 1 taken after impact tests.
Assembly damage included cracked header ceramic breaking vacuum seal; broken
anode ceramic and displaced anode electrode; displaced cathode assembly; change
in cathode radius of curvature; loss of heater lead connection; and loss of cathode
coating.

18286
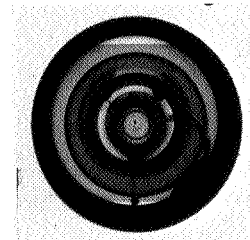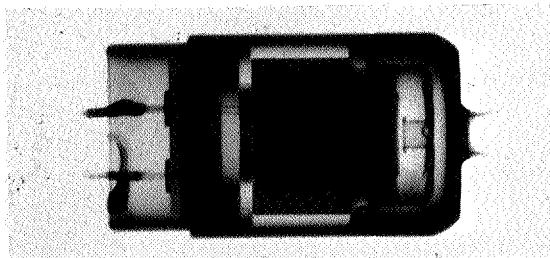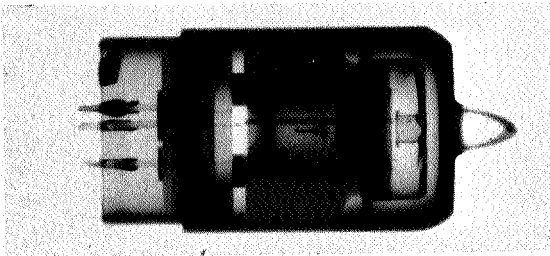
Fig. 39 – Radiograph of Electron Gun Design No. 2 taken after impact tests.
Assembly damage included cracked heater ceramic; deformed cathode cone
support; and deformed anode electrode (not visually detectable).
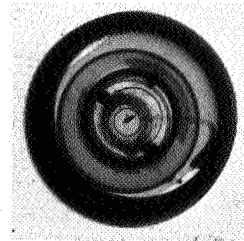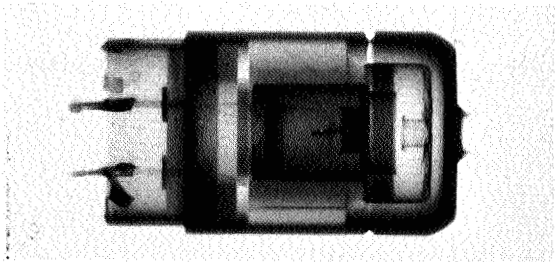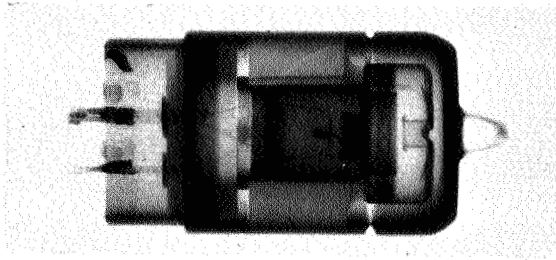
Fig. 40 - Radiograph of Electron Gun Design No. 3 taken after impact tests. Assembly damage included cracked heater ceramic; deformed cathode support cone; and chipped anode ceramic.

18288

Body Pole Piece

Ceramic Insulator

Collector Body

Brazed Joint

Brazed Joint
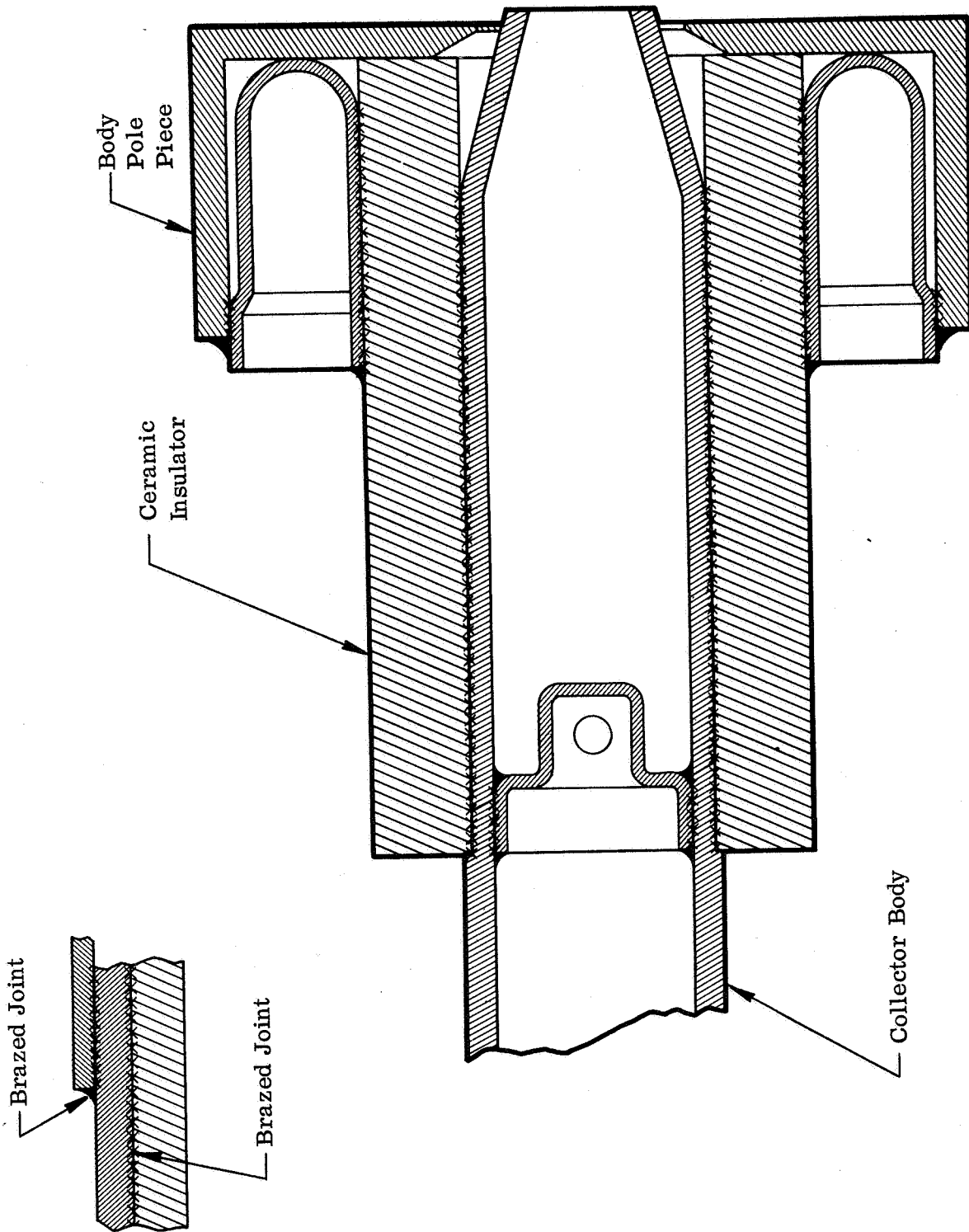
Fig. 41 -Collector shock test assembly. Unit remained undamaged after series of shocks to 12, 500 G in all principal planes.
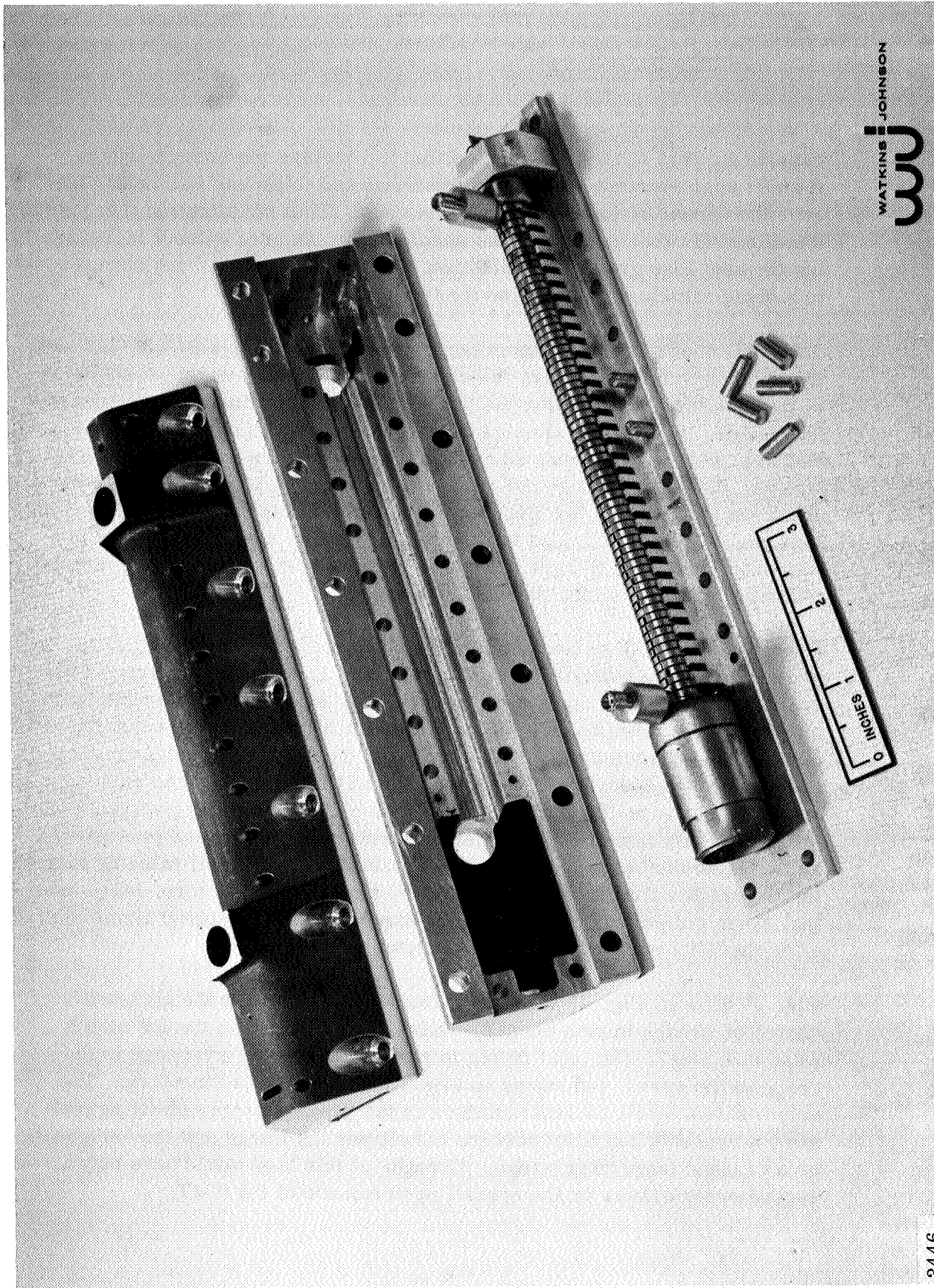
3446

Fig. 42 - Photograph of capsule parts used for the high impact TWT tests. Capsule parts are made in cast form from aluminum alloy 357. The tube is shown in the foreground mounted to the capsule bottom.

cathode support structure was modified to increase the cone strength.
A short cone segment of the same material and thickness was spotwelded
over the upper 40 percent of the base cone. This modification increased
the effective cross section of the cone in the weak area without increas-
ing the heat loss greatly. In addition, the anode electrode was changed
to a dome structure to increase its strength.

Table XII shows the shock tests performed on the WJ-398 S/N 3 TWT and
the relative values of several electrical and RF parameters. A summary
of the test results indicating the damage and test conclusions is shown in
Table XIII. Mechanical damage to the tube capsule is shown in Fig. 43
and Fig. 44. Cathode cone damage can be seen in the radiograph of Fig. 45.

After the test series, the TWT was removed from the capsule and the elec-
tron gun assembly removed for examination. The remainder of the tube
was examined using X-rays. Fig. 46 shows a radiograph of the assembly
indicating the lack of any detectable damage.

Changes in tube RF performance were observed after Tests No. 4, 11, 12,
and 13. Changes measured after Tests 4 and 11 were due to reduced beam
current while performance changes measured after Tests 12 and 13 were
attributed to altered beam optics. Careful analysis of the test data, X-ray
photos, and dissected tube parts attributed the changes to a deformation
in the cathode supporting cone which altered the location of the cathode
surface relative to the gun electrodes thus changing the gun perveance and
emission characteristics. RF performance returned to near pre-test
values when the beam current was increased to its nominal value by increas-
ing the anode voltage. No damage to the slow-wave structure, beam focus-
ing, beam collecting, or RF coupling structures, which could significantly
alter the TWT performance, was detectable.

Fig. 47 through Fig. 49 show performance results after the complete
series of 15 high impact shocks. Only minor changes in the RF match
were observed. The input match in particular showed no change in the
shape of the curve, indicating no alteration to the helix structure. The
output shows small periodic changes in the VSWR pattern indicating pos-
sibly a broken glaze fillet between the supporting wedge and the helix wire,
or a cracked supporting wedge. Changes of this kind would have only
second order effects on the overall performance of the TWT.

TABLE XII

SUMMARY OF SHOCK TESTS PERFORMED ON THE WJ-398 S/N 3 TWT

Test No.	Plane	Impact Level (G)	TWT CURRENTS					Relative Drive Level (dBm)	Relative Power Output Level (dBm)	Remarks
			I_F (A)	I_A (mA)	I_H (mA)	I_C (mA)	I_K (mA)			
1	X	JPL Pretest 950	.88	.026	8.5	45.5	54.02	-2.2	8.05	
			.88	.034	8.5	45.5	54.03	-0.9	8.05	
2	+Y	800	.88	.027	8.7	45.5	54.20	-0.8	8.07	
3	+Z	Unknown	.88	.027	8.6	45.5	54.10	-0.9	8.08	
4	-Y	6850	.88	.020	9.3	43.0	52.30	-0.1	7.55	(-1.1/8.2) when anode increased to $V_A = 458.7$ V
5	+X	5500	.87	.020	10.1	44.5	54.60	-2.0	8.20	$V_A = 458.7$ V
6	+Z	6000	.87	.023	10.0	44.5	54.60	-1.7	8.25	"
7	-Z	6200	.87	.021	9.9	44.2	54.10	-1.7	8.25	"
8	-X	6880	.86	.019	9.8	44.3	54.10	-2.0	8.25	"
9	+Z	9500 to 10,000	.86	.028	9.6	44.1	53.70	-0.9	8.25	"
10	-Z	8700	.86	.022	9.4	44.5	53.90	-1.8	8.20	(-/8.2) when anode increased to $V_A = 506$ V
11	-Y	8130	.86	.020	9.4	42.5	51.90	-0.4	7.92	$V_A = 506$ V
12	-X	8500	.86	.024	10.1	44.0	54.10	-1.4	8.05	"
13	+X	8300	.86	.022	9.2	43.5	52.70	-0.9	8.30	

Input   Output

Z   X   Y
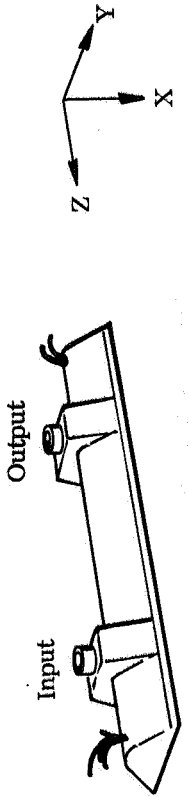
TABLE XIII

SUMMARY OF TWT SHOCK TEST RESULTS AND CONCLUSION

Physical damage to assembly.

    1. Transverse crack in capsule casting.

    2. Collector high voltage lead severed - caused by fixture.

    3. Indentation in top of capsule - caused by defect in fixture.

    4. Capsule ends deformed in longitudinal direction.

    5. Displaced cathode assembly (deformed cathode support).

Test Conclusion.

    1. Capsule redesign required; change to stronger wrought material; alter pin location and thickness of end walls.

    2. Stronger cathode support required.
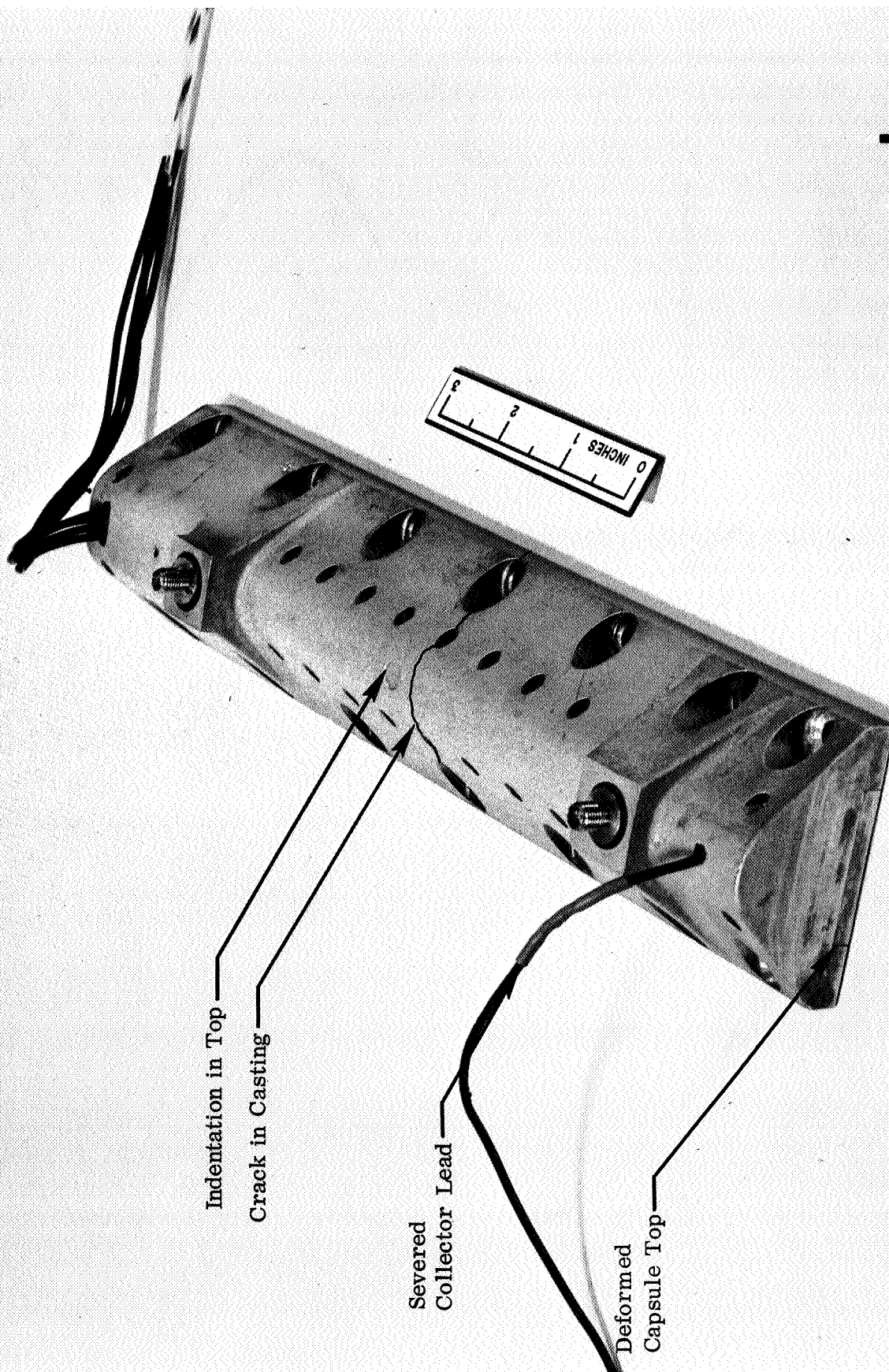
Fig. 43 - Top view of the WJ-398 S/N 3 after high shock test series showing damage to capsule. Crack in casting (shown accentuated) followed line of minimum material between mounting bolt base and taper pin hole. Indentation in top and severed collector lead caused by fixture deficiency. No adverse effects on tube performance were attributable to these items.

3445-1

Crack in Casting

Altered Taper Pin Fit

Deformed Capsule Top

WATKINS JOHNSON
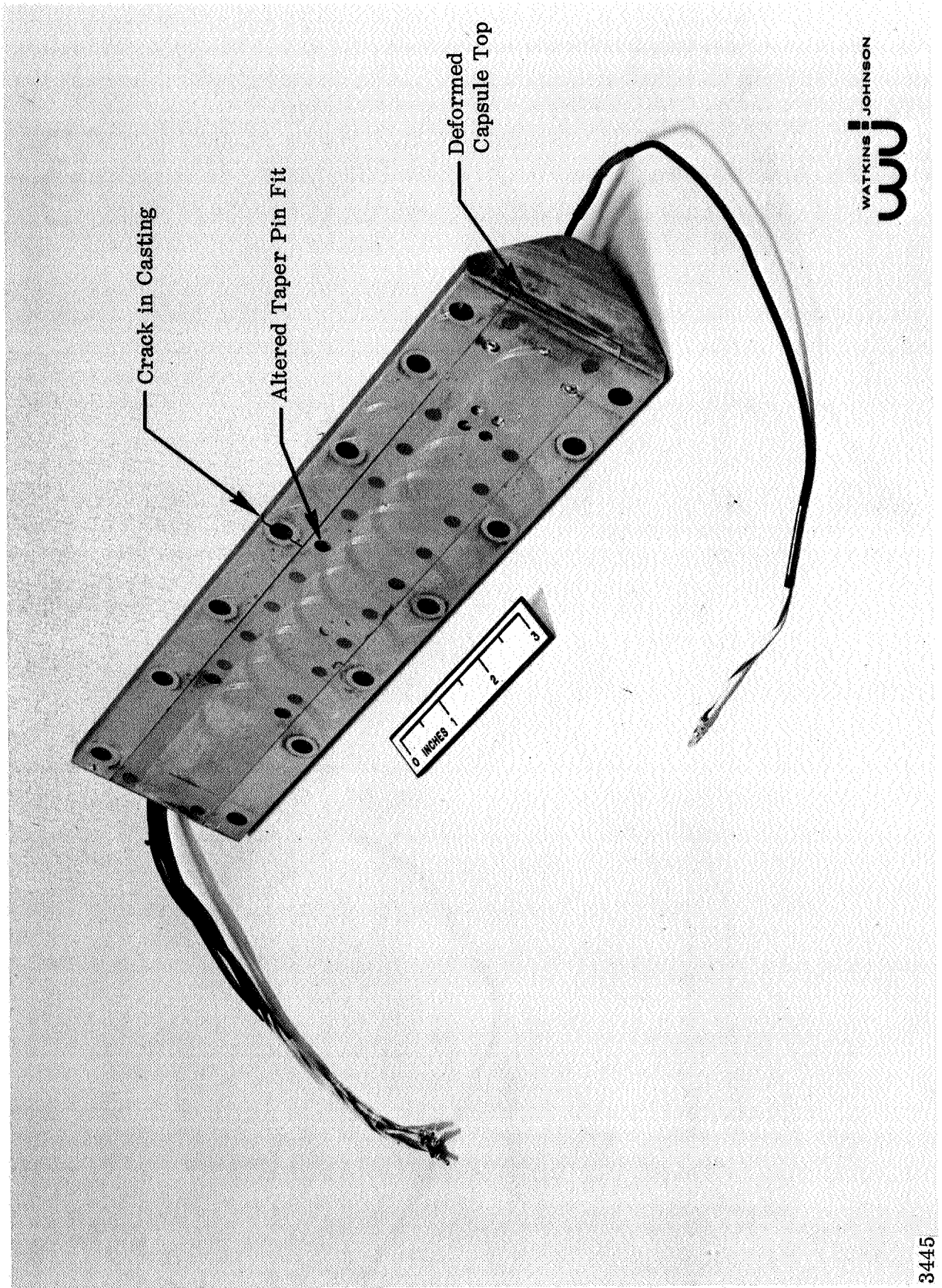
3445

Fig. 44 – Bottom view of the WJ-398 S/N 3 after high shock test series showing damage to capsule.
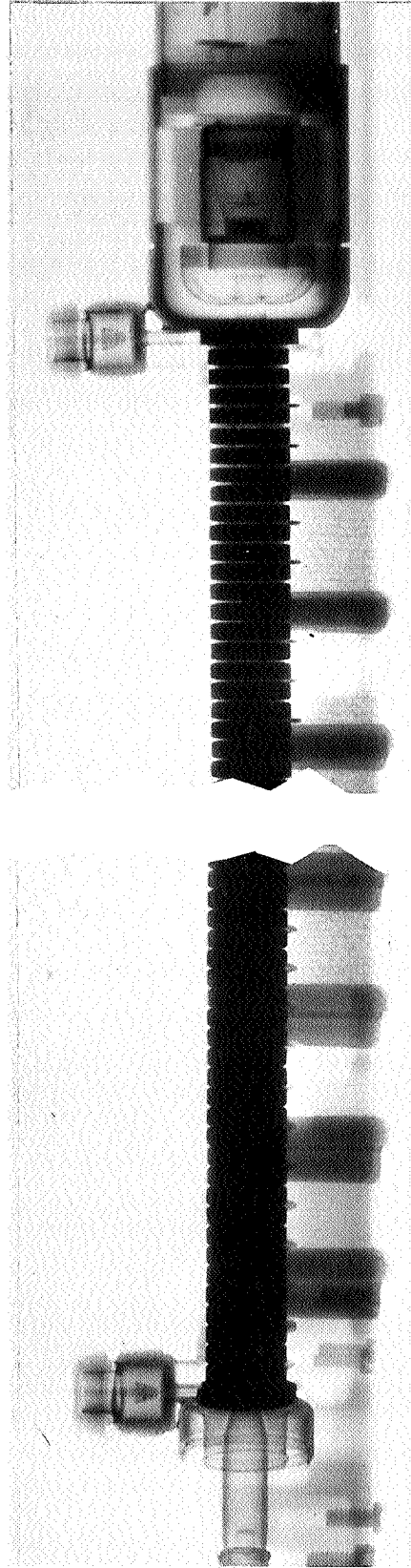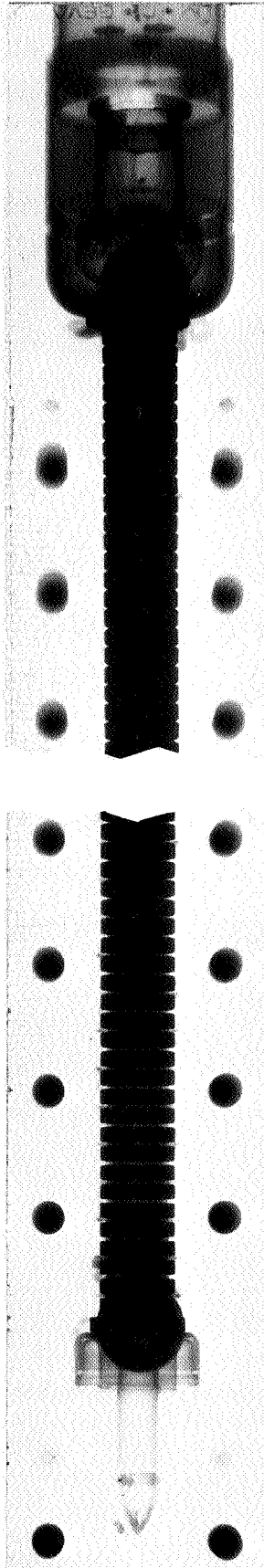
Fig. 45 – Radiograph of the encapsulated WJ-398 S/N 3 after high shock test series. Only detectable damage to vacuum tube and assemblies is shown at the base of the cathode support cone.
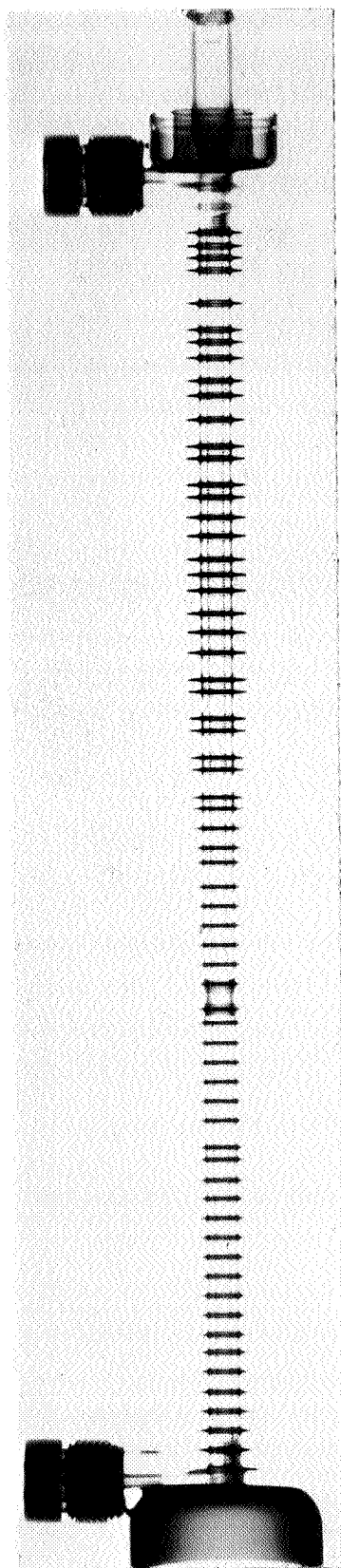
Fig. 46 - Radiograph of the body and collector assemblies (with magnets removed) of the WJ-398 S/N 3 taken after high shock test series. No detectable physical damage to these assemblies was found.

WJ-398, Serial No. 3

TWT Input

TWT Output

Frequency – GHz
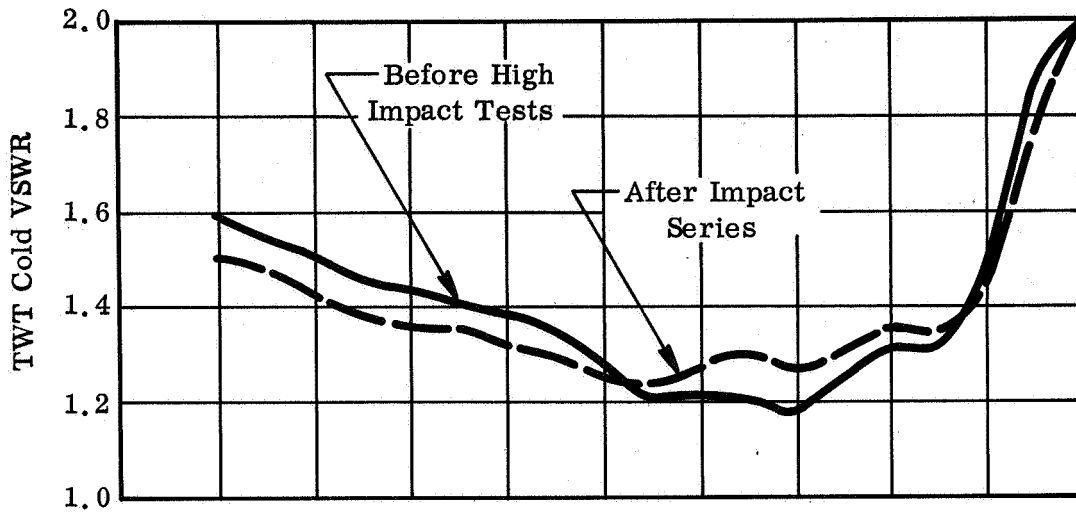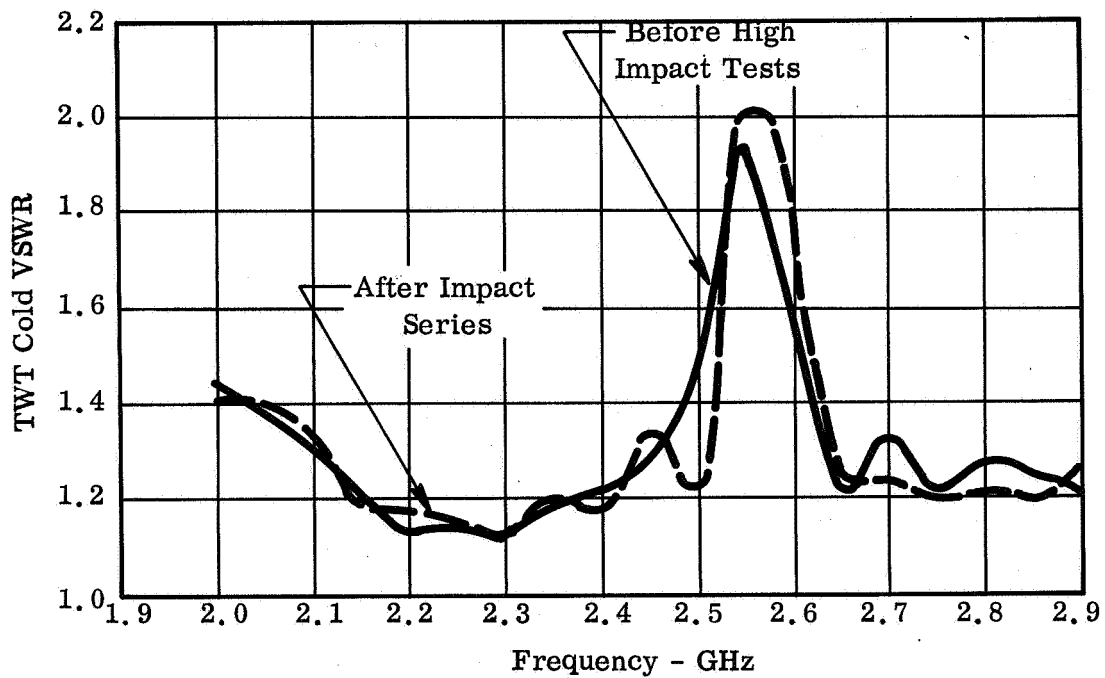
Fig. 47 – Comparison of the WJ-398 S/N 3 RF match after high impact series showing only minor changes in VSWR.
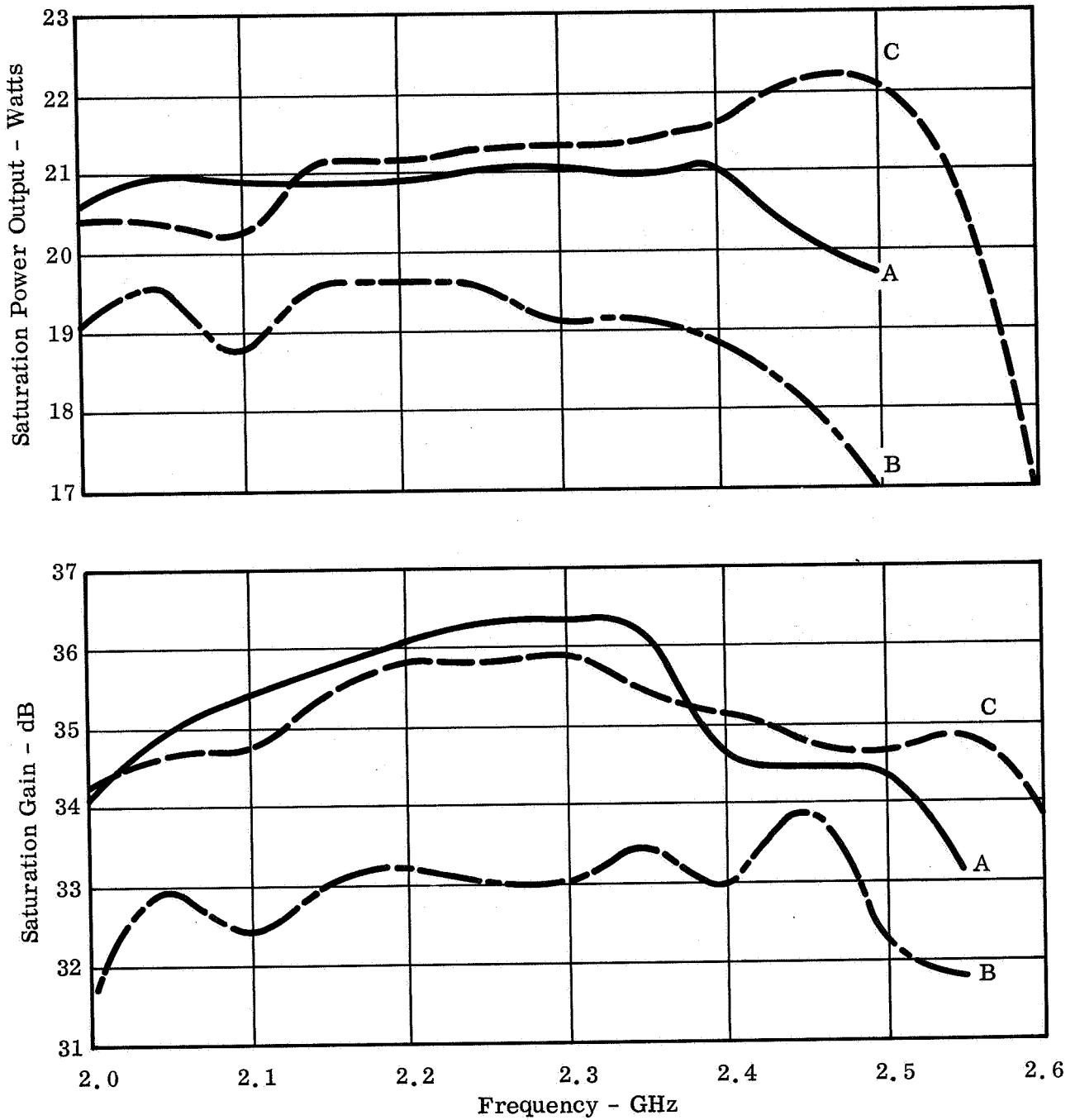
A – Performance before shock test series.

B – After test series with same operating voltages as "A".

C – After test series with same operating voltages as "A" except anode increased to give same beam current as "A".

Fig. 48 – Performance comparison of WJ-398 S/N 3 after shock test series.
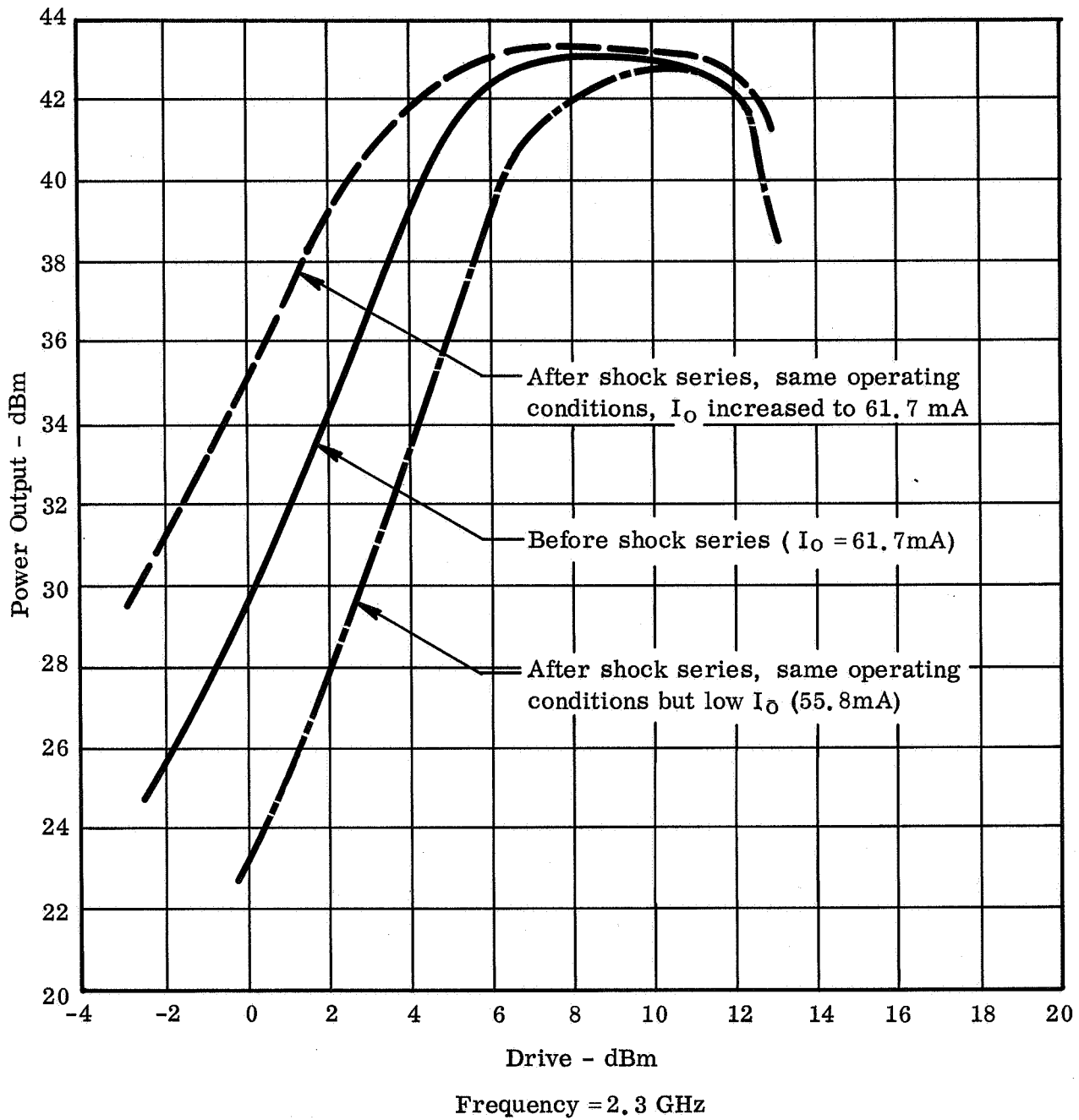
Fig. 49 - WJ-398 S/N 3 Power transfer characteristic comparison after high impact shock series.

The upper part of Table XIV shows a performance comparison which would be of interest to the spacecraft mission engineer. The TWT is operating with fixed voltages and RF drive. While the power output is lower by 2.3 dB, the TWT is no longer drive to saturation. If the drive level had been set at 10.1 dBm so the TWT was saturated at the same drive level in both cases, the power output would have been only 0.18 dB below the pretest value. The lower half shows the comparison with fixed drive and TWT voltages with the exception of the anode voltage which has been increased to give the same beam current. Note, even with the improperly generated electron beam, the TWT saturation performance is very nearly identical.

In summary, the TWT after being subjected to a total of 15 high impacts including all six directions of orientation, was capable of very nearly identical performance. It should be noted, in an actual system only a single shock would be encountered. Damage which did occur included two items – tube capsule and cathode support structure.

The capsule design was modified to use a high strength aluminum alloy in wrought form. In addition, the physical location of the taper pins was altered to increase the material thickness around the pins. Details of the modified design are discussed in the section describing the End Item TWT.

Additional studies were made on the cathode cone support. An investigation of a number of alternate materials was conducted as well as a re-evaluation of the heat treating procedure for Hastelloy alloy B material. The materials considered were Inconel 718, Inconel 625, and Rene' 41. Both Inconel 718 and Rene' 41 are age hardenable materials which means their strength characteristics are improved by aging at its precipitation temperature for a finite time such as 16 hours. However, in some cases, the strength does not remain at its "hardened" value but degrades over time at temperature. For this reason, these two materials were considered undesirable.

Table XV gives a detailed description of the cathode cone assemblies tested under high G loading. Each assembly consisted of a cylindrical button made of 220 nickel which weighed 1.6 times the weight of the cathode assembly used in the traveling-wave tube, a support cone made of the material as noted in Table XV, and a cylindrical base to which the cone was mounted for testing. Since impact tests could not be economically

TABLE XIV

WJ-398 S/N 3 PERFORMANCE COMPARISON
AFTER SHOCK TEST SERIES

"TELEMETRY" DATA COMPARISON (Spacecraft Conditions Constant)		
Parameter	Before Shock Series	After Total of 15 Impacts
Frequency	2.3 GHz	2.3 GHz
Power Output	43.23 dBm = 21.05W	40.92 dBm = 12.4W*
Gain (Constant Drive = 6.9 dBm)	36.3 dB	34 dB
Overall Efficiency	25.6%	---
DC Power	82.4W	73.3W
TWT Input VSWR	1.39	1.32
TWT Output VSWR	1.11	1.13

* Tube not driven to saturation. If increase drive to 10.1 dBm, saturated power output is 19.1W - only 0.18 dB below pretest value for same drive.

LABORATORY PERFORMANCE COMPARISON (Beam Current Constant)		
Parameter	Before Shock Series	After Total of 15 Impacts
Frequency	2.3 GHz	2.3 GHz
Saturation Power Output	43.23 dBm = 21.05W	43.35 dBm = 21.6W
Saturation Gain	36.3 dB	36.25 dB
Beam Efficiency	23.1%	23.8%
Overall Efficiency	25.6%	25.4%
Input VSWR	1.39	1.32
Output VSWR	1.11	1.13

TABLE XV

CATHODE CONE SHOCK TEST ASSEMBLIES

SAMPLE	CONE MATERIAL	MATERIAL THICKNESS (Inches)	HEAT TREATMENT * (°C)
1	Hastelloy B	0.002	1175
2	Hastelloy B	0.002	980
3	Hastelloy B	0.002 With 0.002 Outer Cone	1175
4	Inconel 625	0.002	980
5	Hastelloy B	0.003	1175
6	Hastelloy B	0.003	980
7	Inconel 625	0.003	980
8	Hastelloy B	0.004	1175
9	Inconel 625	0.004	980

* 15 minutes wet H_2, Rapid Cool

run under conditions duplicating the operating temperature of the TWT assembly, the test cones were tested at room temperature. The increased mass of the button compensates for the reduced strength of the cone material at operating temperature and for the limitations of the shock test equipment. For example: the yield strength of Hastelloy B at 750 degrees C is 1.45 times lower than at 23 percent C and Inconel 625, 1.5 times lower. Thus, the 10,000 G pulse for the TWT should be increased to 15,000 G for the cone assemblies; or since the test equipment cannot reach 15,000 G, the mass of the button was increased with a 10,000 G shock pulse.

Table XVI shows the results of the test, and Fig. 50 shows an X-ray photograph of the assemblies after test. A list of conclusions based on the test results as well as other influencing factors is shown in Table XVII. The 0.003 inch Inconel 625 material annealed at 980 degrees C   is the preferred material.

C.   TEMPERATURE STERILIZATION

The requirement that sterilization be accomplished by heating of the tube to 145 degrees C for a total period of 108 hours can have an appreciable effect upon the PPM focusing magnets. Based upon manufacturers data for the platinum-cobalt magnet material, the magnetic field strength would decrease with increasing time and temperature. Under sterilization conditions the magnetic field for platinum-cobalt in free space would decrease to 88 percent of the initial value. The effect of temperature on a magnet under the magnetic loading conditions found in an actual PPM magnet stack had to be determined.

A number of experiments were run to determine the effects of the sterilization condition on the magnetic field and to determine the final magnetic design. Degradation in magnetic field was found to be a function of the magnetic loading conditions and the previous state of the magnetic material.

When a magnet stack similar to the geometry shown in Fig. 51, using magnets which had been saturated with a dc field and then demagnetized with a reversing polarity field, was measured, the average peak axial magnetic field degraded less than 2 percent after three sterilization cycles. When a magnet stack using magnets magnetized and demagnetized in the same manner but tested in a geometry similar to Fig. 52, there was an initial degradation after the first cycle of approximately 5 percent. If the magnets are saturated with a dc magnetic field and not stabilized with a reversing field, when tested in a stack similar to Fig. 52, the initial degradation increases to approximately 12 percent.

TABLE XVI

CONE ASSEMBLY TEST RESULTS
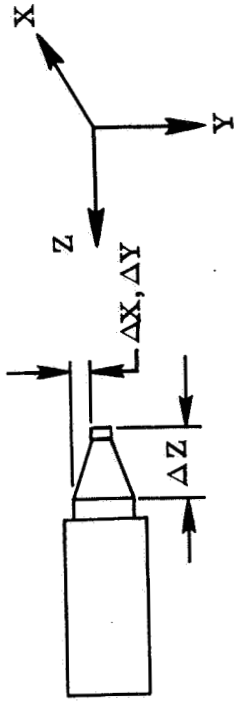
Sample	Dimensional Change – Inches *				Remarks
	X plane (10,750G̅)	Y plane (10,750G̅)	Z plane (10,750G̅)	X plane (12,960G̅)	
1a, 1b, 2a					Untested
2b	0.019				Gross Damage
3a	0.003	0.011			Damaged
3b			0.0007	0.003	Damaged
4a			0.001	0.027	Gross Damage
4b	0.003 to 0.004	0.055			Gross Damage
5a		0.016			Damaged
5b	0.006	0.009	Damaged by Fixture		Fixture Damage
6	0.002	0.003	0.0003	0.001 to 0.002	Undamaged
7a		0.002	0.0002	0.001	Undamaged
7b	0.001	0.003	0.019	0.004	Damaged
8a	0.001			0.0004	Minor Damage
8b			Damaged by Fixture		Fixture Damage
9a	0.002	0.003 to 0.004		0.0004	Minor Damage
9b			Damaged by Fixture		Fixture Damage

* Dimensions readable to ±0.0001; repeatable to ±0.001.

- 88 -
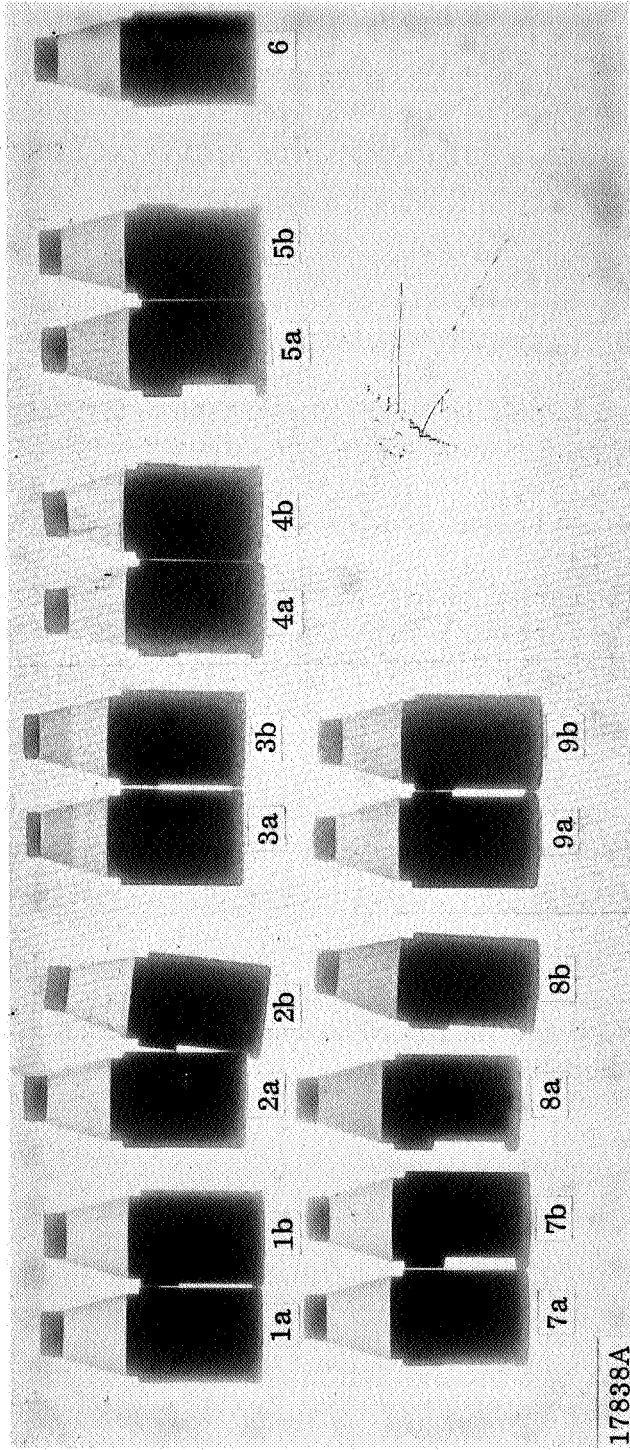
Fig. 50 – Radiograph of WJ-398 cathode cone assemblies after shock tests.

TABLE XVII

CONE ASSEMBLY TEST COMMENTS AND CONCLUSIONS

Comments

1. Cones 6 and 7a gave the best results both visually and dimensionally.

2. Cones 3a and 3b held up better than anticipated; however, investigation of the radiograph showed these items did not have the heavier button.

3. Cones 8a and 8b showed greater damage than 6 and 7a.

4. The use of a heavier button, to compensate for the reduced material strength at temperature, over stresses the base of the cone – where most cone damage occurred.

5. Cold tests do not include influence of changes in elongation of material.

6. "All else being equal" Inconel 625 is preferred to Hastelloy B since it is not an age hardenable material – strength may reduce with age at temperature.

Conclusion

The preferred material is 0.003 inch thick Inconel 625 annealed at $980^{\circ}C$ in wet H_2 for 15 minutes with rapid cooling.

Magnets

Body Tubing

Helix Assembly
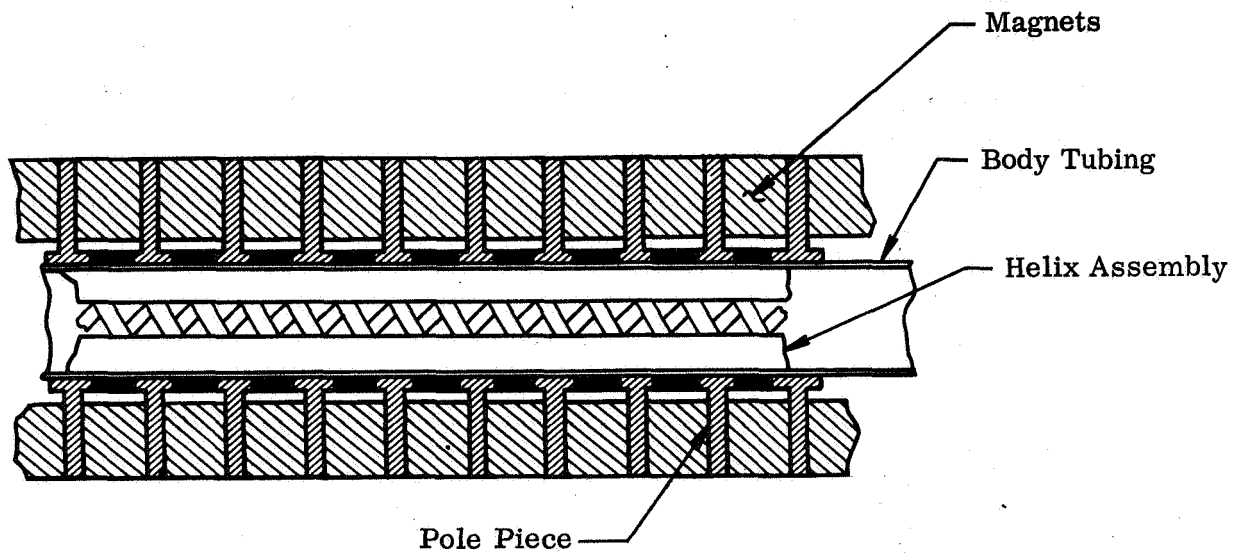
Pole Piece

Fig. 51 –Beam focusing structure using pole pieces and magnets with equal outer diameters.

Magnet

Helix Assembly

Pole Piece

Body Tubing
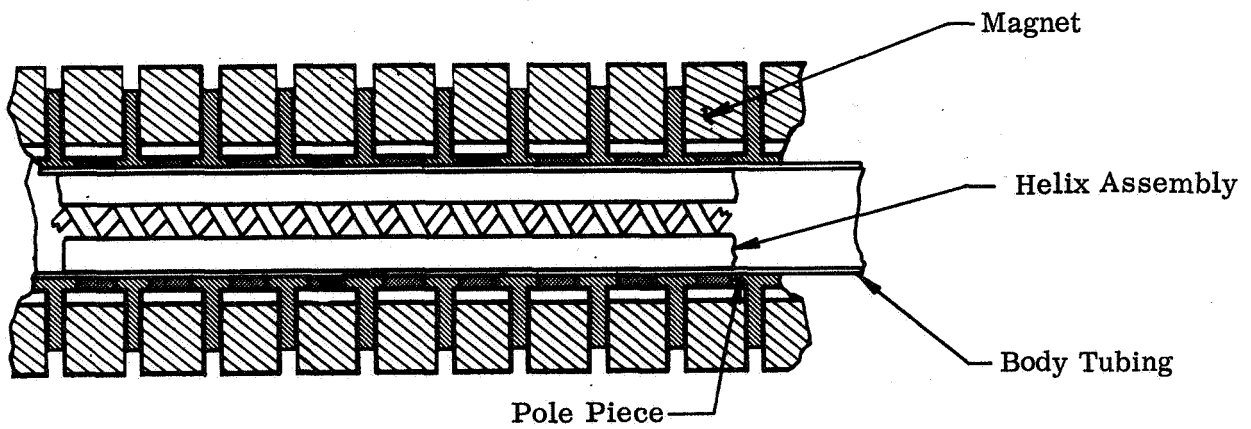
Fig. 52 –Beam focusing structure using pole pieces with a smaller outer diameter than the magnet.

18257

- 91 -

The reverse polarity magnetic field accomplishes the same stabilization effect as the temperature cycle as long as the subsequent temperature range does not exceed the prestabilized range.

The under cut pole piece geometry is necessary for the impacting support; moreover, it has the beneficial effect of increasing the axial field since the external leakage fields are reduced. Thus, the overall maximum magnetic field level can be increased to a level to compensate for the degradation experienced during stabilization.

Magnets are thus prestabilized using a reversing magnetizing field and then in addition are temperature prestabilized on the TWT at 150 degrees for 36 hours.

Fig. 53 shows the helix interception as a function of depressed collector voltage both before and after the tube is put through the temperature stabilization cycle. Helix current increased after the cycle but returned to values lower than the pre-cycle figures after readjusting the focusing, indicating the absolute magnitude of the magnetic field change only slightly. After these prestabilization procedures – reversing field and temperature – the TWT was encapsulated and the temperature sterilization cycle repeated. Helix interception after the cycle (without adjustment) was within 1.7 percent of its pre-cycle value. Tube S/N 4 – the End Item TWT – when processed in the same manner, showed similar results. RF performance was unchanged.

D.   ELECTRICAL DESIGNS

During the program three TWT's, representing two different electrical designs, were manufacturered and tested. Both designs were based on the parent tubes, the WJ-274 and the WJ-274-1. Table XVIII shows the design parameters for these three tubes with the WJ-274-1, and the WJ-274 S/N 13 added as a reference.

The performance characteristics versus frequency for the WJ-398 S/N 1 are shown in Fig. 54. At 2300 MHz the tube delivers 22.4 watts with 41 dB gain and an overall efficiency including heater of 29.3 percent. The WJ-398 S/N 4 which is of the same design as S/N 1 delivered 23 watts with 41 dB gain and 32 percent overall efficiency. (Refer to Fig. 3). Fig. 55 shows the same characteristics for the WJ-398 S/N 1 with the helix voltage optimized for maximum efficiency at each frequency. In this figure beam efficiency is presented rather than overall efficiency. As shown in the figures, the performance is optimum at a frequency between 2200 to 2300 MHz. Fig. 56 shows a comparison of the performance characteristics versus helix voltage for tubes S/N1
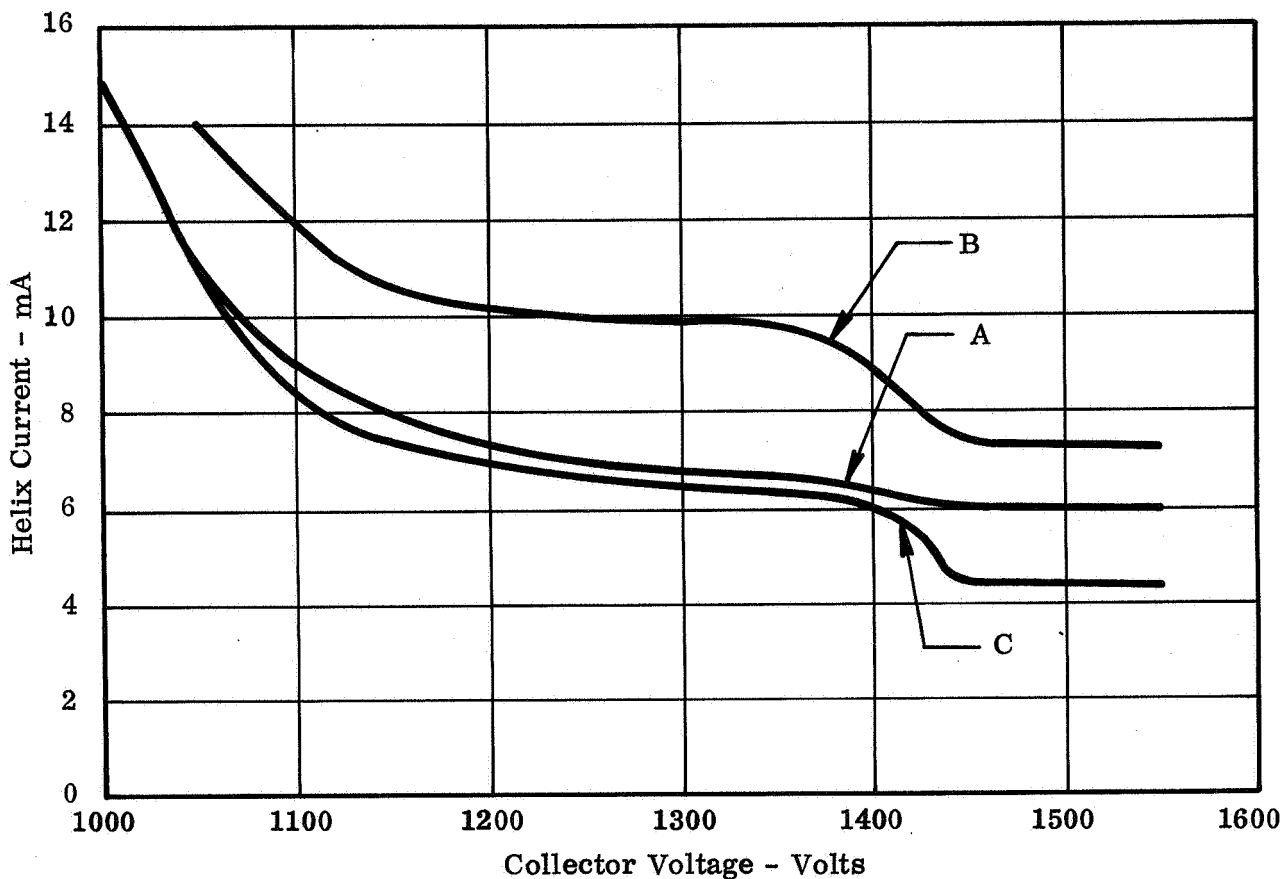
$V_A = 2000\ V$ $P_{out} = 16\ W\ Nominal$

$V_H = 1460\ V$ $Gain = 40\ dB\ Nominal$

$I_o = 61\ mA$ $F = 2.3\ GHz$

$P_{htr} = 4.5\ W$

A. Before Temperature cycling
B. After 150 °C bake for 24 hours
C. After bake and refocusing

Fig. 53 - Depressed collector characteristics of WJ-398 S/N 3, for various conditions related to temperature sterilization.

TABLE XVIII

TUBE TO TUBE
VARIATION IN DESIGN

Tube	Helix TPI		Active Helix Length	
Serial Number	Input	Output	Input	Output
1	54	60	2.07"	2.70"
2	Assembly discontinued in process................			
3	54	61.3, 56	1.75"	2.46", 0.61"
4	54	60	2.07"	2.70"
WJ-274-1	54	60	1.2"	2.70"
WJ-274 S/N 13	61.3	61.3, 56	1.75"	2.46", 0.61"
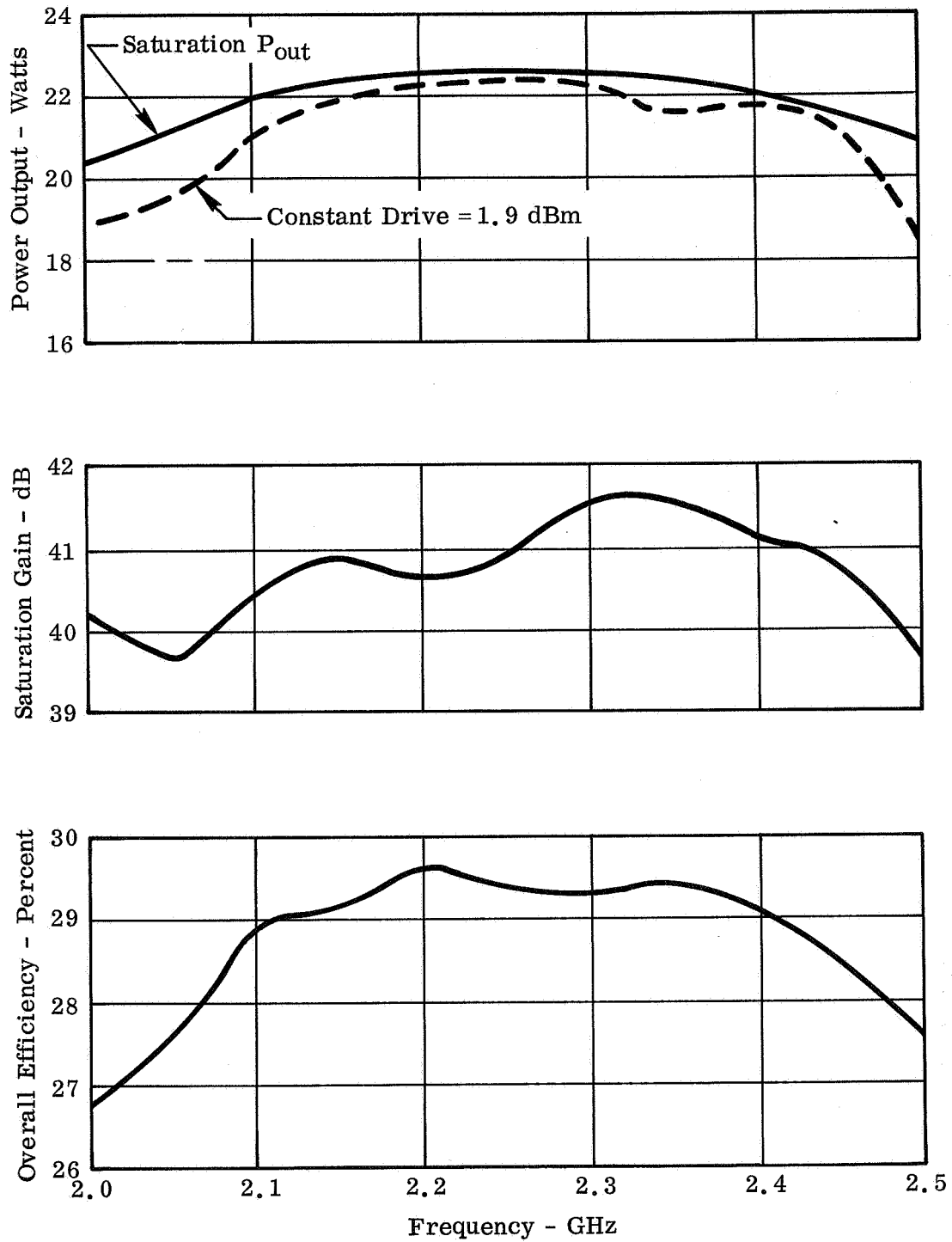
Fig.54-Power, gain, and overall efficiency characteristics for the WJ-398 S/N 1.
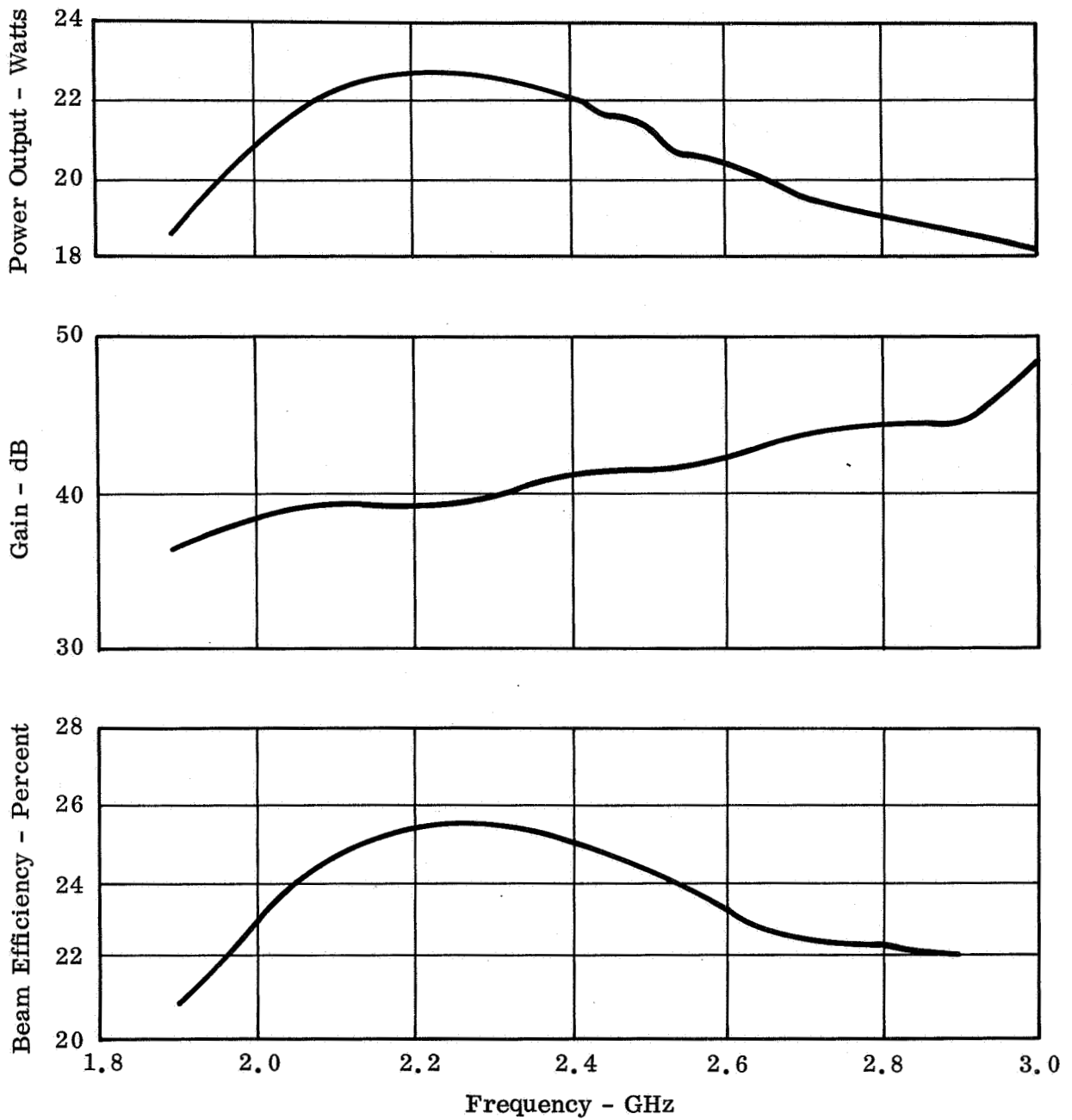
Fig. 55 – Power output, gain, and beam efficiency characteristics for the WJ-398 S/N 1. Helix voltage optimized at each frequency.

Fig. 56-Performance characteristics of the WJ-398 S/N 1 and S/N 3 TWT's.
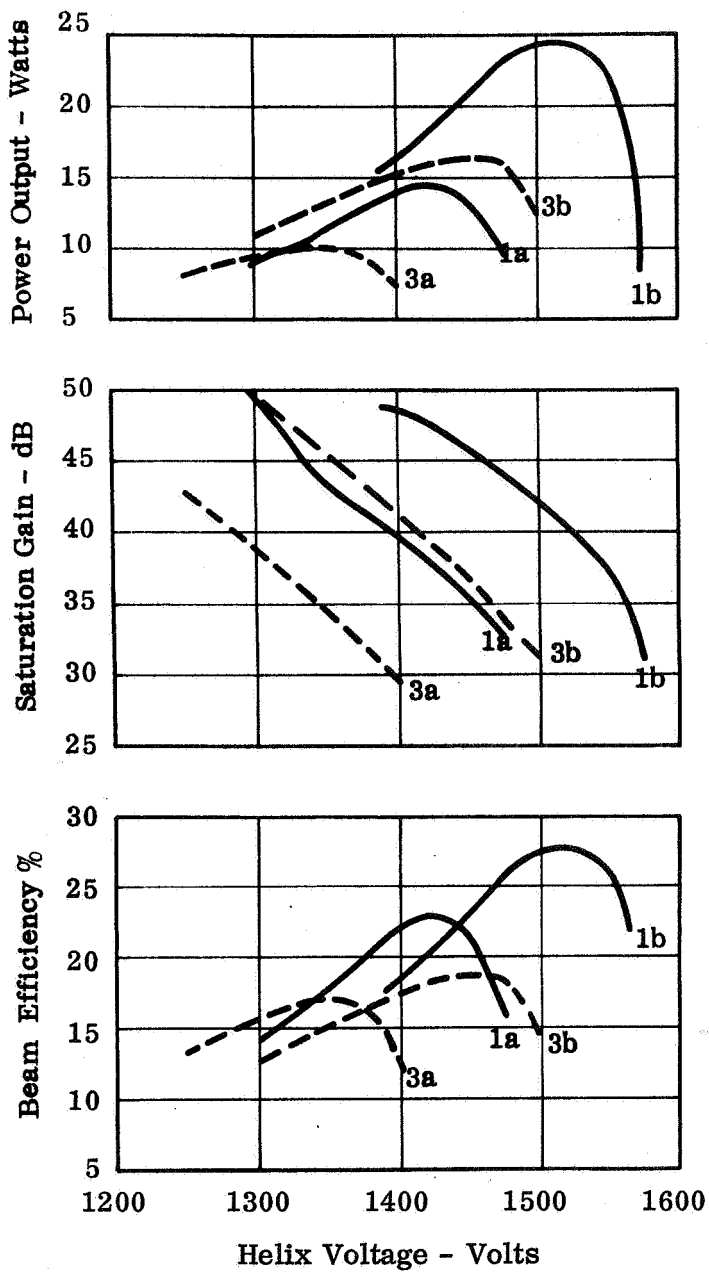
WJ-398 S/N 1 — — —   WJ-398 S/N 3 ————

1a, 3a   1b, 3b

$I_o = 44$ mA $I_o = 60$ mA

Frequency $= 2.3$ GHz

and S/N 3. The power transfer characteristics for the two tubes is shown in Fig. 57. The WJ-398 S/N 1 has greater saturation gain due to the longer length and lower TPI of the input helix.

E. MAGNETIC LEAKAGE FIELD

Early in the program, an encapsulated WJ-274-1 TWT was tested at the Jet Propulsion Laboratory facility to determine the magnetic leakage of a TWT which is magnetically similar to the then undeveloped WJ-398. The measured field at a distance of three feet had peak values of ± 17, ± 14, and ± 1 gamma in the three principal planes. Test data sheets of this test are shown in Appendix IV.

Leakage fields can be reduced using magnetic shielding material. However, the properties of the materials are susceptible to modifications by large shock or other aging mechanisms; and stray magnetic fields from other sources can induce magnetism in the shield. Another approach to reducing the magnetic fields at the location of sensitive instruments on the space craft is direct magnetic field compensation. Compensation cannot be obtained for the total radiated magnetic field of the traveling-wave tube, but compensation at preferred locations can be obtained. The compensating magnet material can be chosen to have the same temperature coefficient of magnetic field with temperature as the tube and compensation can be made to work over a wide temperature range. The use of a redundant amplifier in the system would allow placement to give a magnetic field of the opposite polarity at the location of sensitive instruments. The advantage of field compensation techniques are that the magnetic shields are eliminated entirely and the possibility of changes in magnetization of the shields at low level by stray magnetic fields is eliminated.

The WJ-398 design is magnetically similar to the WJ-274-1. The total stack length includes 68 platinum-cobalt ring magnets compared to 58 for the WJ-274-1. However, the leakage field does not increase proportionately since adjacent magnets tend to cancel one another. In addition, the pole pieces of the WJ-398 have been undercut relative to the magnet outer diameter. This has the beneficial effect of reducing the leakage fields.

Throughout the design phase of the TWT, the magnetic leakage requirement was considered in order to reduce the leakage fields. Only non magnetic materials were chosen except where magnetic materials were necessary for proper operation of the TWT. At this time, magnetic leakage field measurements have not been made on the WJ-398 TWT. The prototype hardware is now being evaluated at the Jet Propulsion Laboratory.
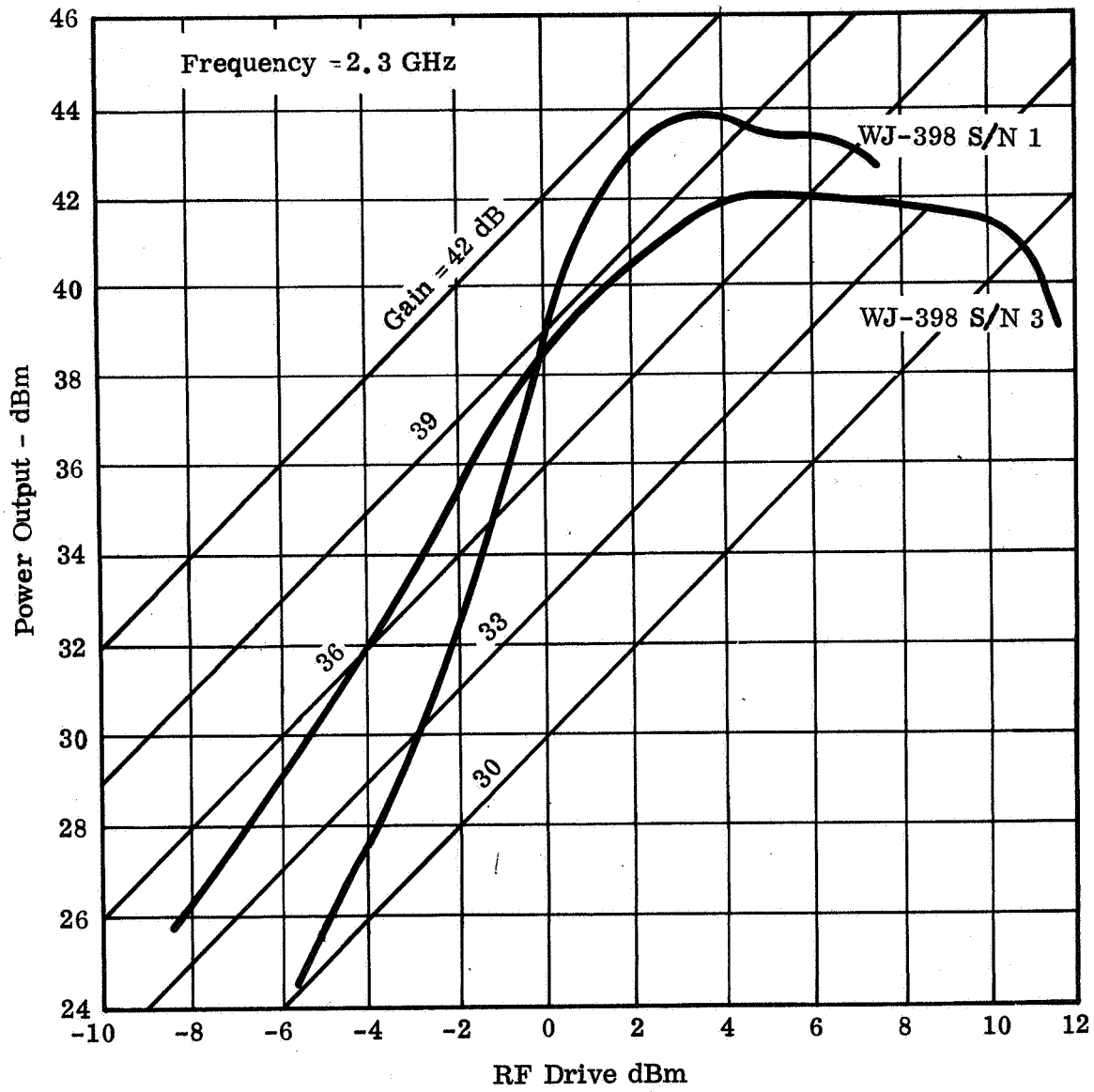
Fig. 57 - Power transfer characteristics of the WJ-398 S/N 1 and WJ-398 S/N 3 TWT's.

F.   Thermocouples, normally used to determine the cathode operating temp-
erature on long life TWT's, could not be used in the WJ-398 due to the high
impact requirements. Nevertheless, knowledge of the cathode operating
temperature is important to determining the life expectancy of this tube.
The rate of reduction of the barium oxide molecule to the metal barium
which is responsible for the low work function of the oxide cathode, is depen-
dent on the cathode temperature. The optimum operating temperature for
a TWT of this type is between 720 degrees to 740 degrees C. One method
of determining the cathode temperature without the use of thermocouples is
to determine the correlation between the cathode temperature and heater
characteristics of the TWT with similar data obtainable during the manu-
facture of the TWT.

During the manufacturing phase, every cathode focus electrode assembly is
vacuum fired using RF heating with the help of the filament power. After
this procedure, the assembly is cooled to room temperature and the cathode
heated to operating temperature using the heater power alone. At this point,
the temperature can be measured optically as a function of filament power.
If a test diode, which is identical to the TWT geometry so that the thermal
losses of the heater are the same as in the completed tube, is then tested,
the true cathode temperature of the TWT can also be determined.

After the correlation factor is determined, the cathode temperature of future
tubes can be determined by correcting the temperature measured during the
vacuum firing procedure. Fig. 58 shows a plot of the true cathode tempera-
ture (optically measured) versus applied heater power for the two cases of
interest. Also shown in the resulting reduction factor used when the focus
electrode assembly characteristics have been determined to obtain the
cathode temperature of the complete TWT assembly.

When a given focus electrode assembly is placed in the TWT, the cathode
operating temperature can be approximated by reducing the T_{cath} vs P_{htr}
curve obtained during the vacuum firing operation by the factor shown in
Fig. 58. The temperature is only approximate to the extent of the tube to
tube variations in the effective thermal path from the focus electrode to the
outer surface of the TWT envelope.

The data shown in Fig. 58 is for a structure like that used in Tube S/N 3.
However, the cathode support cone has since been modified to a single cone
made from Inconel 625. Therefore, the data of Fig. 58 is not directly appli-
cable to the prototype tube. An additional correlation experiment must be
performed before any flight units are manufactured.
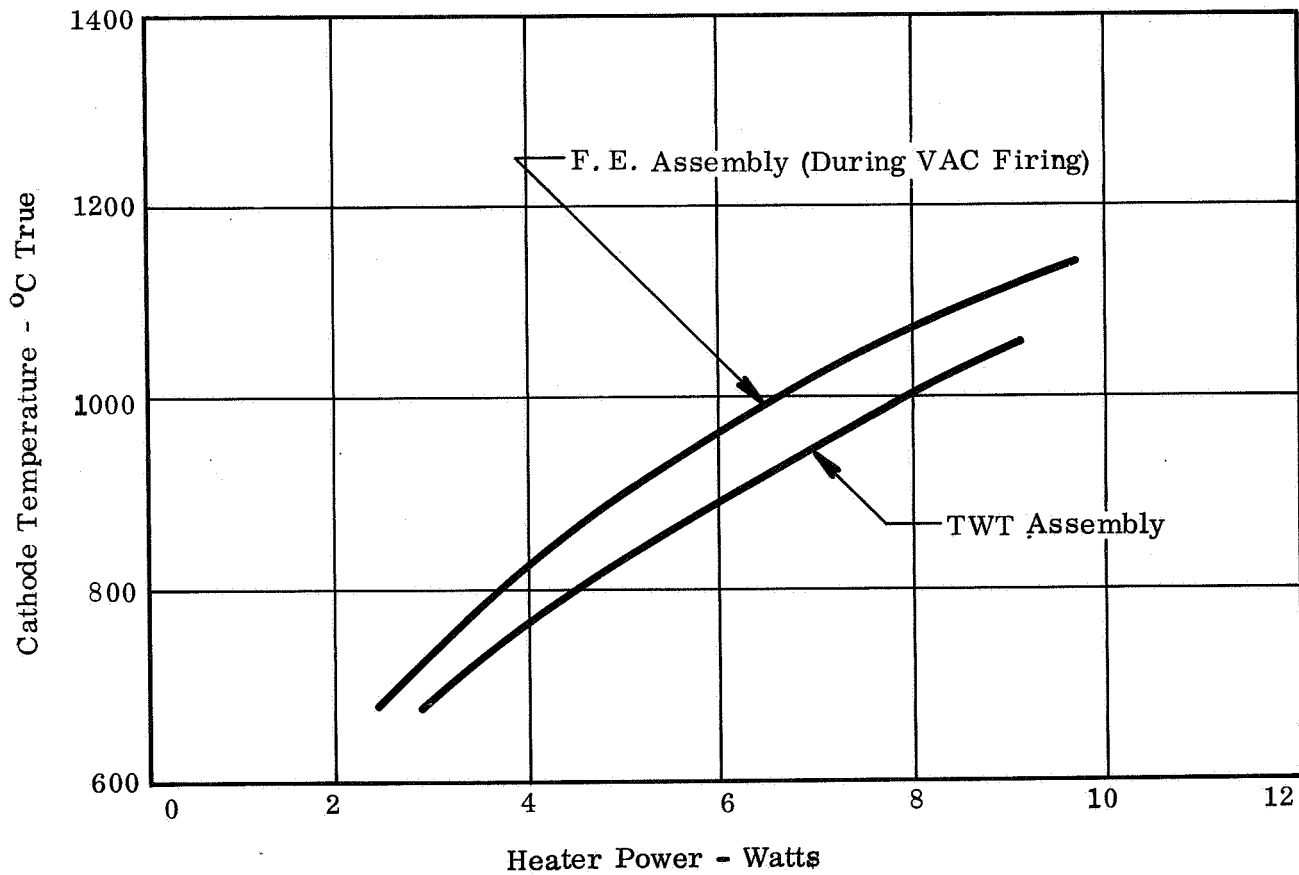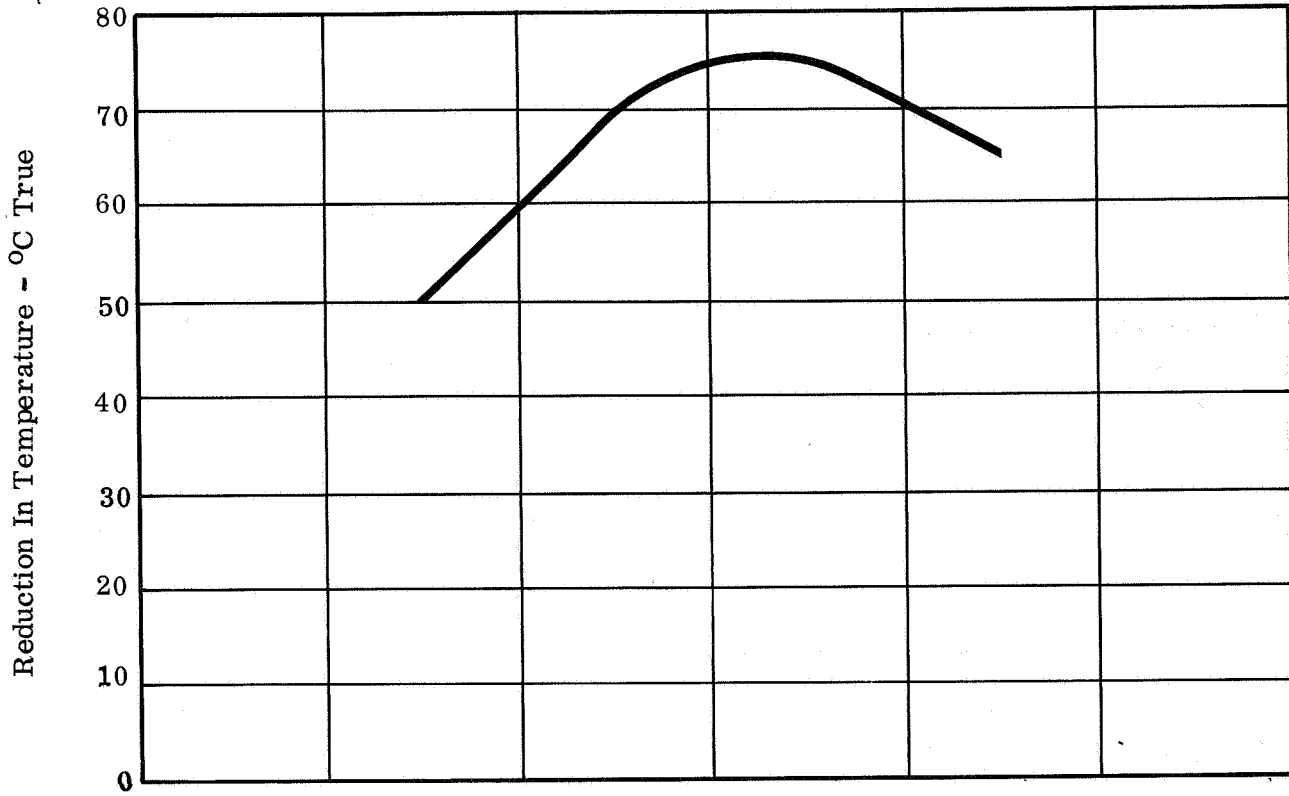
Fig. 58 - Cathode temperature, heater power characteristics of the
WJ398 S/N 3 electron gun structure.

17302

- 101 -

SECTION IV

TWT RELIABILITY AND LIFE

The inherent reliability of the traveling-wave tube amplifier is determined by the design of the two necessary constituent components - the traveling-wave tube and the output filter.

A reliability analysis has been performed by the supplier for the filter which shows an in-service MTBF of 11,000,000 hours. Due to the highly passive nature of this component, the lack of significant environmental test data and more importantly adequate failure mode criteria, no further theoretical analysis is deemed possible. Coupled with this information should be considered the fact that the active nature of the TWT makes the tube the limiting component with respect to the total amplifier reliability. Therefore, the remainder of this report concerns itself solely with the traveling-wave tube reliability and life.

A. RELIABILITY OF THE TUBE

Reliability of the tube is controlled by three basic aspects:

1. Reliable design.

2. Reliable construction.

3. Testing of the finished units.

1. Reliable design depends almost entirely on engineering experience in tube construction techniques and tube performance. Knowledge of tube performance under vibrational and other physical stresses can lead to a design choice. Within a device as complicated as a traveling-wave tube there are many facets of construction which bear upon the ultimate reliability. They have to do with methods of metal joining, support techniques of hot and cold parts, insulation techniques and many others. As can be seen, these depend to a great extent upon the engineering experience of the designer. Many times choices are made that ultimately may not prove to be optimum. These faults can be revealed by thorough testing both from the electrical and environmental standpoint and by constructing many samples.

2. Reliable construction is controlled by careful attention to high reliability and quality assurance procedures. It is Watkins-Johnson procedure to establish a tube construction and process control book for a tube at the completion of

the development phase. This book consists of complete assembly, sub-assembly and parts drawings, plus material lists and process control sheets. The book is so organized that by following its procedures step by step, the tube can be completely constructed and tested.

In addition to this, quality control sheets are generated for major subassembly operations. These sheets are so designed that critical steps and inspections must be done, and in most cases measured answers must be recorded. Each tube has a folder which accompanies it throughout the construction and testing phase and the quality control sheets are kept in this. Process of such items as helix phase velocity, attenuation profile, cathode vacuum firing, and cathode breakdown, are included in the folder. In the testing and final encapsulation phase test data sheets are filled out. In this way, it is assured that all required tests and measurements are performed.

Therefore, one can see that with the above type of documentation used in the fabrication of the tube, careful records of each tube assembled are available. In this way, repeatable performance is obtained; but more important, a detailed history of the fabrication of each tube is available and can be used to evaluate or predict its behavior.

3. <u>Final Quality Assurance Testing</u> is performed on the units on a 100 percent basis to determine that no marginal or defective unit is delivered to the customer. Throughout this testing phase, a complete running time log is maintained. A typical sequence of tests is as follows:

<u>Pre-Encapsulation Test</u>

This test establishes the tube performance versus frequency, drive power, etc.

<u>Stabilization of Magnets</u>

The non-operating tube assembly is cycled through 150 degrees C for 36 hours minimum to assure that the magnetic field is stable.

<u>Encapsulation and Age</u>

After encapsulation, the tube is aged under full RF conditions for a total of 300 hours minimum to assure full cathode activity and stability.

Pre-Environment Test

This test is performed to establish data for comparison with post environment tests.

Environment Tests

a. ## Vibration

The tube is vibrated in two transverse and one longitudinal plane over the vibration frequency range at some predetermined peak acceleration level which is chosen to pick out marginal tubes but which is not so large that the tubes can be damaged.

b. ## Temperature Sterilization

The tube is soaked, in a non-operating mode, at a temperature of 145 degrees C for 36 to 40 hours to assure stable performance after the sterilization cycle.

c. ## Temperature (as part of End Item Test)

Power output tests are made and tube element currents are monitored for five temperatures: Room ambient, low temperature limit, room ambient, high temperature limit, and room ambient.

d. ## Final Tests

This test establishes the final performance of the deliverable tube and is compared with the pre-environment tests to determine if any gross performance changes have taken place.

Fig. 59 shows the test sequences for the WJ-398 TWT prior to acceptance testing with the filter. Each tube has 400 hours of operation before the final acceptance test is performed on the amplifier. In this way, marginal and early failures are rejected. During the test sequence, detailed documentation of the performance of each tube is maintained.

It is seen that the reliability of a tube is a function of many facets of design, controlled construction and quality assurance testing. It cannot be assumed

that just good electrical design will necessarily result in high reliability tubes being delivered to the customer. It takes a carefully planned sequence of the operations of construction and testing to guarantee a product with a high degree of reliability.

B. TUBE LIFE

In a properly designed traveling-wave tube, tube life is determined by the wear-out life of the cathode. Experience has shown that the cathode life can be many tens of thousands of hours if a few simple precautions are followed. The three major precautions are:

● Maintenance of a very high vacuum throughout the life of the tube with freedom from poisoning agents, (i.e., $<10^{-9}$ mm Hg pressure).

● Prevention of ions in reaching the cathode from the helix and collector region by the simple expedient of operating the anode at a higher voltage and the collector at a lower voltage, than the helix.

● Controlling the reduction rate of the metal barium from the barium oxide coating of the cathode.

When the first two factors are provided for, the third factor becomes the controlling item and will determine whether the cathode will continue to perform for only a few thousand hours or for a life of over 100,000 hours. It is within the control of the tube designer to determine where within this wide range his tube will lie.

1. Tube Cleanliness. The assembly techniques used to obtain ultra-clean tubes with good cathode "activity levels" include the following operations:

●Selection of materials with low vapor pressures and free from contaminants,

● Rigorous parts and subassembly cleaning,

● Environmental control of the ultra-clean final assembly area,

● Pre-exhaust vacuum processing,

● Controlled atmosphere brazing system, and

●Extensive high-temperature, double vacuum, bakeout including cathode conversion at the high temperature.

All parts used in the tube are pre-cleaned using the normal degreasing and acid-etching techniques employed throughout the tube industry. After this operation, they are recleaned in a separate controlled atmosphere facility using deionized water and isopropyl alcohol with ultrasonic agitation. Mineral base acids and alkali solutions are prohibited in this facility.

Subassemblies which can be cleaned after fabrication are done so in the special cleaning facility; subassemblies which are not cleanable are built in the ultra-clean assembly benches which incorporates laminar flow filtered air. The air in these benches is passed through absolute filters so that particles larger than two (2) micron in size are essentially eliminated. The two (2) micron and larger particle count within these benches is less than 6-2/3 particles per minute with a sampling rate of 100 cubic centimeters per minute.

The cathode focus electrode assembly receives its own vacuum firing at temperatures up to 1000 degrees C in a sealed glass envelope prior to spraying the cathode and inserting the assembly into the gun stack. Immediately after breaking the glass vacuum envelope, the components are RF brazed in a controlled atmosphere. After RF brazing, the air in the tube is evacuated by an ion pump which is started by a cryogenic pump. The entire bakeout oven is also evacuated to limit the diffusion of gases through the walls of the tube which would result in a permeable gas within the tube. This diffusion of gases is quite large at the high bakeout temperature. Tests with appendage pumps on the tubes have shown that the pressure within the tube after the aforementioned assembly techniques and processing is considerably less than 10^{-9} mm of mercury pressure.

2. <u>Ion Block.</u> Ordinarily ions created in the helix region will be drawn to the lower potential of the cathode surfaces ultimately causing deactivation of the coating. The ions can be blocked from reaching the cathode by operating the anode at a slightly higher voltage than the helix and depressing the collector voltage. This drains the ions into the collector. In addition, the beam interception to the anode should be maintained at a low level to minimize ion formation in the cathode-anode region.

The potential profile for the WJ-398 shows an anode operating 450 volts above and a collector 400 volts below the helix potential. Anode interception is less than 80 microamps.

3. <u>Controlling Reaction Rate of Barium.</u> Aside from catastrophic failures, the most important parameter affecting life is the electron producing capability of the cathode or the "activity" of the cathode. The parameters which are most important in determining this level are:

- Cathode temperature,

- Cathode base material,

- Composition, density and thickness of cathode coating (BaO),

- Cathode current density, and

- Cathode environment.

Of the various parameters listed that affect the "activity" level of a cathode, the cathode environment is the only one that is not directly amenable to measurement. The cathode temperature can be determined using the method described in a previous section. The composition of the cathode base material can be minutely analyzed. The composition, density, and thickness of the cathode coating can be measured extremely accurately. Finally, from the cathode dimensions and beam current, the emission current density can be determined.

The cathode environment is a description of the amount and type of gases and ions which contact it during operation. This environment cannot be measured and will vary with different tube types. However, in terms of long life tubes, the goal for any type of tube envelope is to minimize the effect of this environment by minimizing the residual gas pressure and also excluding materials that are especially harmful to the cathode.

It has been shown that the material responsible for the low work function of the surface of the oxide cathode is the metal barium. It is only necessary to have a monomolecular layer of free barium on the surface of the cathode to achieve the low work function. The source of the barium is the barium oxide coating on the surface of the nickel cathode body. The barium is released by one of two means. The barium oxide molecule can be broken down either by electrolytic action or by chemical reduction. The principal means in the situation under discussion is by chemical reduction. During electron emission, the BaO coating acts as an n-type, excess-impurity

Column Number			1	2	3	4
	Requirement Paragraph		3.4.3 & 3.4.4	3.4.2	3.4.6	
	Procedure Paragraph		4.4.3.1	4.4.3.2	4.4.3.3	
Row Number	Manufacturing Acceptance Test — Parameter		RF Power Out and Drive Level	Power Consumption	Input VSWR	Relative Power Out and TWT Currents
	Procedure Paragraph	Test				
1	4.4.3	Nominal Performance	X	X	X	
2	4.4.5	Post Temperature Sterilization	X	X		
3	4.4.6	Vibration				X
4	4.4.7	Post Vibration	X	X		
5	4.4.8	Final Performance	X	X	X	

Fig. 59 – WJ-398 Acceptance Test Sequence

semiconductor, with the Ba as the impurity donor. These Ba donors are lost by evaporation and chemical reaction with gases and ions in the tube. The continual replacement of these lost donors is essential to prevent decline of emission and subsequent failure of the tube. The production of the Ba donors is a result of chemical reaction between the BaO coating and certain impurities in the base nickel. These impurities are refered to as reducing agents. The reducing agent reacts with the BaO coating to form an impurity oxide. The chemical equation for this reaction is given in Equation (1).

$$R + BaO \rightarrow RO + Ba \qquad\qquad (1)$$
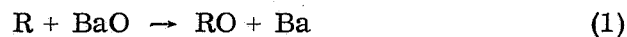
where

$$R = \text{reducing agent}$$

$$BaO = \text{barium oxide.}$$

The impurity oxide is produced at the interface between the nickel base and the coating. Free Ba atoms formed by this reaction diffuse into the BaO coating to maintain the desired donor level. The chemical reaction as given in Equation (1) is very strong to the right side of the equation hence, the Ba production is determined by the diffusion rate of the reducing agent.

The diffusion rate of the reducing agent from the nickel core is determined by the type of reducing agent and cathode temperature. A cathode nickel containing a reducing agent with a high diffusion constant will produce more donors/sec as compared to one with a low diffusion constant. The cathode temperature is involved since the diffusion constant is dependent upon this temperature. Provided that a sufficient amount of reducing agent is available in the nickel core, then the end of tube life will occur when a substantial part of the barium oxide coating is depleted. For sustained emission, the required value of the donor production rate is indirectly dependent upon the cathode current density. The higher the cathode current density, the higher the required operating temperature, thus a larger donor production rate must be maintained.

The prototype tube design uses 220 nickel for the cathode button. Since this alloy contains varying amounts of the reducing agents, carbon, magnesium, and silicon, fundamental studies of donor-production rates cannot

be conducted. Thus, the depletion rate of the coating cannot be predicted by calculations. However, life test results on medium power and low noise TWT's using 220 cathode nickel show long life capabilities in the range from 10,000 hours to 50,000 hours. The following is a brief summary of pertinent life test results at Watkins-Johnson Company:

Medium Power Tubes

The WJ-227 is a 10 watt, S band, PPM focused traveling-wave tube. A total of 10 tubes were placed on life test beginning on 2 October 1961. The results of this life test program has demonstrated that the MTBF of the WJ-227 is 42,100 hours. Cathode loading for the WJ-227 is approximately 100 mA/cm^2.

The WJ-237 is a 2.5 watt, 1.85 to 1.95 GHz PPM focused traveling-wave tube. This tube was developed for NASA as a backup tube for Project Syncom. One tube was placed on life test 11 September 1962. As of 24 June 1966 this unit had accrued 31,241 running-time hours. Cathode loading is approximately 100 mA/cm^2.

Low Noise Amplifiers; Tubes and Power Supplies
(cathode loading considerably below 100 mA/cm^2)

The WJ-252 is a 1.2 to 1.4 GHz TWT. A total of seven tubes were placed on life test during the period 4 January 1963 to 10 June 1963. As of 12 October 1967 five units have each accrued greater than 37,858 hours each with two of them in excess of 41,558 hours. Based on life test data the following MTBF and Confidence factor can be computed:

MTBF	Confidence Factor
88,100 hours	50 percent
44,400 hours	90 percent
28,200 hours	99 percent

The WJ-268 is 1.0 to 2.0 GHz TWTA. One amplifier was placed on life test 25 August 1963. As of 12 October 1967 this unit was performing within specification and had accrued 36,015 running-time hours.

The WJ-269 is at 2.0 to 4.0 GHz TWTA. An amplifier placed on test 11 June 1964 is performing in specification and has accrued 29,123 running-time hours as of 12 October 1967.

The WJ-271 is a 4.0 to 8.0 GHz TWTA. An amplifier placed on test 13 September 1965 is performing in specification and has accrued 17,459 running-time hours as of 12 October 1967.

The WJ-276 is an 8.0 to 12.0 GHz TWTA. Two amplifiers have been placed on life test since 22 September 1964. As of 26 October 1967 these units have accrued a total of 46,957 running time hours. One unit has 26,942 hours to date.

Cathode Design

It is seen that for a long-life cathode design, the tube engineer must go through the following process: First, minimize cathode current density consistent with other good design practices. Then, choose a cathode material with a reducing agent that is known to have good long life capabilities. Possibly the best example of this ultra pure nickel with a known single reducing additive of approximately 0.1 percent zirconium.[1] Second, choose a cathode temperature which, from past experience, is compatible with the current density. From this temperature and cathode material chosen, it is now possible to calculate the diffusion rate of the reducing agent for various cathode thicknesses. This diffusion rate must be sufficient so that with the cathode temperature and current density chosen, the cathode is "active". For example, Kern[1] says that the donor production rate of 10^{10} to 10^{11} atoms/cm^2-sec is sufficient to maintain "activity" for a cathode loading of 200 mA/cm^2. Finally, the maximum amount of barium oxide coating is desired. Depletion of this item must occur before the reducing agent is consumed. The maximum coating density and thickness is restricted based upon experience. Too thick or too dense a coating will cause peeling or physical separation of the cathode and the coating. An optimum value for the coating seems to be 1.1 gm/cm^3 density and 0.0015 inches thick.

Predicting Cathode Coating Depletion for Ultra-Pure Zirconium-Doped Nickel

To determine the cathode depletion, one must first solve the equation for the diffusion of the reducing agent in the nickel core. Initially, the atoms of the reducing impurity are distributed uniformly throughout the nickel.

When the cathode is heated, the reducing impurity atoms react with the BaO at the interface of the coating and the nickel to form the impurity oxide and free barium, as mentioned earlier. The removal of impurity atoms from the coated surface layer of the nickel creates a concentration gradient. At the elevated temperatures of the cathode, this gradient induces diffusion of the impurity atoms toward the depleted surface layer.

Calculations were made to predict the useful cathode life for the WJ-398 design. The following assumptions were made in the calculations:

1. Barium oxide evaporation rate is negligible.

2. A single reducing agent in the ultra pure cathode base nickel.

3. Carbon has been removed from the cathode nickel by proper wet hydrogen furnace firing.

4. Cathode is unbounded in the y-z plane.

The following parameters are given by the WJ-398 design:

1. Cathode loading of 212 mA/cm^2.

2. Cathode nickel thickness of 0.030 inches.

3. Zirconium reducing agent content of 0.15 percent by weight.

4. Cathode coating 1.5 mils thick with a density of 1.1 gm/cm^3.

Fig. 60 shows the diffusion constant of zirconium through pure nickel as a function of temperature. The values were obtained from D. Maurer of Bell Telephone Laboratories in a telephone conversation with Dr. George Wada of Watkins-Johnson Company. Fig. 61 shows the time in hours for 100 percent depletion of the cathode coating as a function of true cathode temperature. Notice on this figure that with a cathode temperature of 720 degrees C, total cathode coating depletion occurs after 114,000 hours. At a cathode temperature of 735 degrees C, total cathode coating depletion occurs at 90,000 hours.
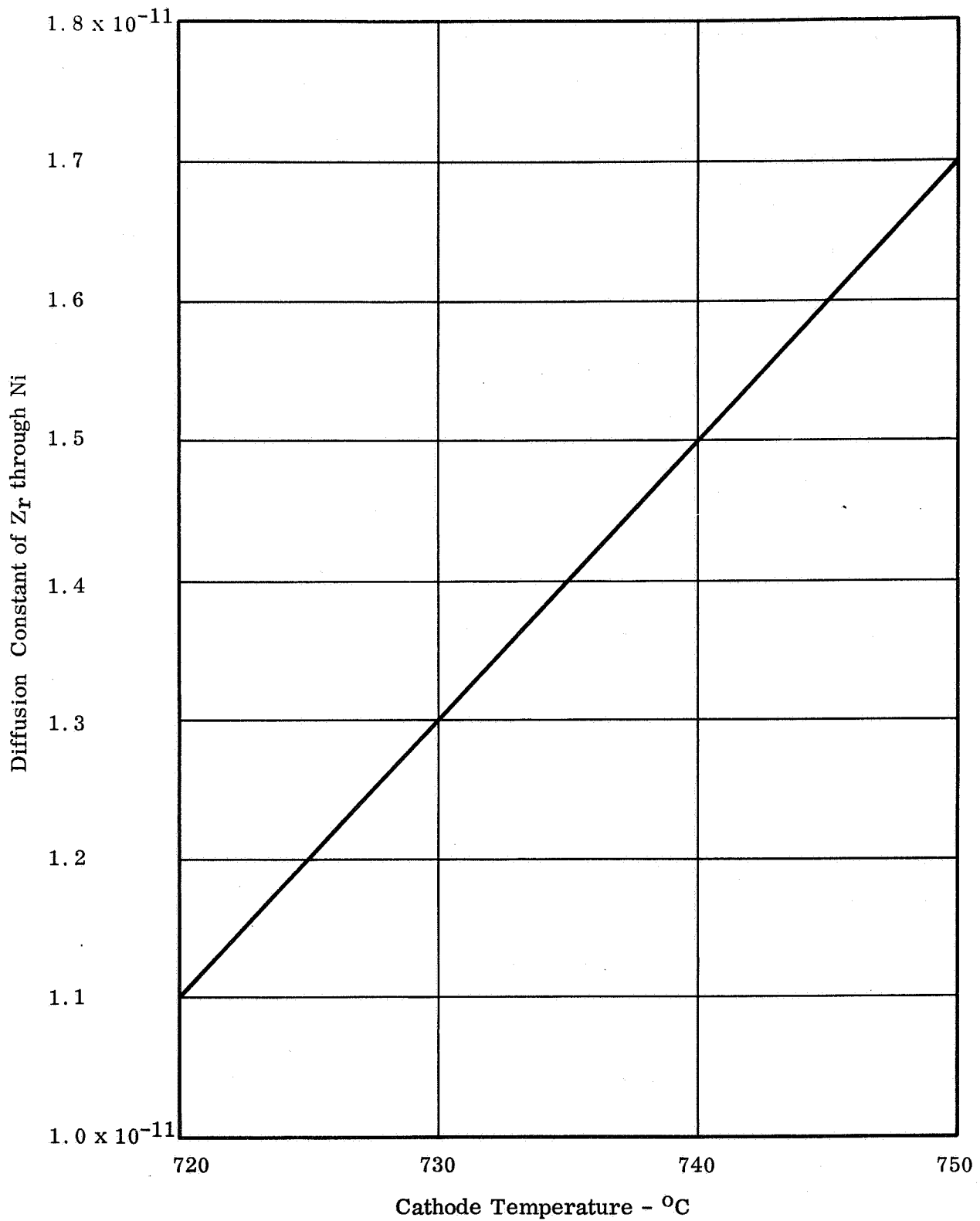
Fig. 60 – Diffusion constant of zirconium through pure nickel versus true cathode temperature.

- 113 -

15130
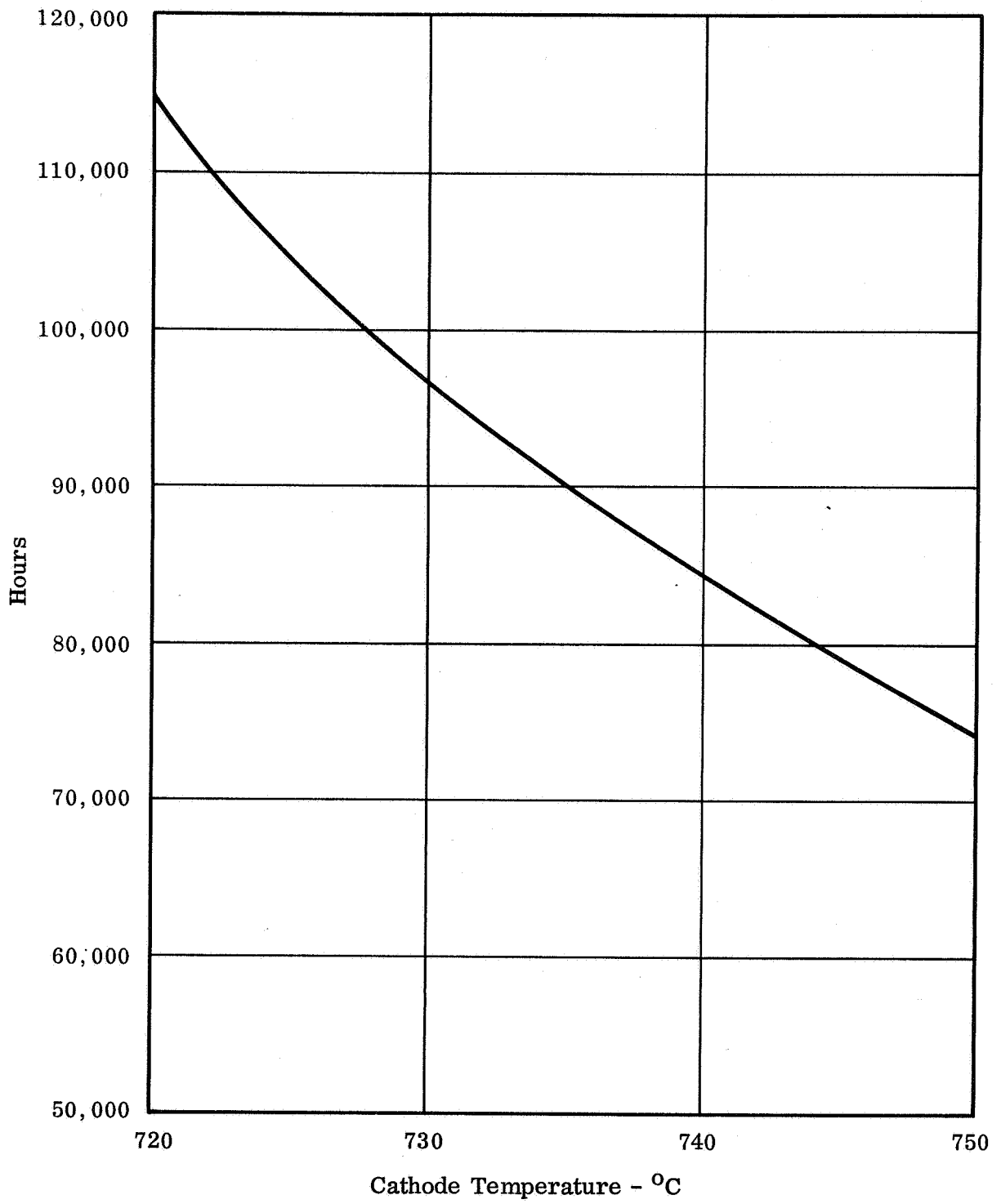
Fig. 61 —Time for 100 percent cathode coating depletion vs. cathode temperature.

15132

Fig. 62 shows the arrival rate of the zirconium reducing agent to the cathode surface after 50,000 hours of tube operation, as a function of true cathode temperature in degrees centigrade. In this calculation, the cathode temperature is held constant from time equal zero to 50,000 hours. For example, if the cathode temperature is held at 720 degrees C, then after 50,000 hours the arrival rate will be 2.2×10^{10} atoms/cm^2-sec. If the cathode temperature was held at 750 degrees C, then after 50,000 hours, the arrival rate will be 2.15×10^{10} atoms/cm^2-sec. It should be pointed out that the donor production rate is twice that shown in Fig. 62 because of the chemical reaction: $Zr + 3 BaO = BaZrO_3 + 2 Ba$ Notice here that over the cathode temperature range of 720 to 750 degrees centigrade, after 50,000 hours the donor production rate is within the range specified by Kern[1].

Finally, in Fig. 63 is shown the percent of cathode coating depletion, after 50,000 hours of tube life as a function of true cathode temperature. The amount of cathode coating depletion that signifies end of life is a matter of debate.

Referring back to Fig. 61, Fig. 62 and Fig. 63, it is seen that the cathode temperature of 720 degrees C originally chosen, should provide life in excess of 50,000 hours. For example, the donor production rate after 50,000 hours operation is sufficient as illustrated in Fig. 62 and that only 80 percent of the cathode coating will be depleted after this time.

The previous calculations have to be extended due to the increase in the cathode thickness determined during development as necessary for the high impact requirement.

Fig. 64 shows donor production rate, percentage zirconium depletion, and percentage coating depletion as a function of cathode thickness. The prototype design has a cathode thickness of 0.050 inches.

The results of these calculations are shown in Table XIX. As indicated on Table XIX, after the tube has operated for 50,000 hours, 91.5 percent of the cathode coating will be depleted with the cathode at a temperature of 735 degrees C. Also, at the end of this time, 45 percent of the zirconium additive in the base nickel would have been consumed and the donor production rate would be 5.3×10^{10} atoms/cm^2-sec. As mentioned previously, a donor production rate of 10^{10} to 10^{11} atoms/cm^2-sec. is required for sustaining emission for this cathode loading. Therefore, by these calculations the WJ-398, using 0.15 percent zirconium doped high purity nickel, should have a useful life of at least 50,000 hours.

[1]H.E.Kern, "Research on Oxide-Coated Cathodes", Bell Telephone Laboratories Record, Dec. 1960.
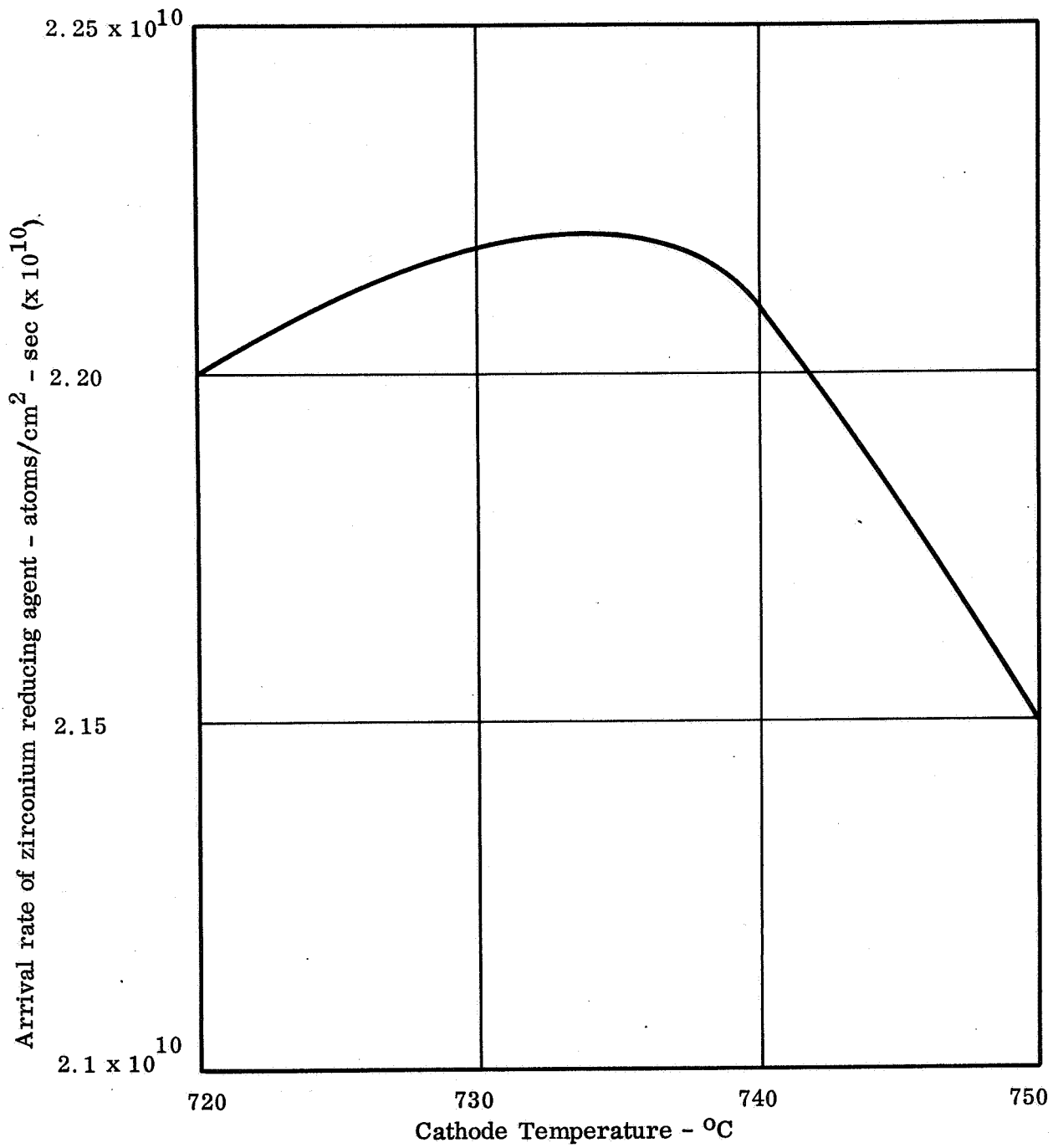
Fig. 62 – Arrival rate of zirconium reducing agent to the cathode surface as a function of cathode temperature, in °C, after 50,000 hours of life. In this calculation the cathode temperature is held constant from time equal zero to 50,000 hours.

15131A
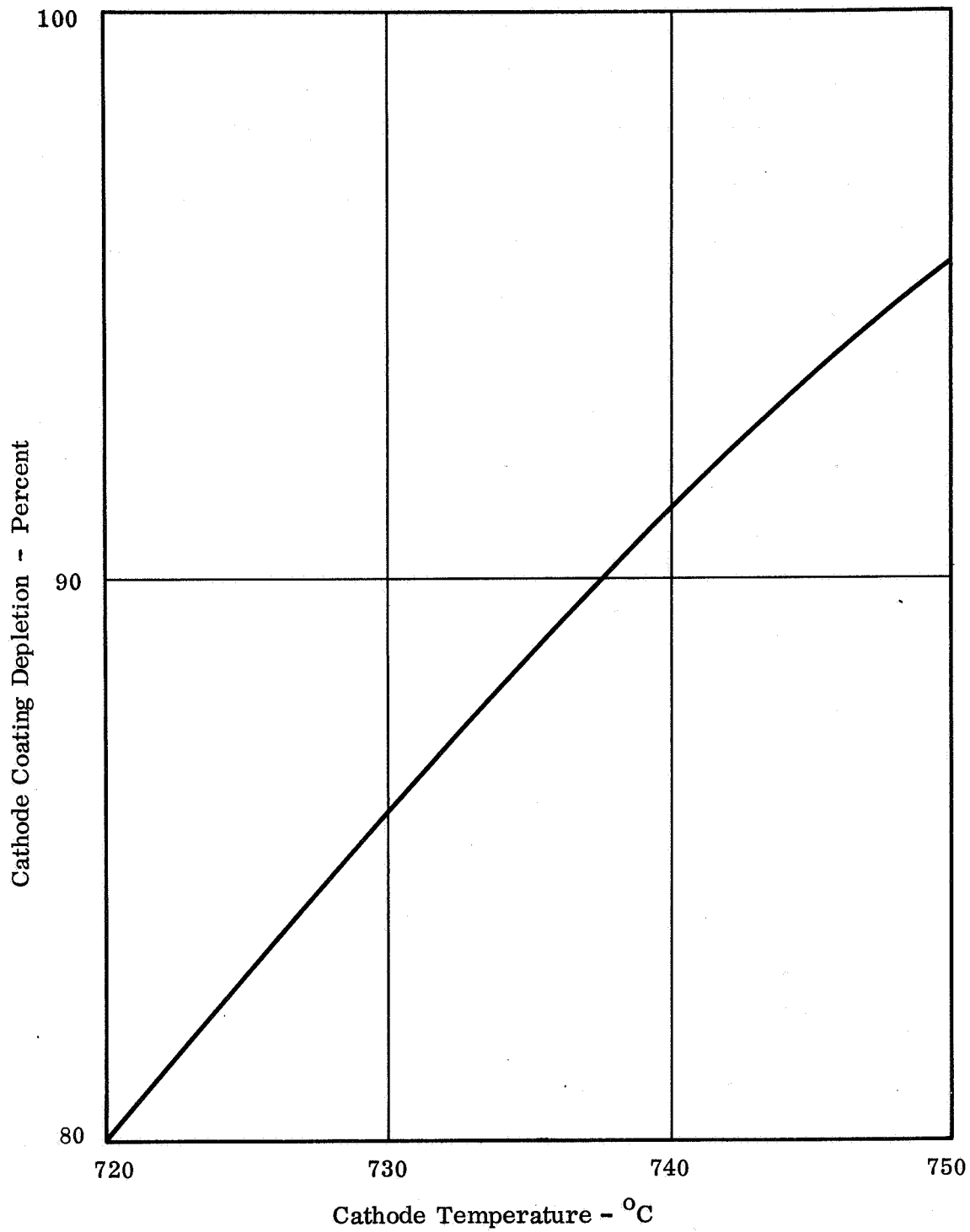
Fig. 63 – Cathode coating depletion vs. cathode temperature after 50,000 hours for the WJ-251 TWT.
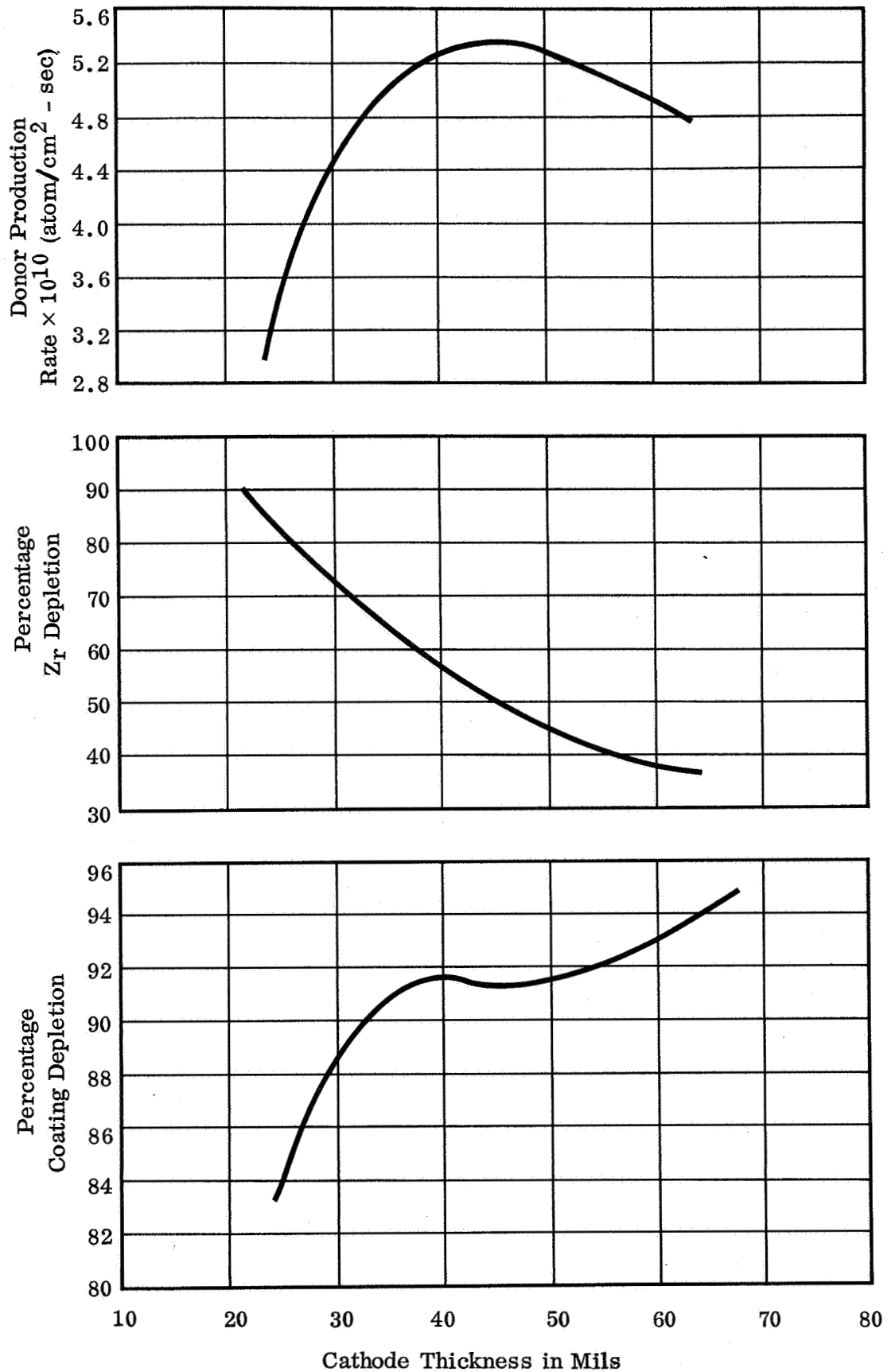
Fig. 64 – Donor production rate and zirconium and coating depletion rates as a function
of cathode thickness for the WJ-398 design after 50,000 hours of life at 735° C. Cathode
nickel is high purity 0.15 percent zirconium doped material.

18299

TABLE XIX

THE WJ-398 CATHODE CALCULATIONS
(Using Zirconium Doped Ultra Pure Nickel)

After 50, 000 hours of tube operation, the WJ-398 cathode would be in the following condition:

Cathode coating depletion	91. 5 percent
Zirconium additive depletion	45 percent
Donor production rate	5.3×10^{10} atoms/cm^2/sec

Above calculations are for a cathode temperature of 735 degrees centigrade.

SECTION V

RECOMMENDATION FOR ADDITIONAL DEVELOPMENT

A number of items discussed in the previous sections of this report warrant additional study and development to either correct non-specification performance or improve the predictability of the life and shock capability of the design.

Three recommendations for additional study and development will be presented:

1. Modify the helix design to improve the overall tube efficiency to greater than the specification requirement.

2. Change the cathode material to ultra-pure nickel with a single additive agent of 0.15 percent zirconium.

3. Evaluate a statistical sample of tubes to confirm the shock environment capability of the design.

1. <u>High Efficiency Improvement.</u> Concurrent with, or since, the high impact development, a number of traveling-wave tubes have been developed in the S-band area which have increased the efficiency state-of-the-art for space type hardware to greater than 40 percent.

    The WJ-274-6, which is electrically and dimensionally very similar to the WJ-398, has shown performance of 26 watts power output, with 42.3 percent overall efficiency including heater power. Table XX shows the final performance data of the WJ-274-6 S/N 3. This tube was delivered to the Jet Propulsion Laboratory in December 1967. Other tube designs in the WJ-274 family of tubes have demonstrated overall efficiencies as high as 44 percent at the 26 watt power level. These tube designs are entirely compatible with the existing WJ-398 physical geometry and high impact construction techniques.

    Other tube types in the S-band telemetry band have demonstrated overall efficiencies as high as 45 and 46 percent at the power levels between 50 and 100 watts.

    The efficiency improvement development could be kept within the existing constraints of the WJ-398 high impact design without altering size, geometry or shock capability.

TABLE XX

FINAL DATA

FOR THE

WJ-274-6 S/N 3 TRAVELING-WAVE TUBE

Frequency (GHz)	Helix Current (mA)	Saturation Power Output (Watts)	Saturation Gain (dB)	Overall Efficiency (%)
2.10	8.6	23.75	28.65	38.5
2.15	8.4	24.30	28.95	39.4
2.20	8.2	24.60	28.30	40.0
2.25	8.1	24.85	27.55	40.4
2.30	8.1	25.15	26.90	40.9
2.35	8.2	26.00	25.95	42.3
2.40	8.2	26.00	24.65	42.3
2.45	8.0	25.15	24.00	41.0
2.50	7.4	23.45	22.70	38.4

2. High Purity Cathode Nickel. As discussed in Section IV, the expected life of a traveling-wave tube using a 220 nickel cathode cannot be calculated because of the numerous impurity elements and various concentrations. Useful life must be determined by actual life test. Existing data indicates a useful life of between 10,000 and 40,000 hours.

On the other hand, single-additive high-purity nickel such as 0.15 percent zirconium-doped nickel, has well known properties making life predictions calculable. As shown earlier, the WJ-398 design with a high-purity, 0.15 percent zirconium-doped nickel has an expected life of approximately 50,000 hours.

To take advantage of the predictable nature of the high-purity nickel, the WJ-398 design should be modified to include this material.

3. Statistical Evaluation of Design. Because of the unusual nature of the high impact environment, the WJ-398 design should be evaluated using a statistical sample rather than the usual single unit type approval. The sample should be manufactured under full quality assurance provisions and be large enough to give an acceptable confidence factor to the shock capability of the design.

APPENDIX I

END ITEM ACCEPTANCE TEST SEQUENCE
AND TEST RESULTS

Column Number			1	2	3	4	5
Requirement Para. No.			3.4.3 and 3.4.4	3.4.2	3.4.6	3.4.3 and 3.4.7	3.4.8
Procedure Para. No.			4.4.4.1	4.4.4.2	4.4.4.3	4.4.6.4	4.4.6.5
Parameter			RF Power Output and Drive Level	Power Consumption	Input VSWR	Load VSWR	Noise Figure
Row Number	Procedure Para. No.	Test					
1	4.4.4	Nominal Performance	x	x	x		
2	4.4.5	Temperature	x	x			
3	4.4.6	Final Performance	x	x	x	x	x

End Item Test Sequence

Figure 3 End Item Test Sequence

TESTED TO PROCEDURE NO. WJ 102041 Rev. __B__	AMPLIFIER DATA SHEET	MODEL NO __WJ-398 FS-507__ SERIAL NO __4__ __11__

1	2	3	4	5	6	7	8	9	10	11	12	13	14	15	16	17	18	19	20	21	22	23	24	25	26	27	28	29

END ITEM TEST SIGN-OFF

Thomas Bobo / E. R. Dornseif C   Responsible Test Technician/Engineer

27 OCTOBER 1967   Date

WITNESSED/REVIEWED BY:

10/27/67   Test Engineer
E. R. Dornseif

10-30-67   WJ Q.A. & R
Date

WATKINS · JOHNSON COMPANY ELECTRON DEVICES ELECTRONIC SYSTEMS PALO ALTO CALIFORNIA	CODE IDENT 14482	DIV	NO. 102041	SHEET 27

B DS- 1   x

AMPLIFIER
DATA SHEETS

MODEL NO. WJ-398 FS 607

SERIAL NO. 4   11

1	2	3	4	5	6	7	8	9	10	11	12	13	14	15	16	17	18	19	20	21	22	23	24	25	26	27	28	29

RUNNING TIME LOG

LOG NO. 3   PREVIOUS LOG NO. 2

DATE	ACTION		RUNNING TIME (Hours)	ACCUMULATIVE TIME TO DATE (Hours)	INITIAL	REMARKS
Mo/Day/Yr.	ON	OFF				
10/25/67	11:00	1700	6	415	𝒟 ᵗ𝐵	Nominal Performance
10/26/67	0830	1800	9-1/2	424-1/2	𝒟 ᵗ𝐵	Temperature
10/27/67	0900	1000	1	425	sa.ᵗ	Final

CODE IDENT	DIV	NO		SHEET
14482	-	102041		28

B DS - 2 x	AMPLIFIER DATA SHEET	MODEL NO WJ-398, FS-607 SERIAL NO 4 11

1	2	3	4	5	6	7	8	9	10	11	12	13	14	15	16	17	18	19	20	21	22	23	24	25	26	27	28	29

OPERATORS CHECK SHEET

TEST	MEASUREMENTS	DATA SHEET NUMBER	PROCEDURE PARAGRAPH	BY	DATE
Nominal Performance 4.4.4	Power Output and Drive	DS - 7	4.4.4.1	JAB	25 Oct '67
	Power Consumption	DS - 8	4.4.4.2	JAB	25 Oct '67
	Input VSWR	DS - 9	4.4.4.3	JAB	25 Oct '67
Temperature 4.4.5	Rel. Power Output & Drive	DS - 13	4.4.5.2	JAB	26 Oct '67
	Power Consumption	DS - 13	4.4.5.2	JAB	26 Oct '67
Final Performance 4.4.6	Power Output and Drive	DS - 7	4.4.4.1	JAB	26 Oct '67
	Power Consumption	DS - 8	4.4.4.2	JAB	26 Oct '67
	Input VSWR	DS - 9	4.4.4.3	JAB	26 Oct '67
	Load VSWR	DS - 10	4.4.6.4	SWD	27 Oct '67
	Noise Figure	DS - 11	4.4.6.5	SWD	26 Oct '67

B DS - 3 x	AMPLIFIER DATA SHEET	MODEL NO WJ-398 FS 607 SERIAL NO 4 11

1	2	3	4	5	6	7	8	9	10	11	12	13	14	15	16	17	18	19	20	21	22	23	24	25	26	27	28	29

DISCREPANCY HISTORY

Discrepancy Number	Test Name	Discrepancy	Disposition	Date
1	Load VSWR	Instability Corrected 10/26/67 *SW*	Adjust Vc and rerun final performance	10/26/67
2	Power Consumption	Exceeds specification Spec: 60 watts Actual: 75.19 watts max.	Continue test *SW*	10/26/67
3	Input VSWR	Exceeds specification Spec: 1.2:1 Actual: 1.45:1 max.	Continue test *SW*	10/26/67

WATKINS · JOHNSON COMPANY ELECTRON DEVICES ELECTRONIC SYSTEMS PALO ALTO, CALIFORNIA	CODE IDENT 14482	DIV	NO. 102041	SHEET 30

| B DS - 4 x | AMPLIFIER DATA SHEET | MODEL NO WJ-398   FS-607 |
| | | SERIAL NU ___4___   11 |

1	2	3	4	5	6	7	8	9	10	11	12	13	14	15	16	17	18	19	20	21	22	23	24	25	26	27	28	29

FAILURE-REPAIR HISTORY

FAILURE OCCURRED IN TEST	DATE	DESCRIPTION OF FAILURE	TFR NO.
		NONE	

CODE IDENT 14482	DIV	NO. 102041	SHEET 31

| B DS - 5 x | AMPLIFIER DATA SHEET | MODEL NO. WJ 398 FS 607 |
| | | SERIAL NO. 4   11 |

1	2	3	4	5	6	7	8	9	10	11	12	13	14	15	16	17	18	19	20	21	22	23	24	25	26	27	28	29

PHYSICAL CHECK SHEET

WEIGHT

			Requirement Limit
Traveling-wave tube	3.12	lbs.	3.5 lbs. max.
Filter	0.53	lbs.	1.0 lb. max.
Amplifier (total above)	3.65	lbs.	4.5 lb. max.

INSPECTION

1. **Pre-Test Check**

   Inspector: _____

   Date: _____10/25/67_____.

2. **Post-Test Check**

   Inspector: _____

   Date: _____10-30-67_____

WATKINS · JOHNSON COMPANY	CODE IDENT	DIV	NO.	SHEET
ELECTRON DEVICES ELECTRONIC SYSTEMS	14482		102041	32
PALO ALTO CALIFORNIA				

ᵇ DS - 6 x	AMPLIFIER DATA SHEET	MODEL NO WJ-398 FS-607
		SERIAL NO 4 11

1	2	3	4	5	6	7	8	9	10	11	12	13	14	15	16	17	18	19	20	21	22	23	24	25	26	27	28	29

TRAVELING-WAVE TUBE VOLTAGES AND CURRENTS

TEST CONDITIONS

RF Frequency: 2300 MHz

RF Drive: Sufficient to saturate tube

SPECIFICATION RANGES

Anode: 1850 - 2050 Vdc: 0-0.5 mA
Helix: 1387 - 1587 Vdc:0.2-9.0 mA
Collector:987-1187 Vdc: 48-61 mA
Filament: 4.5-5.5 Vdc: 0.7-1.0 A

ELEMENT	VOLTAGE		NOMINAL CURRENTS	
ANODE	1963	Vdc	0.07	mA
HELIX	1493	Vdc	7.0	mA
COLLECTOR	1190	Vdc	53.5	mA
FILAMENT	4.75	Vac	0.84	A

CODE IDENT 14482	DIV	NO. 102041	SHEET 33

1	2	3	4	5	6	7	8	9	10	11	12	13	14	15	16	17	18	19	20	21	22	23	24	25	26	27	28	29

POWER OUTPUT AND DRIVE LEVEL

TEST CONDITIONS	SPECIFICATION LIMIT
RF Frequency: As Specified	RF Power Output: 43 dBm, (20 w) min.
RF Drive: sufficient to saturate amplifier	RF Drive: 18 dBm, max
TWT Voltages: Per DS-6	

RF Frequency (MHz)	Power Input P_m(dBm)*	$P_{i(RF)}$(dBm)	Power Output P_m(dBm)*	P_o(dBm)	Po (w)	Gain (dB)
2290	-7.7	2.3	3.65 (39.7)	43.35	21.60	41.05
2300	-7.6	2.4	+3.65(39.7)	43.35	21.60	40.95

* See appropriate calibration sheet for conversion from monitor power to true power

Power Consumption (Reference Only)

Parameter / Electrode	Voltage (vdc)	Current (mA)	Power (watts)
Frequency: 2300 MHz			
Anode	1966	0.07	.13
Helix	1493	7.0	10.40
Collector	1100	53.5	58.90
Filament	4.75Vac	.84 A	4.00
Total	—	—	73.43

B DS- 8 NP	AMPLIFIER DATA SHEET	MODEL NO WJ 388 FS-607
		SERIAL NO 4 11

1	2	3	4	5	6	7	8	9	10	11	12	13	14	15	16	17	18	19	20	21	22	23	24	25	26	27	28	29

POWER CONSUMPTION

TEST CONDITIONS	SPECIFICATION
RF Frequency: 2300 MHz RF Drive: As specified Voltages: Per DS-6	60 watts, maximum at saturation

Parameter	Voltage (Vdc)	Current (mA)	Power (w)
RF Drive: None			
Anode	1966	.031	.061
.Helix	1493	0.390	..58
Collector	1100	60.1	66.00
Filament	4.75	.84	4.00
Total			70.641
RF Drive: 4 db below saturation			
Anode	1966	0.084	.165
Helix	1493	2.75	4.10
Collector	1100	57.8	63.50
Filament	4.75	.84	4.00
Total			71.765
RF Drive: Sufficient to saturate			
Anode	1966	.076	0.15
Helix	1493	6.90	10.30
Collector	1100	53.60	59.00
Filament	4.75	.84	4.00
Total			73.45
RF Drive: 4 dB Above Saturation			
Anode	1966	.08	0.157
Helix	1493	7.1	10.60
Collector	1100	53.4	58.70
Filament	4.75	.84	4.00
Total			73.457

B DS- 9 NP	AMPLIFIER DATA SHEET	MODEL NO WJ 398 FS-507
		SERIAL NO 4 11

1	2	3	4	5	6	7	8	9	10	11	12	13	14	15	16	17	18	19	20	21	22	23	24	25	26	27	28	29	

OPERATING INPUT VSWR

TEST CONDITIONS	SPECIFICATION LIMIT
RF Frequency: As specified RF Drive: Sufficient to saturate TWT Voltages: Per DS-6	1.2:1 maximum

RF Frequency (MHz)	VSWR	Cold VSWR (Ref. Only)
2290	1.40	1.18
2295	1.38	1.20
2300	1.38	1.20

CODE IDENT 14482	DIV	NO. 102041	SHEET 36

B DS - 10 NP	AMPLIFIER DATA SHEET	MODEL NO WJ 398 FS-507 SERIAL NO 4 11

1	2	3	4	5	6	7	8	9	10	11	12	13	14	15	16	17	18	19	20	21	22	23	24	25	26	27	28	29

LOAD VSWR

TEST CONDITIONS	SPECIFICATION LIMITS
RF Frequency: 2300 MHz RF Drive: Sufficient to saturate tube TWT Voltages: Per DS-6 Load: As specified	Power Output: 43 dBm min (1.2:1 load) 42 dBm min (5:1 laod) No Instability

Load (VSWR)	Power Input		Power Output		TWT Currents			Insta-bility Remarks
	P_m(dBm)	$P_i \left(\frac{dBm}{RF}\right)$	P_m(dBm)	P_o(dBm)	I_a (mA)	I_h (mA)	I_c (mA)	
1.2:1	-7.8	+2.2	+3.70	43.4	.073	7.0	53.6	-
0 5:1	-7.8	+2.2	+3.10	42.8	.130	7.8	53.5	none
1	-7.8	+2.2	+3.40	43.1	.110	6.5	54.0	none
2	-7.8	+2.2	+3.70	43.4	.12	7.8	52.5	.3 dB AM

NOTE:

Instability corrected by increasing collector voltage. After voltage adjust all post temperature nominal performance tests were repeated.

| B DS- 11 NP | AMPLIFIER DATA SHEET | MODEL NO WJ 398 FS-607 |
| | | SERIAL NO 4 11 |

1	2	3	4	5	6	7	8	9	10	11	12	13	14	15	16	17	18	19	20	21	22	23	24	25	26	27	28	29

NOISE FIGURE

TEST CONDITIONS	SPECIFICATION LIMIT
RF Frequency: 2300 MHz RF Drive: Sufficient to increase receiver output by 3.0 dB above no drive conditions TWT Voltages: Per DS-6	35 dB max

RF Frequency (MHz)	Generator Level (dbm)	Noise * Figure (dB)
2300	86.9	23.58

* Noise figure is calculated as follows:

$$NF = 114 - S_{i(RF)} - C_{bw} - C_L$$

Where

$S_{i(RF)}$ = Generator Level in dBm
C_L = Loss of input cable in dB = -0.95 dB
C_{bw} = 10 Log B = 4.47 dB
B = Receiver Bandwidth in Mc. = 2.8 Mc

| WATKINS · JOHNSON COMPANY
ELECTRON DEVICES ELECTRONIC SYSTEMS
PALO ALTO CALIFORNIA | CODE IDENT 14482 | DIV | NO. 102041 | SHEET 38 |

_DS- 13 T_	AMPLIFIER DATA SHEET	MODEL NO WJ395 FS- 607 SERIAL NO 4 11

1	2	3	4	5	6	7	8	9	10	11	12	13	14	15	16	17	18	19	20	21	22	23	24	25	26	27	28	29

TEMPERATURE

TEST CONDITIONS	SPECIFICATION LIMIT
RF Frequency: 2300 MHz RF Drive: Sufficient to saturate TWT Voltages: Per DS-6	Primary power less than 60 watts, maximum.

Temp. Parameter	+25°C Pre-test V (Vdc)	I (mA)	P (w)	+75°C	-10°C Turn On V (Vdc)	I (mA)	P (w)	-10°C After Stablize V (Vdc)	I (mA)	P (w)
P_o(relative)	–	–	2.75		–	–	–	–	–	+2.90
P_i(relative)	–	–	-7.00	Non Operative	–	–	–	–	–	-7.20
Anode	1966	0.066	.12		–	–	–	1966	.085	.167
Helix	1493	6.9	10.3		–	–	–	1493	7.4	11.06
Collector	1100	53.6	58.00		–	–	–	1100	53.0	58.40
Filament	4.75 Vac	0.84 A	4.00		-Vac	-A	–	4.75 Vac	0.84 A	4.00
Total			72.42				–			73.627

Temp. Parameter	+25°C V (Vdc)	I (mA)	P (w)	+75°C V (Vdc)	I (mA)	P (w)	+25°C Post Test V (Vdc)	I (mA)	P (w)
P_o(relative)	–	–	+2.80	–	–	+2.75	–	–	+2.80
P_i(relative)	–	–	-7.2	–	–	6.80	–	–	-7.0
Anode	1966	.063	.124	1966	.14	.275	1966	.067	.132
Helix	1493	7.0	10.45	1493	7.2	10.75	1493	6.9	10.30
Collector	1100	53.5	58.90	1100	53.2	58.60	1100	53.6	59.00
Filament	4.75 Vac	.84 A	4.00	7.5 Vac	.84 A	4.00	4.75 Vac	.84 A	4.00
Total			73.474			73.625			73.432

APPENDIX II

HIGH IMPACT, BAND REJECT AND HARMONIC FILTER

STATEMENT OF WORK
AND
SPECIFICATION

STATEMENT OF WORK

FOR WATKINS-JOHNSON COMPANY
SPECIFICATION 120000

HIGH IMPACT BAND REJECT AND HARMONIC FILTER

CONTRACT NO. 951287

TABLE OF CONTENTS

REVISION STATUS	SHT NO	1	2	3	4	5	6	7	8	9	10	11	12	13	14	15	16	17	18	19	20	21	22	23	24	25
	ISSUE LETTER	A	A	A																						

APPROVALS	REQ'D	SIGNATURE	DATE
ORIGINATOR	x	ERD/REV	3-23-66
R & D ENG.	x	WEK	
MANUFACT'G			
PROD. ENG.			
Q. A. R.	x		
APPLIC. ENG.			
Design Eng.	x		3-2?-??

CONTR. NO. 951287   PROJ. NO. 404300

WATKINS · JOHNSON COMPANY
ELECTRON DEVICES. ELECTRONIC SYSTEMS
PALO ALTO. CALIFORNIA

CATEGORY STATEMENT OF WORK

TITLE HIGH IMPACT BAND REJECT AND HARMONIC FILTER

CODE IDENT	DIV	NO.	SHEET OF
14482		120001	1 of 3

1.   CONTRACTOR REQUIREMENTS

1.1   Hardware: The contract shall design, fabricate and test:

a. One (1) each band reject and harmonic filter (BRHF),
Qualification Model, in accordance with the requirements
set forth herein and Specification No. 120000 High Impact
Band Reject and Harmonic Filter.

b. Three (3) each BRHF, Production Models, in accordance with
the requirements set forth herein and Specification No. 120000
hereafter referred to as "The Specification".

1.2   Documentation: The contractor shall:

1.2.1   Preliminary Outline Drawing: Provide one (1) reproducible copy of
a preliminary outline drawing and all subsequent changes to the preliminary outline
drawing.

1.2.2   Quality Program Plan: Provide one (1) reproducible copy of the
Quality Program Plan generated in the performance of Paragraph 4.1.1 set forth in
the Specification with complete inspection procedures for each inspection conducted
during fabrication of the deliverable filters.   The Quality Program Plan is to be
approved by Watkins-Johnson Company before fabrication of the filters.

1.2.3   Final Outline Drawing: Submit for approval one (1) reproducible
copy of the Final Outline Drawing.   The Final Outline Drawing is to be approved by
Watkins-Johnson Company before fabrication of the production model filters.   All
changes in the Final Outline Drawing require the prior approval of Watkins-Johnson.

All parts, materials, drawings, fabrication procedures, etc. are to be under
"Customer Control" conditions, and require prior approval by Watkins-Johnson
Company for all changes.

1.2.4   Test Results: Provide one (1) reproducible and six (6) print copies
of all test results generated in the performance of Paragraph 4.5.2 and 4.6.2 of the
Specification.

1.2.5   Semi-Monthly Status Reports: Provide semi-monthly status reports
which can be in the form of informal telephone conferences.   If the need arises, the
status reports shall be more frequent.

2. **Design Analysis and Approval:** Prior to the Qualification Shock Test, a final design review shall be held by the contractor at the contractor's facility. Should Watkins-Johnson Company determine the filter fails to achieve the requirements specified, the contractor shall conduct a redesign effort to correct the deficiencies revealed. Watkins-Johnson Company approval of a redesign shall be required prior to any further fabrication effort. Approval or disapproval shall be forwarded to the contractor within ten (10) working days from receipt of request.

3. **JPL Test Facilities:** JPL will provide, at no cost to the contractor, high-impact testing facilities during the development to assist the contractor in designing to meet the requirements of Paragraph 3.5.3 of the Specification. The contractor will give JPL ten (10) calendar days advance notice of requirements for said JPL test facilities to allow necessary preparation and assure availability. JPL will also furnish one man week of consulting service with regard to high-impact capability.

4. **Final Acceptance:** Final acceptance of all items will be at Watkins-Johnson Company, 3333 Hillview Avenue, Palo Alto, California.

5. **Delivery Schedule:** The contractor shall furnish and deliver the supplies and perform the services required by this Statement of Work, in accordance with the following schedule.

	Items	Delivery of Performance Not Later Than
5.1	One (1) each BRHF, Qualification Model, Paragraph 1.1a	July 11, 1966
5.2	One (1) each BRHF, Production Model, Paragraph 1.1b	August 29, 1966
5.3	Two (2) each BRHF, Production Model, Paragraph 1.1b	September 19, 1966
5.4	Preliminary Outline Drawing, Paragraph 1.2.1	May 23, 1966
5.5.	Quality Program Plan, Paragraph 1.2.2	May 30, 1966
5.6.	Final Outline Drawing, Paragraph 1.2.3	July 11, 1966
5.7.	Test Results, Paragraph 1.2.4	With deliverable hardware
5.8	Status Reports, Paragraph 1.2.5	Semi-monthly, by 1st and 15th of each month
5.9	Design Analysis, Paragraph 2.0	June 6, 1966

WATKINS · JOHNSON COMPANY
ELECTRON DEVICES. ELECTRONIC SYSTEMS
PALO ALTO. CALIFORNIA

CODE IDENT
14482

DIV

NO.
120001

SHEET
3 of 3

HIGH IMPACT BAND REJECT AND HARMONIC FILTER

WATKINS-JOHNSON COMPANY
SPECIFICATION 120000

CONTRACT NO. 951287

TABLE OF CONTENTS

REVISION STATUS	SHT NO	1	2	3	4	5	6	7	8	9	10	11	12	13	14	15	16	17	18	19	20	21	22	23	24	25
	ISSUE LETTER																									

APPROVALS	REQ'D	SIGNATURE	DATE
ORIGINATOR	x	ERD/REV	3-23-66
R & D ENG.	x	WEK	3-24-66
MANUFACT'G			
PROD. ENG.			
Q. A. R.	x		3-23-66
APPLIC. ENG.			
Design Eng.	x		3-23-66

CONTR. NO. 951287
PROJ. NO. 404300

WATKINS · JOHNSON COMPANY
ELECTRON DEVICES, ELECTRONIC SYSTEMS
PALO ALTO CALIFORNIA

CATEGORY

SPECIFICATION NO. 120000

TITLE   HIGH IMPACT BAND REJECT AND HARMONIC FILTER

CODE IDENT	DIV	NO.	SHEET OF
14482		120000	1 of 10

1. SCOPE

1.1 Scope: This specification defines the requirements for the design of a Band Reject and Harmonic Filter (BRHF), hereinafter referred to as filter or BRHF.

2. APPLICABLE DOCUMENTS

2.1 The following documents of the exact issue noted constitute a part of this specification to the extent specified herein. Should conflicting requirements exist, the requirements of this specification shall govern.

2.1.1 NASA:

NPC-200-3   "Inspection System Provisions for Suppliers of Space Materials, Parts, Components and Services" dated April 1962.

NPC-200-4   "Quality Requirements for Hand Soldering of Electrical Connections", August 1964.

2.1.2 Jet Propulsion Laboratory:

30250 B   "Environmental Specification Mariner C Flight Equipment".

20016 C   "Workmanship Requirements for Electronic Equipment" dated 8 February 1963.

20030 A   "General Specification, Drawings Standards Procedures", dated 4 March 1963.

3. REQUIREMENTS:

3.1 General Design Requirements:

3.1.1 Description: The Band Reject and Harmonic Filter (BRHF) shall consist of a single integrated assembly.

3.1.2   Application: The BRHF provides output filtering for a traveling-wave tube amplifier package capable of operating while being subjected to a high impact such as could result from unmanned lunar and planetary landings.

3.2   Electrical Design:

3.2.1   Power Capacity: The nominal incident R.F. power is 23 watts CW at a frequency between 2.290 and 2.300 GHz. Maximum incident power in the pass band is 26 watts.

3.2.2   Load VSWR: The maximum load VSWR will be 5:1.

3.3   Mechanical Design:

3.3.1   Magnetic Characteristics:

3.3.1.1   Magnetic Leakage: If magnetic materials are a part of the unit, the BRHF shall not produce a static magnetic field with a magnitude greater than two (2) gamma when measured at a distance of three (3) feet.

3.3.1.2   Changing Magnetic Fields: The magnetic field of the BRHF, if any, shall not change more than one-half (1/2) gamma when measured at a distance of three (3) feet at a rate of less than sixty (60) cps.

3.3.2   Operating Life: The BRHF shall be designed to achieve an operating life greater than 20,000 hours. Operating life shall be considered ended when the BRHF can no longer meet all of the requirements specified herein. The designed operating life shall be supported by analysis sufficient to satisfy Watkins-Johnson Company that the design requirement has been met. The analysis shall include, but not be limited to, analyses of known wearout mechanisms.

3.3.3   Size and Weight:

3.3.3.1   Maximum Allowable: The BRHF size and weight shall not exceed the following size and total weight:

Size:	6 in. x 3 in. x .94 in. (excluding connectors)
Weight:	16.0 ounces

3.3.3.2   Design Objective: A design objective shall be to minimize the BRHF size and weight as specified in paragraph 3.3.3.1.

3.3.4   Impedance: Nominal R. F. input and output impedance shall be 50 ohms resistive.

3.3.5   R. F. Connectors: The unit shall be provided with R. F. input and output connectors on opposite ends and parallel to the units long dimension.

        Input: OSM Jack/Terminal

        Output: OSM Jack/Terminal

3.3.6   Orientation: The unit shall be capable of operating in any position.

3.3.7   Mounting: A single plane mounting surface shall be provided for mounting of the BRHF. This surface shall be one of the maximum area surfaces. Mounting hole configuration shall be consistent with the requirements of the specification.

3.3.8   Identification Marking: Identification marking shall be of a permanent type, such as engraving, which will not be destroyed by application and removal of various encapsulating materials and shall be located on the surface opposite the mounting surface. Identification marking shall include:

      a.   Company name

      b.   Model number

      c.   Serial number

      d.   Input and output terminal identification

3.4   Performance Characteristics:

3.4.1   Pass Band:

3.4.1.1   Frequency: 2.290 to 2.300 GHz

3.4.1.2   Insertion Loss: 0.5 dB maximum

3.4.1.2.1 Design Objective: A design objective shall be to minimize the pass band insertion loss.

3.4.1.3   Input and Output VSWR: 1.2:1 maximum

3.4.2   Stop-Band: The minimum stop-band attenuation shall be as specified below and in Figure 1.
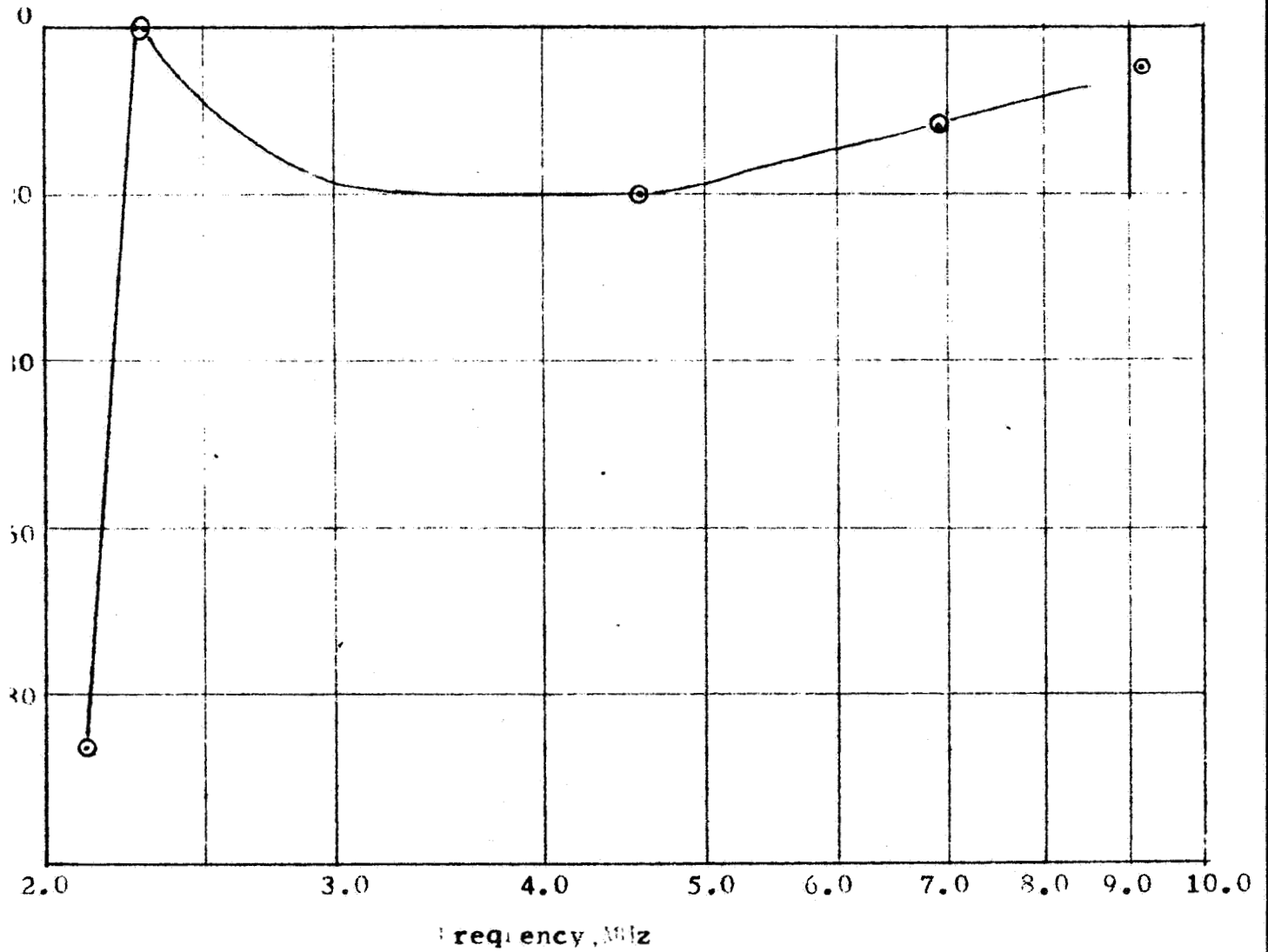
Figure 1.   Stop Band Frequency Characteristics

3.4.2.1 Frequency: 2.108 to 2.128 GHz

3.4.2.1.1 Attenuation: 86 dB minimum

3.4.2.2 Frequency: 4.580 to 4.600 GHz

3.4.2.2.1 Attenuation: 20 dB minimum

3.4.2.3 Frequency: 6.870 to 6.900 GHz

3.4.2.3.1 Attenuation: 12 dB minimum

3.4.2.4 Frequency: 9.160 GHz to 9.200 GHz

3.4.2.4.1 Attenuation: 5 dB minimum

3.5 Environmental Conditions:

3.5.1 Operating Environment: The BRHF shall be capable of meeting all requirements specified herein at any temperature between -10°C and $+75^{\circ}$C with any air pressure between sea level and 10^{-8} mm Hg. with full incident R.F. power (26 watts, CW).

3.5.2 Sterilization Conditions: The BRHF shall be capable of meeting all requirements specified herein both before and after three (3) sterilization cycles consisting of a 145°C storage for a period of thirty-six (36) hours.

3.5.3 High Impact Requirements: The BRHF shall be capable of meeting all requirements specified herein both before and after six (6) 10,000 "G" shocks of duration between one half (.5) and one (1) millisecond one shock to be applied in each direction of three mutually perpendicular planes.

3.5.4 Environmental Requirements: The BRHF shall be capable of meeting all requirements specified herein while being subjected to the environmental conditions of JPL Specification No. 30250 B with full incident R.F. power (26 watts, CW).

3.6 Workmanship: As a minimum the contractor's workmanship specifications shall be in accordance with Rantec Specification "Workmanship Standards", Revision dated 15 April 1966.

3.7   Documentation Requirements:

3.7.1   Drawings: Engineering drawings shall be prepared in accordance with the standard drafting practices of the contractor, with the exceptions specified herein. .

a.   The envelope and/or outline drawing shall reference this specification number.

b.   The following paragraphs of JPL Specification No. 20030A, "General Specification, Drawings Standards Procedures," dated 4 March 1963 apply and are part of this specification: 3.1.4, title block, 3.1.8 drawing change (including all subparagraphs, 3.2 submittal, release, and change procedures for contractor drawings (including all subparagraphs), 4.1, 4.2 and 6.2 definitions (including all sub-paragraphs).

3.8   Reliability: The filter shall be designed such that it will function as intended during and after being subjected to all environments specified herein.

3.8.1   Hand Soldering: Hand soldering of electrical connections shall be in accordance with the procedures and requirements of NPC200 4, "Quality Requirements for Hand Soldering of Electrical Connections".

4.   Quality Assurance Provisions:

4.1   General: The contractor shall establish a Quality Program in accordance with NASA quality document NPC200-3, dated April 1962. In the implementation of NPC200-3, the contractor shall include, but not be limited to, the following:

4.1.1   Quality Program Plan: This plan shall include actions to be taken not only during development but also those planned if a follow-on contract is awarded to produce hardware.

4.1.2   Institute and maintain a system which will ensure maintenance of all R & D documentation to current program status.

4.1.3   Install and maintain a system which will record all tests and results thereof.

4.1.4   Institute and maintain a system which will assure and document conformance of all materials used to applicable specifications and drawings. The system should document usage of any materials for which specifications do not exist, and record the selection process for same.

4.1.5   Institute a Material Review Board for the control of non-conforming materials and maintain records of MRB actions.

4.1.6   Install and maintain an instrument calibration program.

4.2   Test Conditions:

4.2.1   Test Environment: Unless otherwise specified herein, all tests shall be performed under the following conditions:

    a. Atmospheric pressure: between 28 and 32 inches of Mercury.

    b. Temperature: between plus 60°F (plus 15.6°C) and plus 95°F (plus 35°C).

    c. Humidity: Not to exceed 90%.

4.2.2   Tolerances: The maximum allowable tolerances for specified test conditions during environmental testing are to be as listed below:

    a. Temperature: $\pm 5^O$F

    b. Atmospheric Pressure: $\pm 10\%$ at room ambient
                                    $\pm 50\%$ at vacuum

    c. Relative Humidity: $\pm 5\%$

    d. Vibration Amplitude (sine): $\pm 10\%$

    e. Vibration Frequency (sine): $\pm 2\%$

    f. Gaussian Vibration Power
       Spectral Density (25 cps or narrower)
                                    $\pm 3dB$ (5-2000 cps)

    g. Shock: a) Average Amplitude: $\pm 10\%$

                 b) Peak Amplitude: $\pm 35\%$ of average amplitude

                 c) Duration: $+20\%$ -10%

    h. Acceleration Amplitude: $\pm 10\%$

    i. Test Duration: $\pm 5\%$

4.2.3   Test Equipment Calibration: All test measurements shall be made with precision laboratory instruments whose accuracy has been certified at intervals established to ensure continued accuracy and is traceable to national standards.

4.2.4   Temperature Stabilizations: Temperature stabilization shall be considered achieved when the temperature of any randomly picked point on the external surface of the hardware remains within 5 F degrees of the specified test temperature.

4.3   Classification of Tests: Inspection and testing shall be classified as follows:

a.   Acceptance Test: Inspection and functional tests performed on each deliverable filter.

b.   Qualification Test: Functional and environmental tests performed on the qualification model.

4.4.   Inspection: The filter shall be inspected for the applicable requirements listed below in accordance with approved contractor standards and/or procedures.

a.   Completeness of product.

b.   Conformance to drawings.

c.   Nameplate, identification markings.

d.   Workmanship, assembly and fit.

e.   Materials, parts and finish.

f.   Welded and/or soldered joints.

4.5.   Acceptance Test Requirements:

4.5.1   Test Procedure: The acceptance test procedure shall provide procedures to demonstrate the deliverable filter's capability of meeting the requirements of Paragraph 3.4, Performance Characteristics, and associated sub-paragraphs under nominal operating conditions.

WATKINS · JOHNSON COMPANY	CODE IDENT	DIV	NO.	SHEET
ELECTRON DEVICES, ELECTRONIC SYSTEMS PALO ALTO, CALIFORNIA	14482		120000	9 of 10

173-1

Satisfactory performance under the environmental requirements of Paragraph 3.5, Environmental Conditions, and associated sub-paragraphs shall be guaranteed by the contractor, but need not be tested.

4.5.2 **Acceptance Test Report:** As a minimum, the acceptance test report shall include:

      a. Summary of inspection information relevant to Paragraph 4.4 herein.

      b. All pertinent test data

4.6 **Qualification Test Requirements:**

4.6.1 **Test Procedure:** The qualification test procedure shall provide procedures to demonstrate the filter's capability of meeting the requirements of Paragraph 3.4, Performance Characteristics, and associated sub-paragraphs under nominal operating conditions before and after the environmental condition of Paragraph 3.5.3, High Impact Requirements.

Satisfactory performance under the other environmental requirements of Paragraph 3.5, and associated sub-paragraphs shall be guaranteed by the contractor but need not be tested.

4.6.2 **Qualification Test Report:** A Qualification Test Report shall be prepared; and shall include, but not limited to, test data, irregularities observed during test, test results, discussion and analysis of failures, conclusions and recommendations. Sketches, graphs, charts photographs, etc., shall be included as part of the test data as applicable.

5. **Preparation for Delivery:**

5.1 **Preservation and Packaging:** Preservation and packaging shall be sufficient to insure safe delivery. Contractor's procedures equivalent to Military level C packaging shall be sufficient if it meets the requirements of safe delivery above.

5.2 **Marking for Shipment:** The package shall be labeled or stencilled for shipment to destination as specified in the Statement of Work. The package labeling shall include the contract or purchase order number.

6. **Notes**

6.1 "And specified herein" or words to that effect shall be construed to mean to the extent specified in other paragraphs of this specification.

APPENDIX III

RANTEC CORPORATION FINAL REPORT

22 November 1966
Rantec No. 66245-32

Watkins-Johnson Company
3333 Hillview Avenue
Stanford Industrial Park
Palo Alto, California   94304

Attention: Mr. E. Beckmeyer

Subject: Test Results, Band Reject and Harmonic Filter

Reference: Watkins-Johnson P. O. No. 51220
                Specification 120000

Gentlemen:

This is the final report to be submitted in compliance with Para 1.2.4
of Watkins-Johnson Statement of Work No. 120000, Revision A.   This
report includes all data pertaining to the acceptance and qualification
tests.   One (1) reproducible and six (6) print copies are provided.

The data is as follows:
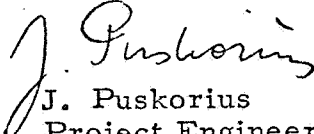
TR-1)   Assembly Display Band Reject and Harmonic Filter
         Model FS-607

TR-2)   Performance Test Report for the FS-607 Prior to Qual Test

TR-3)   FS-607 Filter X-ray before High Impact

TR-4)   FS-607 Filter mounted in the shock fixture

TR-5)   VSWR Measurement Set-up at JPL

TR-6)   VSWR Data before, during and after each impact (original)

TR-6a)   VSWR Data before, during and after each impact (retyped)

TR-7)   Letter by JPL to Rantec regarding the final shock data

TR-7a)   High Impact Test Data by JPL

TR-8)   Performance Test Report for the FS-607 Post Qual Test

TR-9)   FS-607 Filter X-ray after high impact

TR-10) FS-607 Filter Pass Band Reflection plot

TR-11) FS-607 Spectrum Response

TR-12) FS-607 Spectrum Response Plot

During the Impact Tests, due to the shortage of bolts as specified on the Assembly Display drawing, one bolt was substituted by a bolt having markings "FL4 S. C. L." which apparently has higher strength than that specified. Due to the mounting configuration (filter recessed on the mounting plate), this substitution should not be of any consequence to the performed qualification test.

Very truly yours,

RANTEC Division
Emerson Electric Co.

J. Puskorius
Project Engineer

mk

Attachments

SECTION A-A

.100

.003

.020 R
MAX

.5 MIN

.38 TYP
(3) PLCS

NOTES

1. WEIGHT : 9 oz NOMINAL
2. FINISH : GOLD FLASH OVER COPPER PLATE
3. PERFORMANCE PER WATKINS - JOHNSON SPEC. No. 120020
4. SOURCE : FAMTEC CORPORATION
   CALABASAS, CALIFORNIA
   HARMONIC FILTER
   MODEL FS-607

RF CONNECTORS
OSM JACK (2) REQ'D

.94 MAX

.75

45° x .020 MIN
CHAMF

.003

.25 DIA CORNER
RELIEF (4) PLCS

1.374
1.376

2.00

1.374
1.372

1.08

.75 TYP
(4) PLCS

.020 DIA

.338 DIA HOLE ⊕ .020 DIA
.345 DIA SPOTFACE
.625 DIA SPOTFACE
TYP (3) PLCS

OUTPUT

1.00

2.50

2.625
BSC

5.250
BSC

.375

1.375
BSC

.312
BSC

INPUT

MFG TUNING ADJ
(SECURED WITH EPOXY)

.38 REF
TYP (2) PLCS

5.999
5.996
6.75

5.999
6.002
5.250
BSC

2.625
BSC

.376
BSC

1.375
BSC

.313
BSC

.338 DIA HOLE ⊕ .020 DIA
.345
TYP (3) PLCS

.75 MIN
TYP (4) PLCS

MOUNTING REQUIREMENTS
HARDWARE : MS35308 (.312-24) BOLTS
AN960C516 FLAT WASHERS
TORQUE BOLTS TO 330-350 LB IN.

A

A

Rantec No. 66245-32

22 November 1966

PERFORMANCE TEST REPORT

FOR THE FS-607

HIGH IMPACT BAND REJECT HARMONIC FILTER

PRIOR TO QUAL. TEST

Rantec Model No. **FS-607**
Customer **Watkins Johnson**
Customer Part No. _____

Project No. **66245**
Serial No. **11**
Specification No. **120000**

NAME OF TEST	FREQUENCY IN MC											
	2108.0	2118.0	2128.0	2290.0	2295.0	2300.0	4580.0	4600.0	6870.0	6900.0	9160.0	10,000.0
VSWR 1.2:1 Max				1.06:1	1.06:1	1.06:1						
INSERTION LOSS 0.5 db Max				0.25	0.25	0.24						
STOP BAND ATTENUATION	86db min	86db min	86db min	20db min	20db min	12db min	12db min	5db min	5db min
	>95.0	>95.0	>95.0	>30db	>30db	>20db	>20db	>20	>20.0

TESTED BY _R. Wilson_   QC STAMP _____   DATE _10-10-66_

RANTEC CORPORATION
CALABASAS, CALIFORNIA

TR-2

+Y

b) Top View

a) Side View

+Z

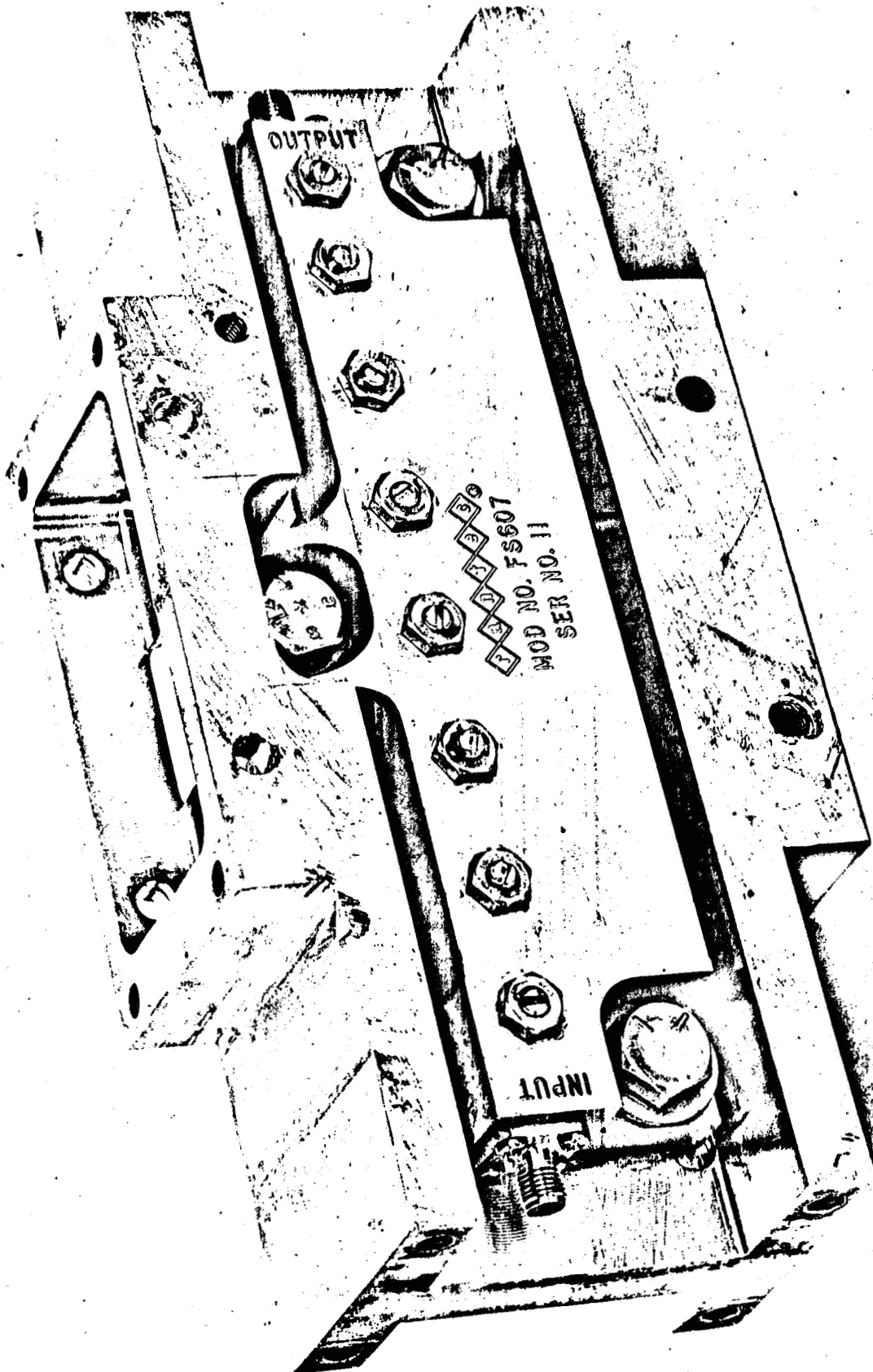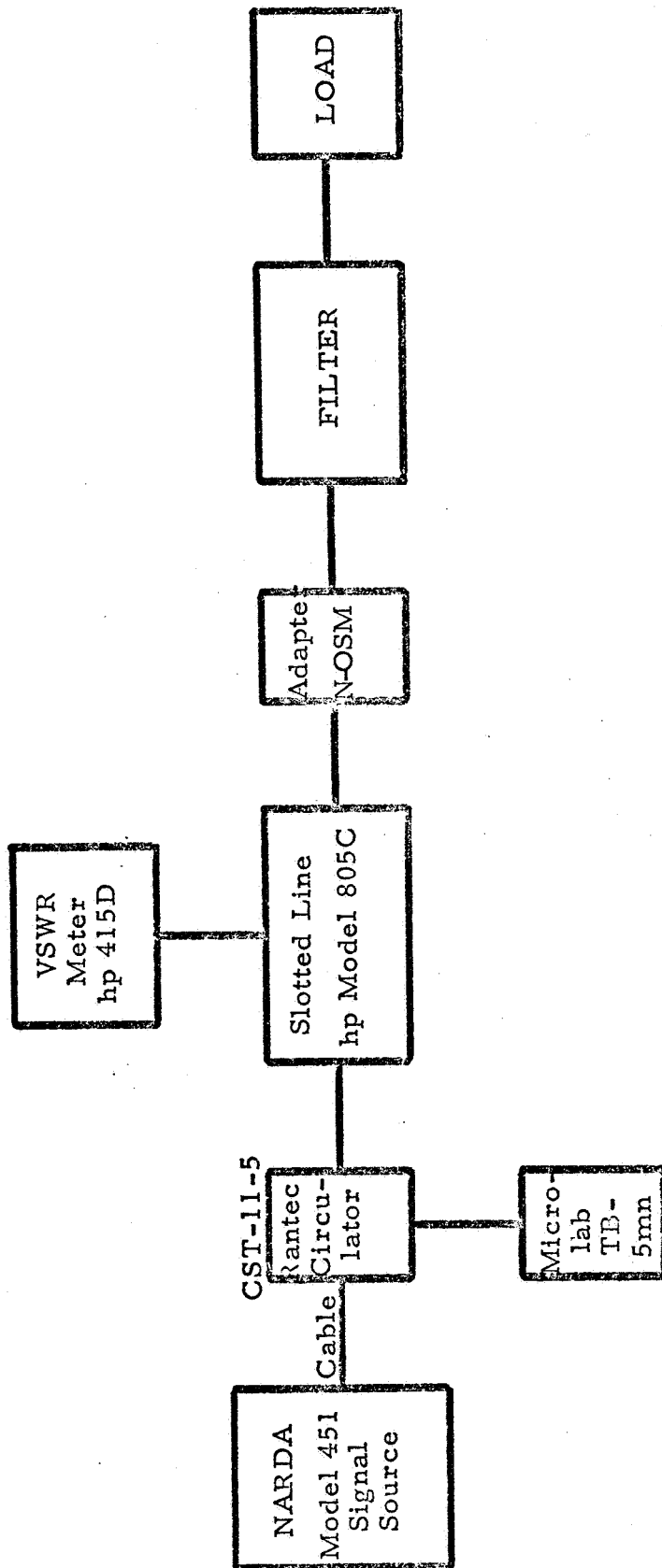+X

Rantec FS-607 Filter Qualification Model
Before High Impact

VSWR MEASUREMENT SET-UP AT JPL

HIGH IMPACT TESTS AT JPL
ON RANTEC FS-607 FILTER
(QUALIFICATION MODEL)

INPUT VSWR (OUTPUT HAS MATCHED LOAD)

Freq (Gc)	On-Test 1st	Repeat	Pre	Pre	+Y	-Y	+X	-X	+Z	-Z	POST TEST -Z	-Z nyud
2.24	2.00	2.10	1.80	1.97	2.15	2.2	2.25	2.30	2.35	2.40	2.55	
2.25	1.41	1.41		1.39	1.42	1.49	1.53	1.51	1.54	1.59	1.55	
2.26	1.21	1.22	1.20	1.21	1.22	1.23	1.24	1.24	1.24	1.24	1.25	
2.27	1.19	1.18	1.18	1.18	1.18	1.19	1.19	1.19	1.18	1.18	1.19	
2.28	1.15	1.14	1.17	1.16	-	-	-	-	-	1.16	1.17	
2.29	1.16	1.15	1.16	1.16	1.15	1.17	1.16	1.17	1.11	1.14	1.14	
2.30	1.15	1.15	1.15	1.15	-	1.15	1.15	1.16	1.14	1.14	1.14	
2.31	1.11	1.15	1.18	1.16	1.15	1.15	1.15	1.19	1.18	1.14	1.15	
2.32	1.17	1.16	1.18	1.19	1.14	1.18	1.17	1.19	1.18	1.17	1.17	
2.33	1.19	1.18		1.22	-	-	-	-	-	1.20	1.20	
2.34	1.23	1.22	1.24	1.26	1.25	1.23	1.22	1.25	1.25	1.24	1.23	
2.35	1.17	1.24		1.31	-	-	-	-	-	-	1.29	
2.36	1.33	1.31		1.34	-	1.34	1.33	1.35	1.35	1.34	1.33	
2.37	1.34	1.36		1.42	1.35	1.39	1.39	1.40	1.39	1.40	1.39	
2.38	1.50	1.44	1.26	1.50	-	1.50	1.48	1.51	1.51	1.50	1.50	
2.39	1.49											
2.40	1.54											
2.42	1.59											

10/24

Not in fixture

for fixture

9300 9350 8750 9800 10400 9600 12000

LEVEL

TI

HIGH IMPACT TESTS AT JPL
ON RANTEC FS-607 FILTER
(QUALIFICATION MODEL)
INPUT VSWR (OUTPUT HAS MATCHED LOAD)

Freq (Gc)	PRETEST				POST TEST						
G Level	1st	repeat			+Y	-Y	+X	-X	+Z	-Z	-Z
					9300	9850	8950	9800	10400	8600	12000
2.24	2.00	2.00	1.80	1.97	2.15	2.2	2.25	2.30	2.35	2.40	2.55
2.25	1.41	1.41		1.39	1.42	1.49	1.53	1.51	1.54	1.59	1.55
2.26	1.21	1.22	1.20	1.21	1.22	1.23	1.24	1.24	1.24	1.24	1.25
2.27	1.19	1.18		1.18	1.18	1.19	1.19	1.19	1.18	1.18	1.19
2.28	1.15	1.16	1.17	1.16	--	--	--	--	--	1.16	1.17
2.29	1.16	1.15		1.16	1.15	1.17	1.16	1.17	1.16	1.15	1.16
2.30	1.15	1.15	1.15	1.15	--	--	--	--	--	1.14	1.14
2.31	1.17	1.15		1.16	1.15	1.15	1.15	1.16	1.14	1.14	1.14
2.32	1.17	1.16	1.18	1.16	--	--	--	--	--	1.15	1.15
2.33	1.19	1.18		1.19	1.19	1.18	1.17	1.19	1.18	1.17	1.17
2.34	1.23	1.22	1.24	1.22	--	--	--	--	--	1.20	1.20
2.35	1.27	1.26		1.26	1.25	1.23	1.22	1.25	1.25	1.24	1.23
2.36	1.33	1.31		1.31	--	--	--	--	--	--	1.29
2.37	1.39	1.36		1.34	1.35	1.34	1.33	1.35	1.35	1.34	1.33
2.38	1.50	1.44		1.42	1.40	1.39	1.39	1.40	1.39	1.40	1.39
2.39		1.49		--	--	--	--	--	--	--	1.46
2.40		1.54		1.50	1.50	1.49	1.48	1.51	1.51	1.50	1.50
2.42		1.59									

10/24 not in fixture　　　10/25 in fixture

TR-6a

CALABASAS, CALIFORNIA
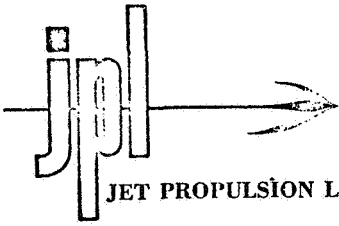
JET PROPULSION LABORATORY *California Institute of Technology • 4800 Oak Grove Drive, Pasadena, California 91103*

17 November 1966

Rantec Corporation
Calabasas, California

Attention: Jonas Puskorius

Dear Jonas;

      Enclosed are two copies of the final shock data for the
filter qualification tests on 25 October 1966. Photographs of the
shock wave shape have been added to the usual data format where
such photographs are available.

Sincerely yours,

W. M. Holmes, Jr.

WMH:at

Encls.

TR-7

PERFORMANCE TEST REPORT

FOR THE FS-607

HIGH IMPACT BAND REJECT HARMONIC FILTER

Post Qual. Test

Rantec Model No. FS-607

Customer Watkins Johnson

Customer Part No. _____

Project No. 66245

Serial No. 1

Specification No. 120000

9200M

NAME OF TEST	2108.0	2118.0	2128.0	2290.0	2295.0	2300.0	4580.0	4600.0	6870.0	6900.0	9160.0	10,000.0
FREQUENCY IN MC												
VSWR 1.2:1 Max.				1.06:1	1.06:1	1.06:1						
INSERTION LOSS 0.5 db Max				0.25	0.25	0.25						
STOP BAND ATTENUATION	86db min	86db min	86db min				20db min	20db min	12db min	12db min	5db min	5db min
	>95	>95	>95				>30	>30	>20	>20	>2?	>2.0

TESTED BY _____   QC STAMP _____   DATE 10-26-66

$+Z$

$+X$

a) Side View

$+Y$

b) Top View

Rantec FS-607 Filter Qualification Model
After High Impact - 25 October 1966
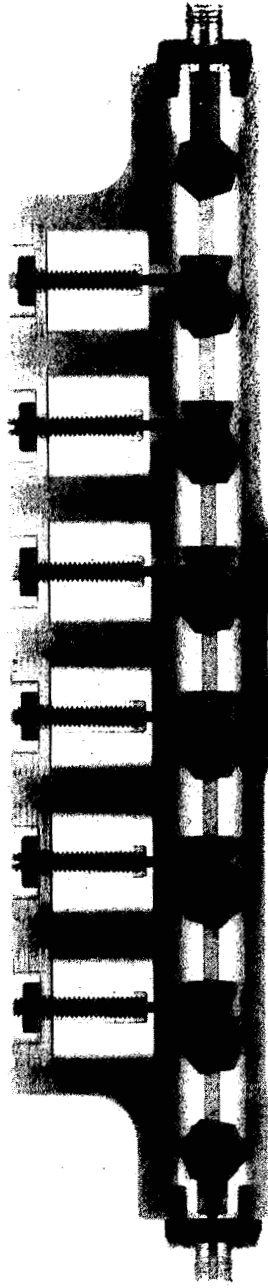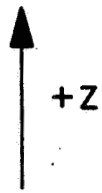
USWR RET LOSS

MODEL NO. FS. 607   TESTED BY H.M. VESTER

SERIAL NO. 11   DATE 11-14-66

FREQUENCY - MC

20-3- db SCALE

10-20 db SCALE

RANTEC CORPORATION
CALABASAS, CALIFORNIA

FS-607 SPECTRUM RESPONSE
S/N 11

Frequency-GHz	Insertion Loss db	Frequency-GHz	Insertion Loss db
2.000	20	3.160	40
2.075	86	3.280	50
2.148	86	3.540	60
2.180	30	3.580	80
2.187	20	3.730	70
2.192	10	3.800	80
2.236	1.0	5.400	80
2.270	0.5	5.480	50
2.290	0.25	5.625	25
2.300	0.25	5.660	50
2.397	0.5	5.670	80
2.420	0.6	6.950	80
2.465	0.3	6.970	50
2.520	0.7	7.060	10.5
2.580	0.3	7.160	50
2.680	2.7	7.280	80
2.760	0.4	9.280	80
2.790	3.0	9.500	8.0
2.815	10	10.500	8.0
2.910	20	11.000	80
3.010	30		

TR-11

FS-607 SPECTRUM RESPONSE

S/N 11

2 November 1966

scale at right

APPENDIX IV

MAGNETIC LEAKAGE FIELD TEST RESULTS
FOR THE WJ-274-1 S/N 5

Component _TRAVELING WAVE TUBE_
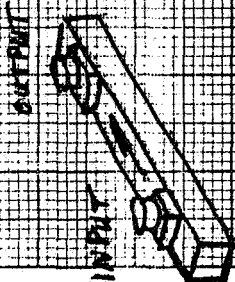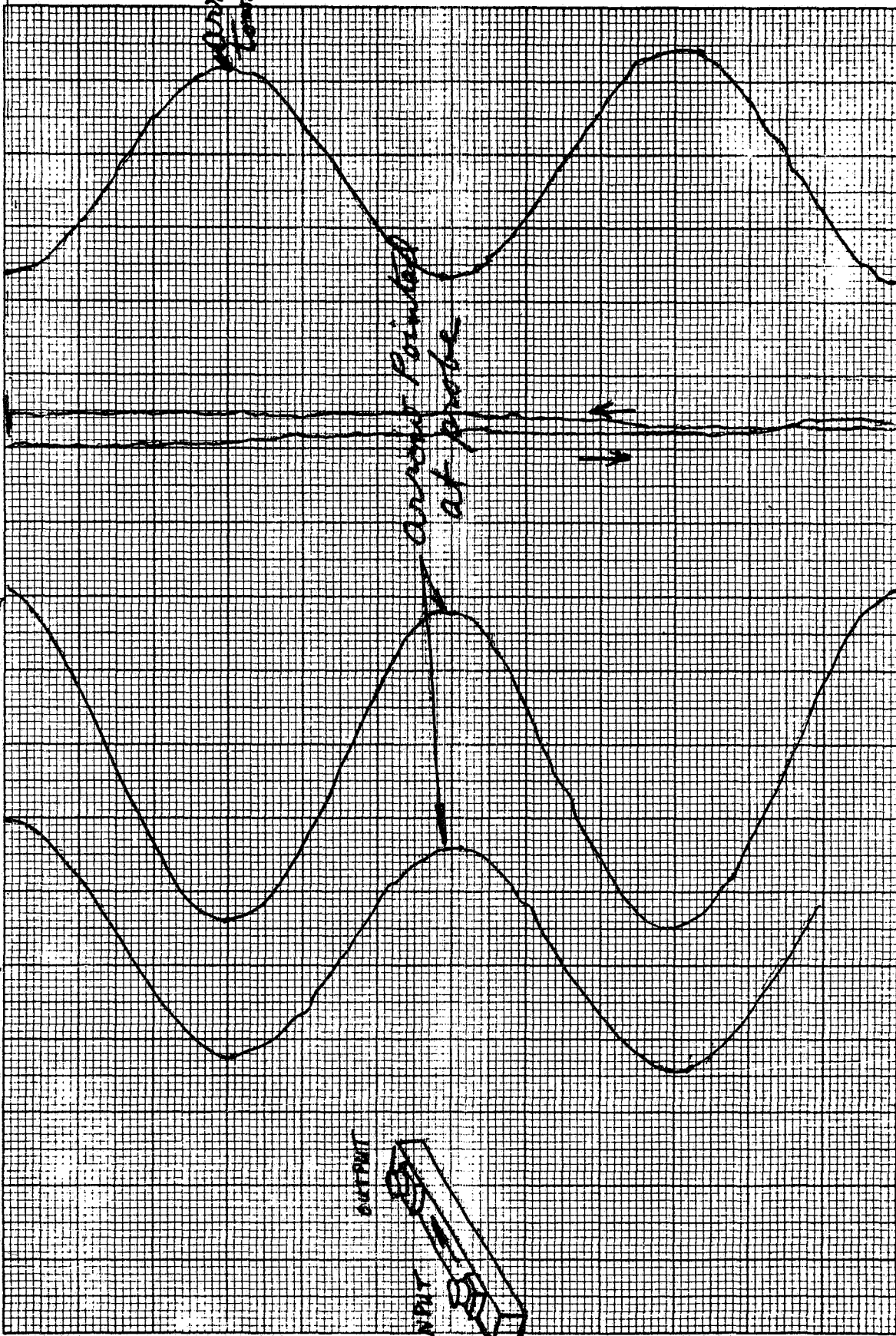_WATKINS-JOHNSON 274-1 #5_

Date _MAR 10, 1966_ Cog. Engr. _MORRIS HOLMES_

Program _VOYAGER_

Orientation for Pos. 1	Orientation for Pos. 2	Orientation for Pos. 3
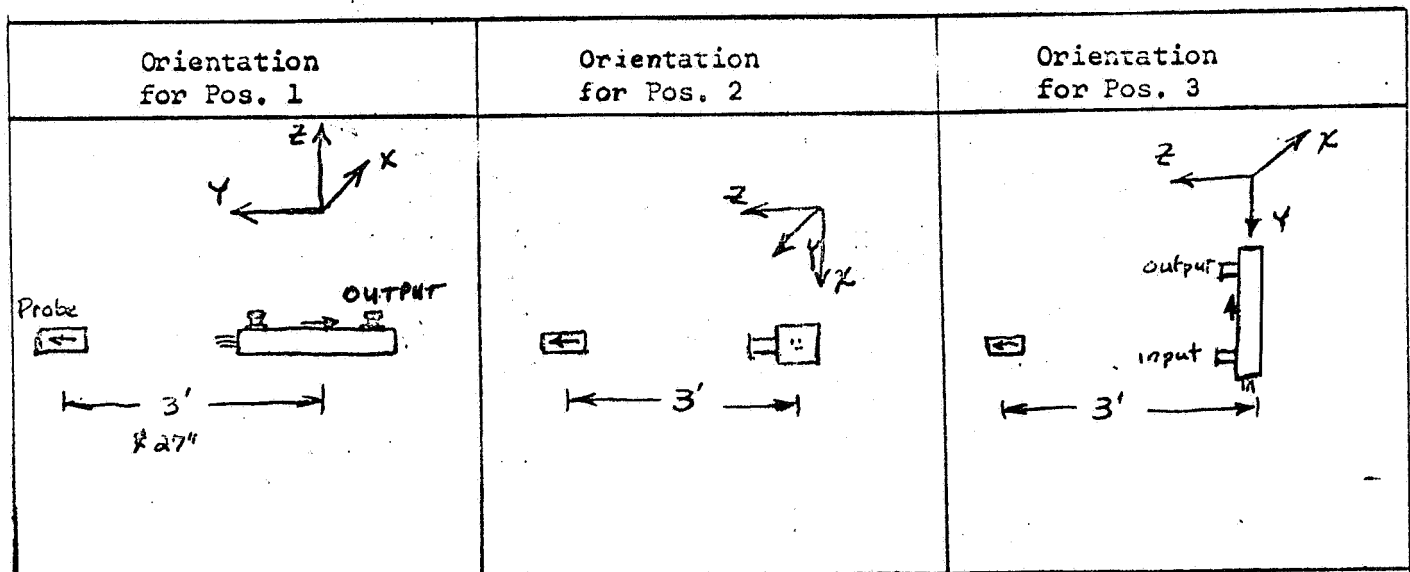
Test	Distance 36"		27"	Equivalent at 36" in.	Remarks
1a	±17γ		69γ	±17 γ	} AS RECEIVED
2a	±14γ			±14 γ	QUADRAPOLE
3a	<1γ			<1 γ	}
1b	±17γ			±17 γ	} Demagnetized 60 cps Ac field
2b	±16γ			±16 γ	25 Gauss RMS. Quadrapole
1c	±16½γ			±16½ γ	} EXPOSED TO 25 Gauss DC field Parallel to long axis in direction
2c	±16γ			±16 γ	of arrow Quadrapole